UNIVERSITY OF NAPLES "FEDERICO II"

PhD in Clinical and Experimental Medicine

CURRICULUM: IMMUNOLOGICAL AND DERMATOLOGICAL SCIENCES

XXIX Cycle

PhD coordinator: Prof. Gianni Marone

PROPERTIES OF MELANIN PIGMENTS FOR THE DEFINITION OF MECHANISMS OF (PHOTO)TOXICITY IN RED HAIR PHENOTYPE AND DEVELOPMENT OF STRATEGIES OF (PHOTO)PROTECTION.

TUTOR/SUPERVISOR

Chiar.mo

Prof. Giuseppe Monfrecola

APPLICANT

Dr. Raffaella Micillo

Index

Chapter 6. Experimental methods

ABSTRACT

In recent years particular attention has been focused on the properties of melanin pigments with regard to their association with some pathological conditions and to their controversial role in the response of skin to solar radiation.

This is especially true in the case of pheomelanins, typical of red hair phenotype, with red hair pale skin, blue-green eyes and freckles. People exhibiting this phenotype have poor tanning capacity, exhibit a UV-susceptibility trait with high tendency to sunburn and an increased risk for skin tumors and melanoma.

On the other hand, eumelanins are commonly believed to be the most important photoprotective factor, even if evidence accumulating over the last decades highlight a much more controversial role of eumelanins in human pigmentation. On these bases, the research work carried out during the PhD course and reported in this thesis was directed at investigating the light-independent effects of purified human hair melanins on keratinocyte cell cultures with particular attention to their pro-oxidant properties and at defining the origin of the broadband absorption spectrum of eumelanin, which underpins their protective shielding effect.

Based on the consideration that, besides eumelanin pigments, the entire melanogenic pathway is relevant to melanocyte function, the effect of carboxyl group substituent of indole precursors on eumelanin properties was evaluated and a suitable derivative of 5,6-dihydroxyindole-2-carboxylic acid (DHICA) was prepared to assess the photoprotective properties for potential application in sunscreen formulations.

Local excess of pigmentation is one of the most common pigmentary disorder[5] whose aesthetically impact has urged the search for efficient strategies for control of skin pigmentation. As a preliminary approach toward the implementation of a novel skin depigmenting agent a conjugate of caffeic acid with dihydrolipoic acid was prepared and tested for its ability to inhibit mushroom tyrosinase activity.

STATEMENT OF CANDIDATE'S CONTRIBUTION TO JOINTLY PUBLISHED WORK

Chapter 1. A part of the concepts presented in this chapter were reported in the commentary "A new light on the dark DNA damages.", **R. Micillo**, S. Lembo, G. Monfrecola, *SKINmed Journal*, **2017**, *15*: 409-411. I surveyed the literature and wrote the manuscript with S.L. and G.M..

Chapter 2. This chapter follows closely a letter to editor that has been published as "Light-independent pro-inflammatory and pro-oxidant effects of purified human hair melanins on keratinocyte cell cultures.", S. Lembo, R. Di Caprio, R. **Micillo**, A. Balato, G. Monfrecola, L. Panzella, A. Napolitano, *Exp Dermatol*., **2016**, DOI: 10.1111/exd.13122. I purified melanins and performed pro-oxidant assays.

A part of the data reported in this chapter has been published in the article "Reverse Engineering Applied to Red Human Hair Pheomelanin Reveals Redox-Buffering as a Pro-Oxidant Mechanism." E. Kim, L. Panzella, **R. Micillo**, W.E. Bentley, A. Napolitano, G.F. Payne, *Sci Rep*., **2015**, DOI: 10.1038/srep18447. I synthesize and extracted the melanin samples.

Moreover some of the data have been published in "Tailoring melanins for bioelectronics: polycysteinyldopamine as an ion conducting redox-responsive polydopamine variant for pro-oxidant thin films" N.F. Della Vecchia, R. Marega, M. Ambrico, M. Iacomino, **R. Micillo**, A. Napolitano, D. Bonifazi, M. d'Ischia, *J. Mater Chem. C*., **2015**, DOI: 10.1039/C5TC00672D. I prepared 5-S-cysteinyldopamine (CDA) and performed HPLC analysis of pro-oxidant properties of p(CDA) films.

Chapter 3. This chapter is an almost complete representation of the publication "Eumelanin broadband absorption develops from aggregation-modulated chromophore interactions under structural and redox control." **R. Micillo**, L. Panzella, M. Iacomino, G. Prampolini, I. Cacelli, A. Ferretti, O. Crescenzi, K. Koike, A. Napolitano, M. d'Ischia, *Sci Rep*., **2017** DOI: 10.1038/srep41532. I prepared monomers and oligomers and carried out experiments.

A part of the concepts presented in this chapter was reported in the review "A reappraisal of the biological functions of melanins and melanogens: The role of 5,6-dihydroxyindole-2-carboxylic acid (DHICA) in skin (photo)protection." **R. Micillo**, L. Panzella, G. Fabbrocini, F. Ayala, G. Monfrecola, *Journal of Plastic Dermatology*, **2014** *101*: 252-255. I surveyed the literature and wrote the manuscript with the other authors.

Chapter 4. A part of the concepts presented in this chapter were reported in the commentary "Melanin pigmentation control by 1,3-thiazolidines: does NO scavenging play a critical role?" A. Napolitano, **R. Micillo**, G. Monfrecola, *Exp Dermatol.*, (**2016**) *25*: 596-597. I surveyed the literature and wrote the manuscript with A.N. and G.M..

CHAPTER 1

1.1 Melanin pigmentation

Melanin pigmentation is believed to be one of the main determinants of sensitivity to ultraviolet (UV) light and susceptibility to sun damage, including photoaging, skin cancer and melanoma and it is important for skin homeostasis.[1]

Together with increasing epidermal thickness, DNA repair mechanisms, apoptosis and antioxidant enzymes, skin pigmentation is one of the endogenous mechanisms developed to protect skin from environmental influences.

Two main varieties of melanin pigments, the black-to-brown indolic eumelanin and the reddish sulfur-containing pheomelanin are known.

Eumelanins are commonly believed to be the most important photoprotective factor, providing protection against sunlight-induced burns, DNA damage and skin cancer, thanks to the broad absorption spectrum and the free radical scavenging properties.[2–5] Epidemiological studies showed an inverse correlation between skin pigmentation and incidence of light-induced skin cancers: people with darker skin (richest in eumelanin) are less prone to skin cancer compared to those with fair skin.[3]

Yet, evidence accumulating over the last decades has highlighted a much more controversial role of melanins in human pigmentation, suggesting a more complex interplay between pigmentation and photoprotection.[6] For example, melanin is known to protect DNA from damage induced by UV radiation, but it is also known to act as a photosensitizer that generates reactive oxygen species (ROS) upon UV irradiation, inducing oxidative base lesions and DNA strand breaks *in vitro* or in cultured cells.[7]

Particular attention has traditionally been focused on the red hair phenotype typically found in individuals of Celtic origin, with red hair pale skin, blue-green eyes and freckles. People that exhibit this phenotype, have a higher ratio of yellow pheomelanin to brown eumelanin[8], have poor tanning capacity, exhibit an UV-susceptibility trait, a high tendency to sunburn and an increased risk for skin tumors and melanoma.[9–12] Pheomelanins are photolable under physiologically relevant conditions[13,14] and can generate ROS following UVR exposure, possibly causing mutation in skin cells and damaging important biological targets.[15]

1.2 Melanin biosynthesis

Under physiological conditions, melanin synthesis in melanocytes is restricted to melanosomes, membrane-bound organelles whose structures differs according with the type of melanin produced: eumelanosomes are elliptical and are characterized by the content of fibrillary matrix, pheomelanosomes are rounded shaped and contains a vesicular matrix.

Melanogenesis is under complex regulatory control by multiple agents interacting via pathways activated by receptor-dependent and -independent mechanisms.[2]

It has long been known that both eumelanins and pheomelanins originate from the tyrosinase-catalyzed oxidation of L-tyrosine whose availability depends either on transport from extracellular space or on hydroxylation of L-phenylalanine to L-tyrosine, a nonobligatory step, operative *in vivo*.

L-tyrosine is hydroxylated by tyrosinase to L-dihydroxyphenylalanine (L-DOPA) (Scheme 1); further steps of melanogenesis can occur spontaneously, at varying rates depending on pH, presence, and concentration of metal cations (particularly zinc and iron), reducing agents, thiols, and oxygen.[16]

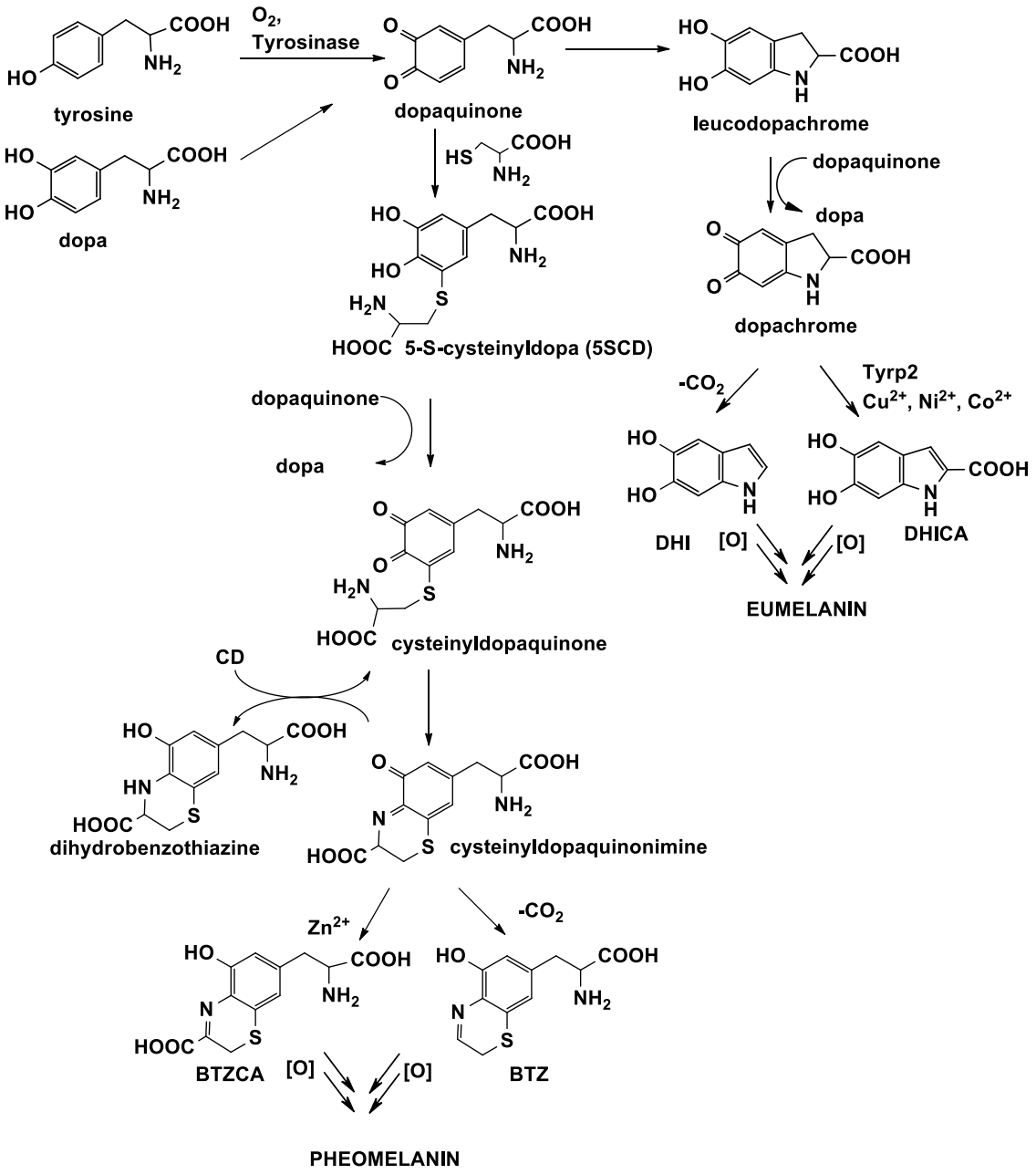

Scheme 1. *Melanogenesis.*

The oxidation product of tyrosine, dopaquinone (common to both eu- and pheomelanogenic pathways), undergoes different fates depending on the presence/absence of cysteine.

Dopaquinone is an orthoquinone which reacts extremely rapidly with thiol compounds but rather slowly with amines, so when concentration of sulfhydryl compounds is low, dopaquinone undergoes an intramolecular reaction of the amino group to give dopachrome via leukodopachrome, followed by a series of oxidation-reduction reactions with production of the intermediates 5,6-dihydroxyindole (DHI) and 5,6-dihydroxyindole-2carboxylic acid (DHICA), that undergo polymerization to form eumelanin. If *in vitro* the decarboxylation of

dopachrome is favored, *in vivo* the tyrosinase-related protein Dopachrome tautomerase (Dct, Tyrp 2) directs the fate of dopachrome toward tautomerization with non-decarboxylative formation of DHICA, a major circulating melanogen.[17]

Also metal cations such as copper, zinc, and iron can affect the composition of the melanin polymer, being involved in the rearrangement of dopachrome to DHICA.[18]

When sufficient levels of L-cysteine are present in melanosomes, it undergoes a non-enzymatically conjugation with dopaquinone forming the isomers 5-S- and 2-S-cysteinyldopa (5SCD and 2SCD) in a ratio of 5:1.[19] As a result, the intramolecular cyclization pathway of 5,6-dihydroxyindole formation leading to eumelanin polymers is decreased or inhibited, and an alternate 1,4-benzothiazine route to pheomelanins becomes dominant. Pheomelanogenesis is also favored at acidic pH because the cyclization of dopaquinone proceeds much slower than the cysteinyldopa quinone cyclization.[9]

Oxidation of cysteinyldopas, *e.g.* 5SCD followed by intramolecular cyclization would then lead to the generation of a transient *o*-quinoneimine which can either undergo redox exchange with the parent cysteinyldopa to give a dihydrobenzothiazine or isomerize with or without concomitant decarboxylation to give 2*H*-1,4-benzothiazine derivatives which undergo oxidative polymerization leading eventually to the pigment.[20,21]

Metal can also affect the reactivity of intermediates of pheomelanogenesis.[22] In the presence of zinc ions, the most abundant trace element present in skin and hair, CD-zinc complexes are formed the undergo oxidation at higher rates with respect to free CD and decarboxylation of the quinoneimine is substantially inhibited so that the 3-carboxy derivative is the main product which persists in the reaction medium for relatively long periods of time due to the stabilizing effect of the metal.[23,24]

Just formed, the 2*H*-1,4-benzothiazine derivatives may follow diverse routes reflecting the presence or the absence of the carboxyl group on the 3-position, and the specific reaction conditions.

Alkaline or hydrogen peroxide treatment of 1,4-benzothiazines leads to a stable 3-oxo derivative (path *a*, Scheme 2).[24]

An intriguing oxidative dimerization process leading to the 2,2'bibenzothiazines (path *b*, Scheme 2*)* can be observed by spontaneous oxidation under mild condition.[20]

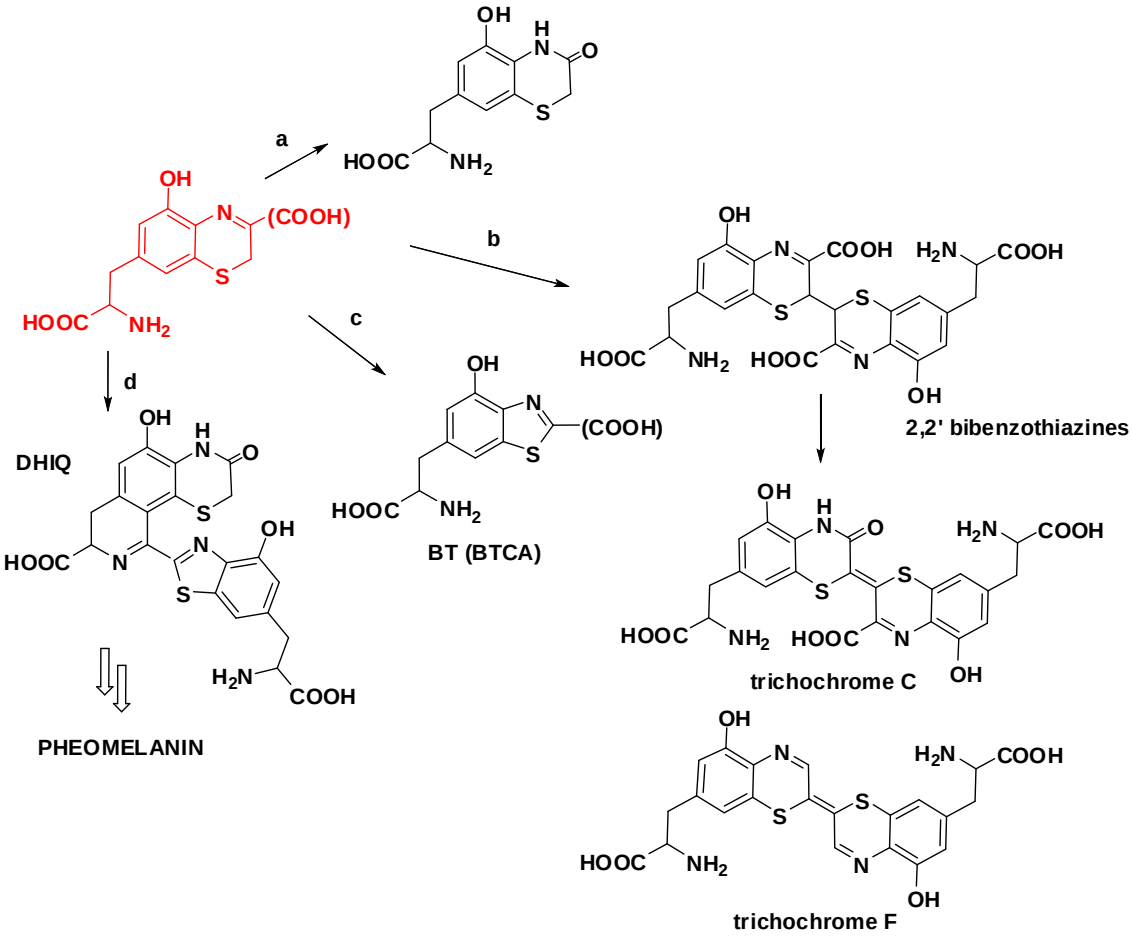

Scheme 2. *Main reaction routes of benzothiazine intermediates of pheomelanogenesis under physiological relevant conditions.*

Further oxidative steps lead to unusual bibenzothiazine derivatives commonly referred to as the trichochromes. These latter comprise four main variants, two of which consist of symmetric bibenzothiazine derivative (trichochromes E and F) while the other two are mixed systems (trichochromes B and C).[25]

By far one of the most typical chemically and biologically relevant characteristic of the 2*H*-1,4-benzothiazines is their tendency to undergo ring contraction either spontaneously or following UV irradiation to give benzothiazole products BTCA and BT (path *c*, Scheme 2).[26] This process has been described as a major post-biosynthetic modification of pheomelanins and the levels of benzothiazole inside the pigment are taken as marker of aging of the pigment itself.[27]

Benzothiazole-carboxylic acids from isomeric cysteinyldopas have been used as markers of high levels of hair pheomelanin and increased risk of skin cancer and melanoma.[28,29]

Pathway *d* in Scheme 2 entails an outstanding sequence of spontaneous chemical processes, which is probably triggered by the coupling of two oxidized benzothiazine species.[30]

The main dimeric product (DHIQ), featuring dihydroisoquinoline and benzothiazole moieties, has been shown to provide the most important building blocks of natural pigments from red hair and chicken feathers.[31,32] Current evidence indicates that most of red hair pheomelanin properties, including UV-visible chromophore and chemical degradation marker profile are matched fairly well by the unusual dimer generated as in path *d*.[31]

Most of natural melanin are considered to be mixtures of eumelanin and pheomelanin so melanogenesis should be considered as "mixed melanogenesis".[8] The ratio of eumelanin to pheomelanin is determined by tyrosinase activity and the availability of tyrosine and cysteine in melanosomes.[33] Kinetic data suggest that pheomelanin production comes first, followed by eumelanin deposition[33,34] so this "casing model" envisages melanin granules consisting of a pheomelanin core covered by an eumelanin surface.[34,35]

1.2 UV radiation, (photo)damage and skin role in (photo)protection

The UV radiation spectrum can be subdivided into ultraviolet A (UVA), from 320 to 400 nm, ultraviolet B (UVB), from 280 to 320 nm and ultraviolet C (UVC) from 200 to 280 nm, but this short wavelength part of the spectrum does not reach the Earth's surface because is absorbed by ozone layer and screened out by atmospheric oxygen.[1]

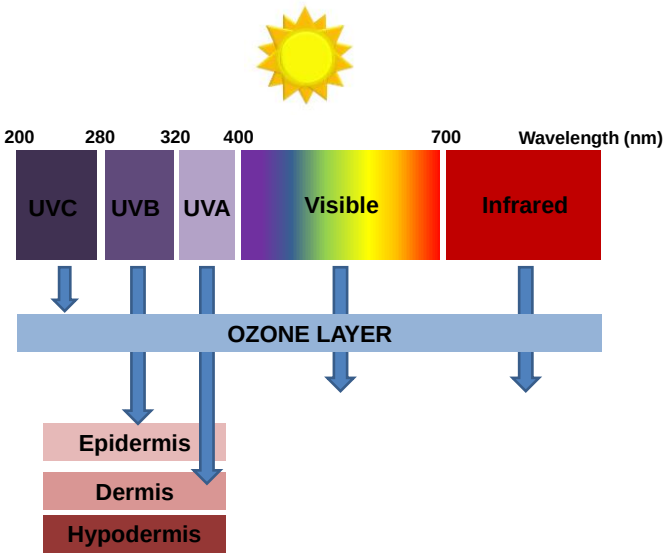

Figure 1. *Schematic representation of electromagnetic spectrum.*

Excessive UVR exposure is known to be responsible for a wide variety of different acute and chronic effects on the skin. Acute responses of human skin to UVR include photodamage, erythema, mutation, immunosuppression, synthesis of vitamin D and tanning. Chronic UVR effects include photoaging and photocarcinogenesis, which is considered to be induced by

mutation and immunosuppression.[36]

UVA and UVB show different properties regarding their biological effects on skin and can act through multiple mechanisms. UVB radiation is more cytotoxic and mutagenic than UVA and can directly damage DNA but is filtered by windows glass, while UVA is able to penetrate in the skin reaching the dermis and it is mainly responsible for indirect DNA damage by ROS generation.[1]

One of the most important photolesions induced by UVB, even at suberythemal doses, are cyclobutane pyrimidine dimers (CPD) that contain a cyclobutane ring arising from the reaction between the carbon-carbon double bond of two adjacent pyrimidine [37].This cycloaddition forces the bases close to each other, altering the DNA structure. The nucleotide excision repair (NER) mechanism can repair dimers but it is sometimes overwhelmed so unpaired dimers can accumulate and possibly lead to skin cancer.[38]

CPDs are responsible for a wide range of acute effects (*e.g.* erythema and inflammatory response), transient effects (suppression of immune function) and chronic effects (DNA mutation and carcinogenesis).[38]

CPDs lead to highly specific mutation, namely (cytosine-cytosine) CC → (tymine-tymine) TT double base substitutions and C→T substitutions at dipyrimidine sites that are known as UVR "fingerprint mutations" or "UV signature mutations".[39] C to T substitutions are typically found in human melanomas.[40]

UVA is able to damage DNA producing reactive singlet oxygen ($^1O_2$) that interacts with guanine (G) moieties, giving oxidized products such as 8-oxo-7,8-dihydroguanine. Moreover UVA can promote the formation of hydroxyl radicals that can induce less specific damages to DNA.

UVA, even if weakly absorbed by DNA, can generate CPDs[41] accounting for a higher induction of T=T CPDs than UVB[42–44] but, while UVB induction of CPDs is associated with the production of (6-4) pyrimidone photoproducts (6-4PPs), in the case of UVA 6-4PPs are not generated.[41,45]

Two different mechanisms seem to be involved in UV-induced melanoma via CPDs. Studies on murine skin showed that CPDs are induced in black and albino mice mainly by UVB radiation while UVA production of CPD is less efficient.[46]

A new mechanism involving melanin has been recently proposed by Premi and coworkers in 2015,[47] suggesting that CPDs are produced in the dark by chemiexcitation,[48,49] *i.e.* the generation of electronically excited molecules by chemical reaction. This work has been the focus of a review article prepared during the PhD course.

According with this study, superoxide ($O_2^{\bullet -}$) ions generated by NADPH oxidase (NOX), and nitric oxide ($NO^{\bullet}$) generated by induced nitric oxide synthase react to give peroxynitrite ($ONOO^-$),[50] an oxidant that is able to generate dioxetanes that by thermolysis are cleaved to two carbonyls. One of these carbonyls is in the high energy triplet state[51] and can transfer energy to DNA in a non-radiative manner bases generating dimers via cycloaddition.

In this contest, melanin would act as molecular vector, acting as a triplet-state carrier. Synthetic eumelanin, DHICA and 5SCD can be oxidized by peroxynitrite and enter the nucleus[47] where they transfer energy to DNA and generate CPDs even hours after UV exposure has ended (delayed or "dark" CPDs). In particular, a product of oxidation of DHICA likely obtained via a muconic-type C-C cleavage or a 1,2-dioxetane mediated C-C cleavage has been identified as a possible triplet-carrier carbonyl.[52]

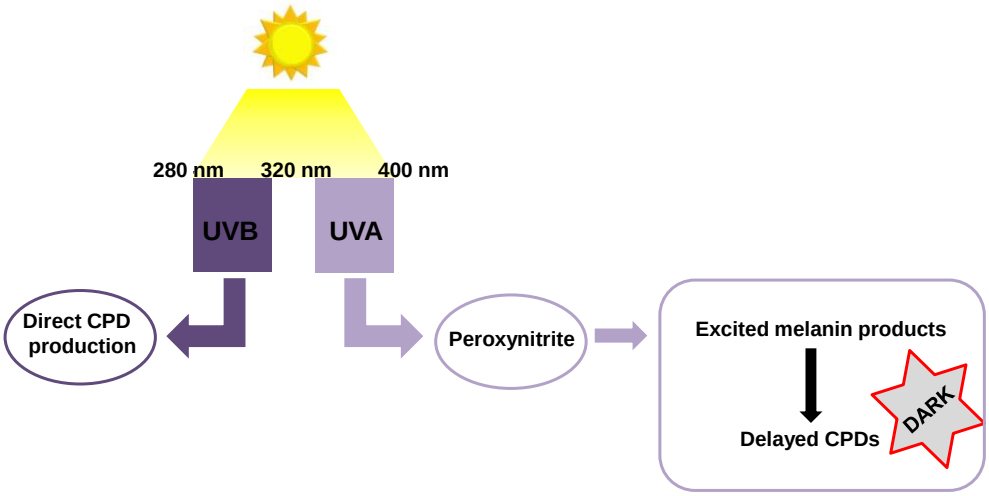

Figure 2. *A proposed mechanism for the bright and the dark pathways of cyclobutane pyrimidine dimers (CPDs) production.*

Human skin has developed two main defense mechanisms against the damaging effects of UV: epidermal thickening and the stimulation of melanin synthesis that play a key role in photoprotection.[1] Epidemiological data strongly support the photoprotective role of melanin as there exists an inverse correlation between skin pigmentation and the incidence of sun-induced skin cancers.[53,54]

UV exposure induces skin pigmentation that follows different phases:

- Immediate pigment darkening (IPD) shows a broad peak in UVA region, occurs within minutes of exposure and fades over some days. It is not due to melanin synthesis but to photooxidation of already formed melanin.[55]
- Persistent pigment darkening (PPD) is mainly induced by UVA and results from oxidation of pre-formed melanin and fades over 3-5 days.[56,57]
- Delayed tanning (DT) can be induced both by UVA and UVB, occurs 2 or 3 days after UV exposure and is completely different from IPD, displaying a different action spectrum.[58] DT results from synthesis of new melanin and it is associated with an increase of tyrosinase activity.[59].

The protective effect of melanin is achieved by its capacity to serve as shielding filter that absorbs UV reducing its penetration through the skin, however melanin role is not merely that of a sunscreen.[60]

For example, melanin is able to quench excited states of photosensitizers and singlet oxygen ($^1O_2$) and to act as scavenger of ROS, playing an important role in protection against oxidative damage.[60]

Actually, synthetic melanin can react with both oxidizing and reducing radicals because the hydroquinone and quinone subunits allow it to act both as electron donor and acceptor. Melanin can also protect DNA from H_2O_2-induced DNA damage through its ability to bind Ca^{2+}.[61]

Even if it is generally accepted that melanin acts as a natural sunscreen and protective agent, the relationship between pigmentation and photoprotection seems to be by far more complex than generally assumed as melanin can also have toxic effects,[7] especially after exposure to UVR.[62–64] *In vitro* studies showed that after UVA irradiation, it generates ROS that can indirectly induce oxidative base lesions, damaging DNA.[65,66]

The tyrosine-derived aromatic rings of the melanin chromophore are excited to the singlet state, decay to the triplet, and transfer an electron to oxygen to yield superoxide.[14] Some evidence also indicates transfer of excitation from the chromophore to oxygen, giving singlet oxygen which can react with several targets. Reaction of superoxide with iron (III) ions and hydrogen peroxide (created by dismutation of superoxide) can lead to the $OH^{\bullet}$ radical, which is capable of causing DNA strand breaks. Melanins subsequently scavenge these active chemical species, but their scavenging capacity can be overwhelmed. In

living skin exposed to UV, it is not known which of these opposing mechanisms predominates.[67]

Pheomelanin, that is especially prone to photodegradation,[13,68] amplifies these effects contributing to the damaging effects of UVR by generation of hydrogen peroxide and superoxide anions.[14,18]

Melanin should then be regarded as a double-edge sword, being carcinogenic as well as protective against cancer, so further investigation on the its role in the UV immune and antioxidant responses and on the chemistry of eumelanin and pheomelanin precursors, would improve our understanding its contribute to the risk of carcinogenesis not only due to UV exposure but even in the dark.

CHAPTER 2

2.1 Pheomelanin pigments: (photo)toxicity and pro-oxidant properties

Since the discovery in 1995 that people with red hair display mutations in the human melanocortin 1 receptor (MC1R), the genetic of pigmentation has been largely investigated.[3]

Indeed, among the more than 120 genes involved in the regulation of pigmentation, only the melanocortin 1 receptor gene (*mc1r)* is known to account for variation in skin and hair pigmentation and in skin cancer incidence. The *mc1r* gene encodes a 317–amino acid G-coupled receptor, MC1R.

Human *mc1r* sequence variants are associated with red hair and fair skin in the Caucasian population.[69–71] These variant alleles are extremely common, and in northern European populations < 50% of the *mc1r* genes encodes the 'wild-type' or consensus protein. Three alleles in particular, Arg151Cys, Arg160Trp and Asp294His together make up 22% of the *mc1r* genes and account for 60% of all cases of red hair. Thus, a single *locus* can contribute significantly to human pigmentary variation.

The MC1R gene is regulated positively by α-melanocyte-stimulating hormone (α-MSH) and negatively by antagonists of MC1R, such as Agouti signal protein (ASIP) and beta-defensin 3, competing with α-MSH.[72,73]

In wild-type eumelanic subjects, MC1R activation induces eumelanin synthesis via tyrosinase activation. Among red haired individuals, homozygous for alleles of the *mc1r* gene can be found, that show varying degrees of diminished function. The main consequence is a decrease in the amount of eumelanin pigments with prevalence of the pheomelanin variant.

At the biochemical level, this change is the result of the drop in tyrosinase activity favoring the concomitant intervention of cysteine in the pathway.

MC1R is even implicated in controlling ROS-induced DNA damage, regulating the levels of two enzymes involved in DNA repair, namely 8-oxoguanine DNA glycosylase (OGG1) and apurinic apyrimidinic endonuclease.[74]

In spite of the many advances carried out in the last years in the elucidation of the structure and biosynthesis of pheomelanin pigments, the relationship between the structural features and the role of the pigments in determining the skin cancer proneness of red hair phenotypes has not been fully elucidated.

Traditionally, the positive correlation between red hair and melanoma has been attributed to both the poor antioxidant and photoprotective properties of pheomelanins compared to the dark eumelanins, and the capacity of pheomelanin to act as photosensitizer inducing generation of ROS upon irradiation with UV light.[7,10,14,75,76]

These effects have been extensively investigated either on cell cultures[10] or in vitro by Electron Paramagnetic Resonance (EPR) oxymetry using synthetic pheomelanins prepared under different conditions showing an enhanced photoreactivity for the synthetic pigments obtained in the presence of zinc ions under which conditions the formation of benzotiazine-2-carboxylic acid BTCA and DHIQ is favored.[75]

Pheomelanin chromophore can be excited to the singlet state;[14] decaying to the triplet it can transfer an electron to oxygen generating superoxide anion or singlet oxygen, both able to damage DNA. Moreover singlet oxygen can destruct the pigment itself.[77]

Evidence has also been obtained that red hair pheomelanins undergo significant structural modifications on exposure to air and solar light during hair growth, being readily photodegraded under physiologically relevant conditions.[28] All these data however have not so far been reconciled into a coherent picture correlating the structure features of the pigment with the photoreactivity.

Two UV-dependent pathways for the induction of melanoma have been identified, which revealed an unexpected and significant role for melanin in melanomagenesis:[46] while UVB is able to induce DNA damage in a direct manner, UVA requires the presence of melanin.

Nonetheless, direct relationship between sun exposure and melanoma is still missing, and issues have been raised of why melanoma is not restricted to sun-exposed areas of the body, and UV radiation signature mutations are infrequently oncogenic drivers.[78]

A further issue of great relevance to the mechanisms of toxicity associated to pheomelanic pigmentation has recently been disclosed by a series of papers that claimed identification of UV-independent pathway for the induction of melanoma.[6,78–80]

Multiple experiments show that an activating mutation of BRAF into red hair mice melanocytes resulted in a high incidence of invasive melanomas in the absence of UV-light.[79] Introduction of an albino allele that inhibits pigment production showed that the absence of pheomelanin is protective against melanoma development.

In addition, pheomelanic mice's skin contained higher levels of oxidative DNA and lipid damage than albino-Mc1re/e mice.[79] These data suggested that the pheomelanin pathway produces UV-independent carcinogenic contributions to melanomagenesis, probably by a mechanism of oxidative damage.

Oxidative damage seems to play a key role in melanoma formation, however the actual mechanisms implicated in pheomelanin-induced UV-independent oxidative stress, DNA damage and melanomagenesis have remained unclear.

Pheomelanin synthesis is associated with increased oxidative stress in the skin. Two possible not mutually exclusive pathways by which the pheomelanin pathway could mediate oxidative stress and melanomagenesis were postulated:[80]

- The pheomelanin biosynthetic pathway envisages the incorporation of cysteine that is mainly stored in glutathione, the most important cellular antioxidant. So it would be the synthesis, rather than the presence of pheomelanin to make the cell more vulnerable to elevated ROS levels oxidative stress.
- Although pheomelanin is not located in the nucleus, it might cause damage by promoting the formation of ROS, which could overwhelm cellular antioxidant reserves and cause oxidative damage to biomolecules.[81] It is known that pheomelanin can generate ROS after UVA exposure, but the study by Mitra and his coworkers[79] showed that ROS generation can occur even in the absence of UV stimulation.

A hint to the peculiar properties of pheomelanins in the dark was provided by a recent work showing that synthetic pheomelanins can behave as pro-oxidant promoting formation of melanin pigments from catecholamines and DOPA, a process requiring the presence of oxygen.[82]

Indeed, in vitro studies with synthetic pigments indicated that both eumelanin and pheomelanin are able to promote DNA strand breaks in the dark,[83] and even act as direct mutagenic agents by generation of CPD in the absence of UV.[47]

The molecular basis to interpret the role of melanins in these processes was provided by in vitro experiments showing that, in the dark and in the presence of oxygen, natural and synthetic pheomelanins can accelerate depletion of two cellular antioxidants, namely glutathione (GSH) and reduced nicotinamide adenine dinucleotide (NADH), by a UV-independent mechanism.[84] High pressure liquid chromatography (HPLC) analysis with

electrochemical and/or UV detection allowed to observe the generation of GSH disulfide (GSSG) and NAD^+, confirming a redox reaction. Natural eumelanin from black hair induced less marked variations. The same study showed that natural pheomelanin is able to promote the oxidation of melanin precursors, for example DOPA and 5SCD, in the dark. Data from EPR experiments suggested that pheomelanin can promote GSH and NADH autoxidation via direct H-atom exchange. The subsequent reoxidation of reduced pheomelanin by oxygen may generate ROS and restore the free-radical population, thus sustaining a redox cycle.[84]

However, neither the effects of melanins at cellular level, nor the possibility that the pigment may display a proinflammatory activity, have been investigated.

Based on this background, part of the research activity of this PhD project was focused on testing the ability of natural melanins to induce an inflammatory response on cultured keratinocytes and to affect the levels of endogenous antioxidants, independently from light exposure.

In order to examine human hair pheomelanin redox properties, a sample of the pigment was provided to Professor Payne of the University of Maryland for its evaluation in an electrochemically-based reverse engineering methodology. Moreover polycysteinyldopamine (pCDA), a red hair-inspired polydopamine-like polymer, was tested for the ability to accelerate the autoxidation of GSH via a redox exchange process.

2.2 Light-independent effects of purified human hair melanins on keratinocyte cell cultures

Immortalized keratinocytes were incubated by Dr. Roberta Di Caprio (University of Naples) and Dr. Serena Lembo (University of Salerno) in the dark with increasing doses of red hair pheomelanin (RHP), black hair eumelanin (BHE) and white hair protein (WHP), purified from untreated hair of healthy volunteers.[85]

Pigments from hair have been widely used as a model for human melanin. It is preferable to use freshly collected hair samples, as photoaging induces structural modifications not only in pheomelanins[28] but also in eumelanins.[86]

Isolation of natural melanin pigments represents quite a difficult task because of the close association of proteins and other biological components with melanin.[85,87,88]

Melanin in human hair is deposited in the form of granules in the medulla, the porous core of the hair fiber and in the cortex surrounding it. Access to the inside of the hair by a proper swelling of the overlapping layers of the external covering, the cuticle, is therefore necessary for pigment release. Current strategies revolve on the attack of the keratin matrix by breaking disulfide bonds and exposure to proteolytic digestion.[89] The enzymatic extraction preserves the integrity of the melanosome, removes most of the external proteins, and therefore should be the preferred choice for isolation of melanin from hair samples.[87]

Homogenization of the finely minced hair sample is required prior to exposure to proteolytic agents to favor their action. This can be achieved by the use of a glass/glass potter such as Tenbroeck homogenizer while other mechanical devices (grinder, ultrasonic disrupters) currently employed for tissue homogenization prove often inappropriate.

Hair was treated with dithiothreitol and subjected to different digestion steps with proteinase K. Every digestion step was followed by centrifugation: the pellet was collected and the supernatant was acidified to allow formation of a precipitate that was combined with the former. The reaction mixture was eventually treated with Triton X-100 for improving proteins solubilization and removal from the pigment. The overall procedure represented in Figure 3 afforded 125 mg starting from 5 g of red hairs. The same protocol repeated on black hairs yielded 157 mg of black hair melanin and 65 mg from white ones.

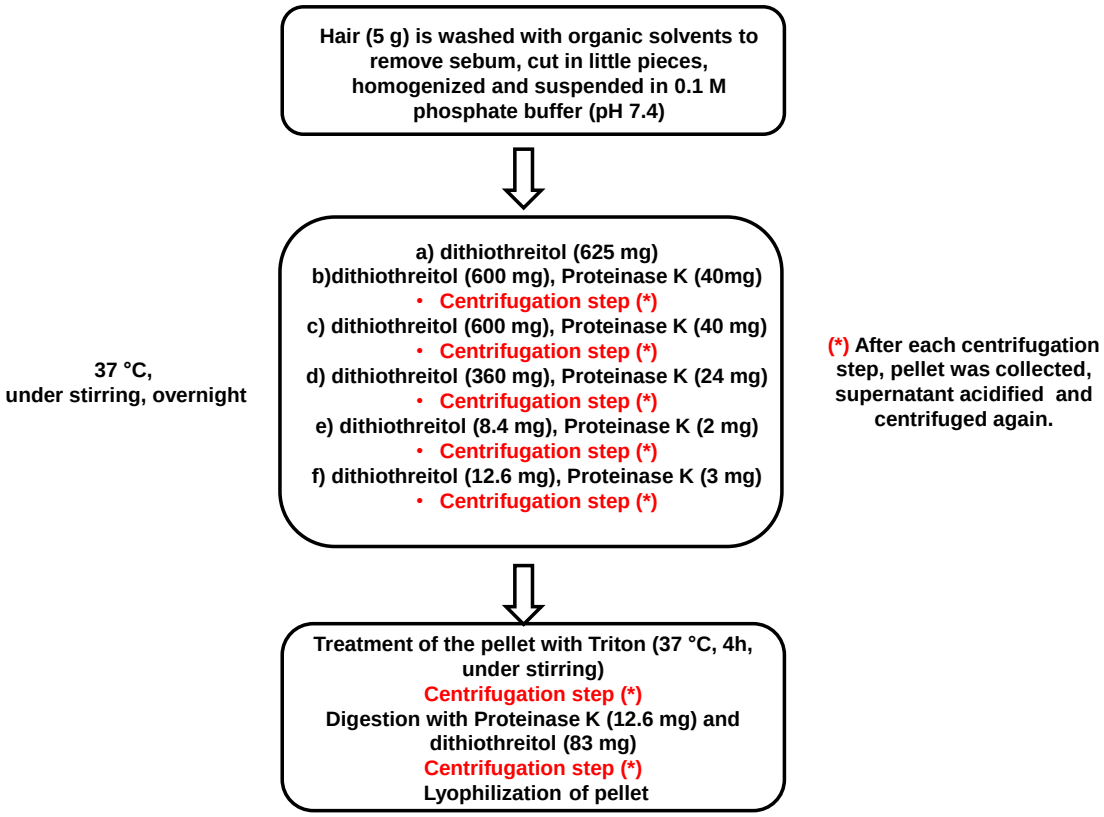

Figure 3. *Schematic outline of the procedure of pheomelanin isolation from human hair.*

Chemical analysis was carried out on the starting hairs and the final purified pigment to assess the degree of pigment enrichment. Degradation of the pigmented tissues by alkaline hydrogen peroxide treatment was followed by HPLC quantitation of the typical structural markers, namely thiazole-2,4,5-tricarboxylic acid (TTCA) for pheomelanin, and 2,4,5-pyrrole-tricarboxylic acid (PTCA) for eumelanin.[90]

Purified red human pheomelanin (RHP) showed an 11-fold enrichment in melanin with respect to the starting hair based on the yields of TTCA. The pigment content in RHP was also estimated as 57% by EPR analysis from the ratio of the double integration of the RHP and a synthetic pheomelanin from 5SCD (CD-mel) spectra. In the case of BHE a 10 fold enrichment was estimated based on the yields of PTCA.

Exposure to RHP or BHE, but not to WHP, moderately decreased keratinocyte viability compared to untreated control cells (Figure 4). Proliferation/apoptosis assessment showed not significant differences.

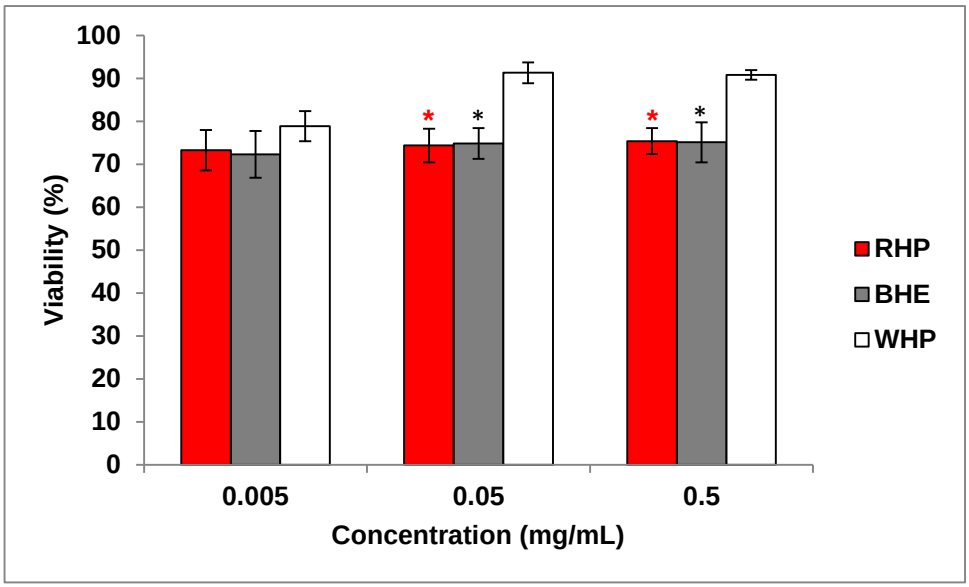

Figure 4. *Viability of HaCat cells after exposure to multiple concentrations (0.005; 0.05; 0.5 mg/mL) of RHP, BHE or WHP for 24 hours. Data are expressed as mean ± SD of three independent experiments, each performed in duplicate (*p<0.05; **p<0.01; ***p<0.001).*

The direct pro-inflammatory ability was investigated through IL-1β, TNF-α and IL-6 gene (RT-PCR) and protein expression (ELISA). IL-1 is one of the most potent proinflammatory mediators and elevated levels of IL-1β have been correlated with melanoma progression; IL-6 (formerly known as BSF-2 and IFN-β) is a pleiotropic cytokine that participates in immunomodulation, hematopoiesis, inflammation, and oncogenesis; it is produced by many cell types, including keratinocytes, and stimulates proliferation in keratinocytes, being essential for wound healing.[91] TNF-α (formerly cachectin) is involved in multiple cellular and inflammatory immune reactions through activation of corresponding receptors. While IL-1β upregulates MC-1R activity and message, TNF-α has the opposite effect.[92]

RHP, and to a minor extent BHE, promoted expression of pro-inflammatory interleukins and oxidative damage, whereas WHP was ineffective. More in detail, after 24 hours, gene expression increase was dose related (Figure 5 a-c) and highly significant for TNF- α and IL-1β (Figure 6a), whereas protein secretion of IL-6 resulted more enhanced than that of TNF- α or IL-1β (Figure 6b). No significant differences in protein expression emerged at 48 hours.

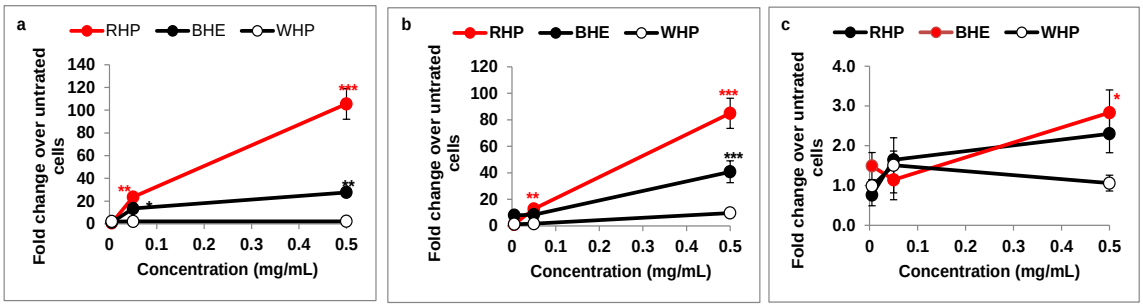

Figure 5. *Dose–response curve for TNF-α (a), IL-1β (b) and IL-6 (c). Data are expressed as mean ± SD of three independent experiments, each performed in duplicate (*p<0.05; **p<0.01; ***p<0.001).*

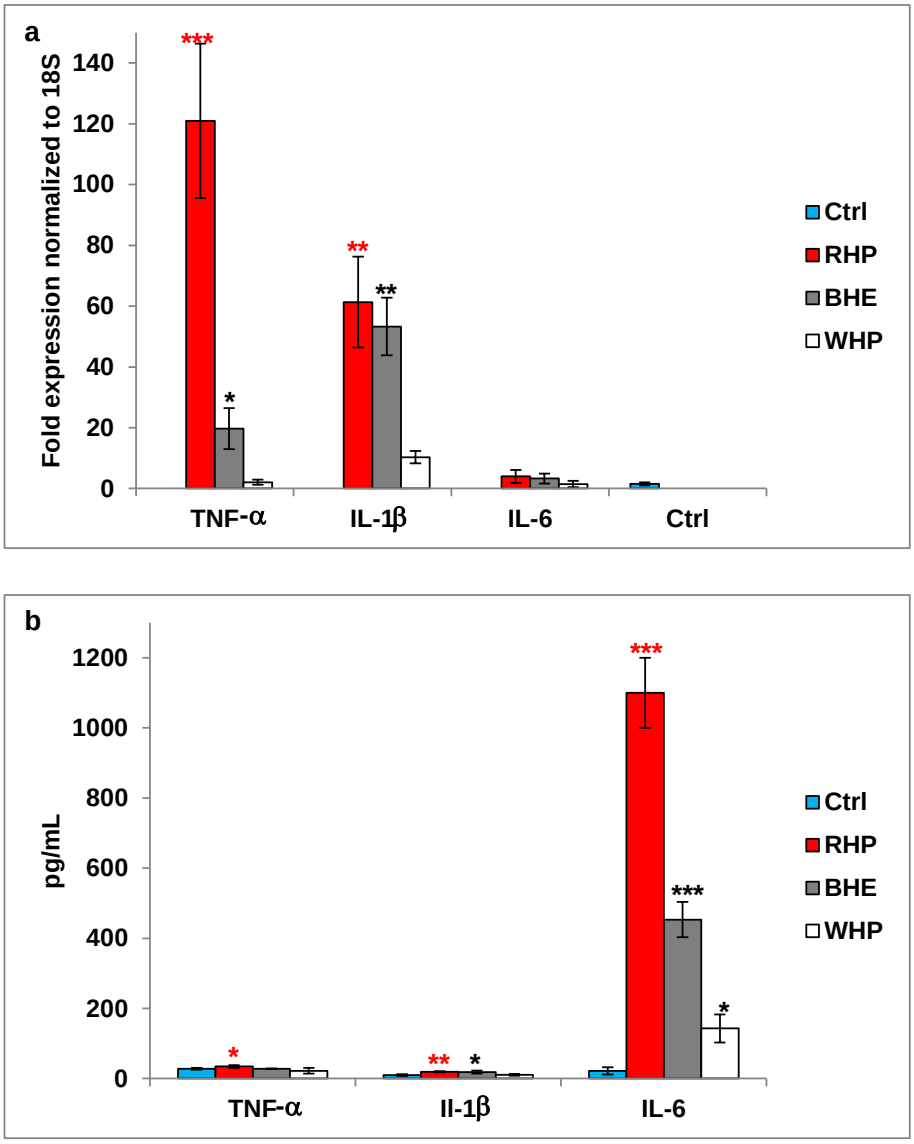

Figure 6. *TNF-α and IL-1β gene expression (a) and protein expression (b) in the absence (Ctrl) or in the presence of RHP, BHE or WHP. Data are expressed as mean ± SD of three independent experiments, each performed in duplicate (*p<0.05; **p<0.01; ***p<0.001).*

The discrepancy between IL-6 gene expression and protein secretion is likely due to an early rise of mRNA, which has already decayed after 24h, when protein has accumulated, also inducing TNF-α negative regulation. TNF-α, IL-1β and IL-6 were studied as pivotal mediators of chronic inflammation, implicated in most stages of tumorigenesis. Although their role is still controversial, up-regulation has been reported in melanoma, also in relation to inflammasome activation, occurring in response to pathogens associated molecular patterns (PAMPs) or (damage associated molecular patterns) DAMPs.[11,12,93]

Pheomelanin can act as a binding agent for drugs and chemicals.[94,95] Thus the long, melanized scalp hair with its capability to trap and/or bind chemicals, toxins, and heavy metals would prevent their access to living tissues. Pigmented hair may also provide antioxidant defense for the skin and hair follicles due to the high capacity of melanin for binding transition metals. This buffering capacity as applied to calcium would imply a role for melanin in cell function, since calcium is a critical second messenger in pigmentation signaling, acting in the transfer of melanosome to keratinocytes, and in epithelial cell differentiation.[96]

In order to ensure removal of possible contaminants that could affect the results so far illustrated, integrative experiments with the 3 compounds (RHP*, BEH*, WHP*) previously washed with EDTA, a strong chelating agent, have been performed to ensure removal of drugs or other substances possibly derived from environmental contamination. No significant differences in terms of toxicity or pro-inflammatory effects were obtained for the EDTA-treated compounds with respect to the untreated ones (data not shown).

In order to explore the direct pro-oxidant ability of RHP, BHE and WHP, the levels of cellular antioxidants and lipid peroxidation markers were determined.

The effect of RHP on the autoxidation of GSH, a primary cellular antioxidant, a substrate for detoxifying enzymes such as glutathione-S-transferase and glyoxalase, and a cofactor of glutathione peroxidase, and NADPH, a central component of the respiratory chain and a critical index of the metabolic state of the mitochondria in terms of energy production and intracellular oxygen levels[97] was investigated.

Pheomelanin pigments are generated within the melanosomes, organelles that contain the biochemical machinery for production of pigments. Hair pheomelanosomes are less regularly shaped than eumelanosomes.[98–101] Once pheomelanosomes are mature, they are transferred to keratinocytes, where they are made available to come into contact with major cellular ingredients including GSH, NADH and other redox active biomolecules. Thus, both in

melanocytes and keratinocytes, the pigment components of pheomelanosomes, which seems to be more accessible than those of the compact eumelanosomes, can induce a depletion of cellular antioxidants at micromolar concentrations. Moreover, it is possible that ROS produced by interaction between pheomelanin and GSH, damage the pheomelanosome surface favoring the contact of the pigment with the antioxidants.

The level of GSH was determined by HPLC with electrochemical detector set at +500 mV *vs.* an Hg/Hg_2Cl_2 reference electrode while in the case of NADPH a UV detector was used (wavelength set at 340 nm). Depletion of either the antioxidants was observed after exposure to RHP and, to a lower extent, to BHE (Figure 7a). These results are in line with the effects of RHP on GSH and NADPH levels, in air equilibrated metal-free buffer.[84]

Moreover, thiobarbituric acid reactive substances (TBARS) assay was performed. This spectrophotometric assay allows to determine and quantify malondialdehyde (MDA) and related compounds, known to be byproducts of lipid peroxidation.[102] MDA can denature proteins, alter apoptosis, and influence the release of proinflammatory mediators, such as cytokines, foster the induction of some inflammatory skin diseases.[103] An increase of TBARS was registered after exposure to RHP and, to a lower degree, to BHE (Figure 7 b). However, as not all lipid peroxidation products generate MDA and MDA is not the only product of fatty peroxide formation, care should be taken in interpreting results from TBARS assay that can only offer a narrow picture of the process of lipid peroxidation.

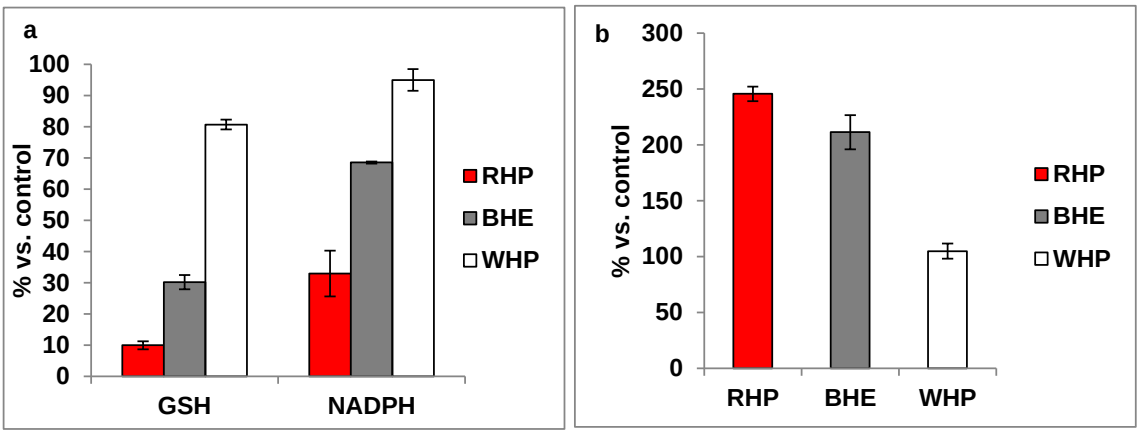

Figure 7. *Levels (expressed as percent of control) of GSH and NADPH levels in keratinocyte cultures after 24 hours exposure to RHP, BHE and WHP (0.5 mg/mL) in the dark (a). Levels (expressed as percent of control) of thiobarbituric acid reactive substances (TBARS) after 24 hours (b). WHP. Data are expressed as mean ± SD of three independent experiments, each performed in duplicate.*

Oxidative stress plays a key role in several inflammatory skin diseases and a correlation between inflammation and cancer has been established.[104,105] As a cross-point between the IL-1β inflammatory pathway and the direct oxidative damage, the expression of cyclooxygenase-2 expression (COX-2) gene was then determined. IL-1β increases COX-2 that is not expressed in normal cells but is increased in melanoma.[106] Exposure to RHP for 24 h in the dark was found to induce a moderate but significant increase of COX-2 expression (Figure 8).

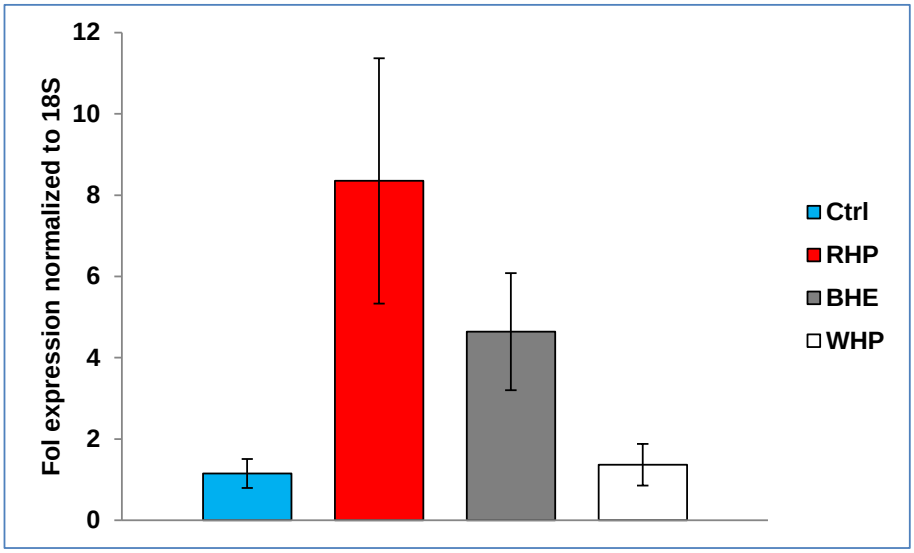

Figure 8. *COX-2 gene expression in HaCat cell in the absence (Ctrl) or in the presence of 0.5 mg/mL of RHP, BHE or WHP. Data are expressed as mean ± SD of three independent experiments, each performed in duplicate (*p<0.05; **p<0.01; ***p<0.001).*

2.3 Pro-oxidant properties of polycysteinyldopamine thin films

Polycysteinyldopamine (pCDA) is a red hair-inspired polydopamine-like polymer[107] derived by the oxidation of 5-S-cysteinyldopamine (CDA). In turn, CDA is an important building block of neuromelanin, a pigment found mainly in the *substantia nigra* of central nervous system. [108,109]

CDA oxidation generates benzothiazine intermediates similar to pheomelanin building blocks by the cyclization of cysteinecatechol conjugates derived from attack of cysteine onto *o*-quinone intermediates.

CDA was prepared by a chemical reaction between dopamine (DA) and cysteine, according to a previously reported method[110] that allows to produce a polymer containing benzothiazine units similar to those found in photoactive red hair pigments.

CDA thin film prepared by Dr. Mariagrazia Iacomino (University of Naples) allowing the polymer (10 mM) to autoxidize in bicarbonate buffer (50 mM, pH 8.5) in the presence of

quartz and glass cuttings. The thin films obtained were characterized by scanning electron microscopy (SEM), tapping mode atomic force microscopy (AFM) analysis and X-ray photoelectron spectroscopy (XPS) as reported.[107]

The ability of pCDA thin films and suspensions to affect autoxidation of GSH and NADH was tested. Data reported in Figure 9 show that both the suspension and the films can accelerate the autoxidation of GSH and NADH in phosphate buffer (pH 7.4), reaching 80% of GSH depletion in less than 3 h.

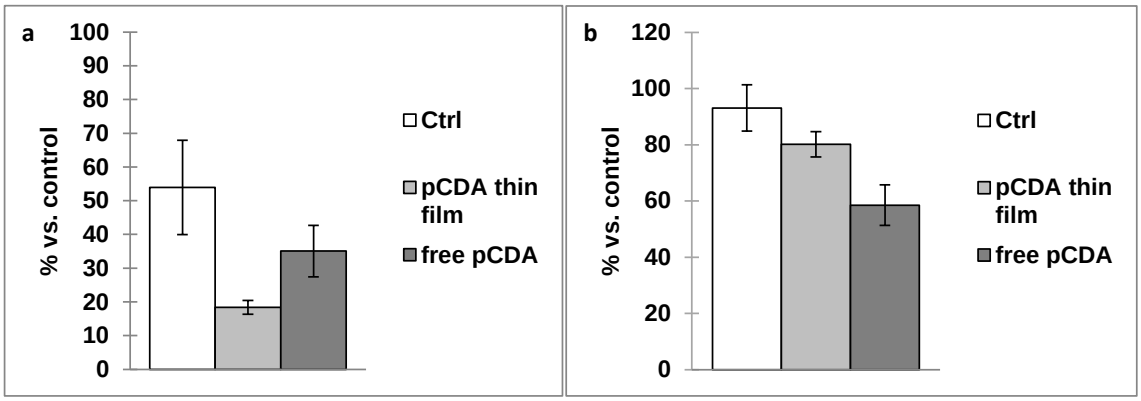

Figure 9. *Effect of pCDA on the autoxidation of GSH at 150 mM (a) and NADH at 300 mM (b) at 3 h reaction time in 0.1 M phosphate buffer pH 7.4 as determined by HPLC-ED/UV. Data are expressed as mean ± SD of three independent experiments, each performed in duplicate.*

In control experiments using pDA the reaction rate was not significantly affected (data not shown). This accelerating effect was not observed under an argon atmosphere, pointing out an essential role of oxygen. Data are in line with the effects of RHP on GSH and NADPH levels, in air equilibrated metal-free buffer,[84] suggesting a redox cycle.

2.4 Pheomelanin pro-oxidant properties: a mechanism from reverse engineering

Another hint suggesting that pheomelanins may contribute to sustaining a chronic oxidative stress condition through a redox buffering mechanism comes from experiments conducted by an electrochemically-based reverse engineering methodology that allows to characterize the functionality of complex technological and biological systems.[111] Pheomelanins and eumelanins pigments isolated from human hair as well model synthetic pigments prepared by enzymatic oxidation of dihydroxyphenylalanine (DOPA) or 5SCD were provided to Professor Gregory F. Payne (University of Maryland) to test their redox activities.

Melanin samples were exposed to complex voltage inputs and output responses were measured. Here is summarized the electrochemical methodology that has been applied:

1) An insoluble melanin sample was entrapped in a non-conducting hydrogel film and was localized near an electrode.
2) Soluble mediators shuttled electrons between the sample and the electrode.[112]
3) Complex input voltages are applied and the potentials were transmitted to the samples through the soluble mediators.
4) Output currents are measured and analyzed to assess melanin redox activity.[113,114]

First model melanins were examined and the results show that even if both eumelanin and pheomelanin are redox-active and can engage in redox-cycling reactions, pheomelanin possess a more oxidative redox potential. Even in the case of natural melanins, a grater pro-oxidant activity is displayed by pheomelanins with respect to eumelanins, suggesting that a redox buffering mechanism is involved in their pro-oxidant activity.

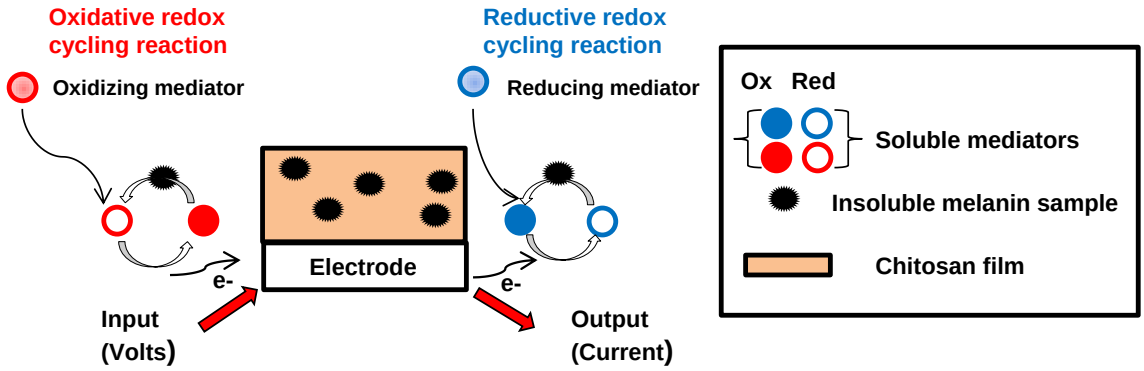

Figure 10. *Scheme of the electrochemical approach to reverse engineer melanin: soluble mediators shuttle electrons between electrode and sample. Complex input voltages are applied while output currents are measure (adapted from Kim et al. 2015).*[115]

CHAPTER 3

3.1 Eumelanin pigments: (photo)protective properties and the origin of the broadband absorption spectrum

Eumelanin synthesis is associated with functionally active melanocortin-1-receptor (MC1R),[1] whose function is regulated by the physiological agonists αMSH and adrenocorticotropic hormone (ACTH) and by one antagonist agouti-signaling protein (ASP).

In wild-type eumelanic subjects, α-MSH stimulates *MC1R* activating the associated G-protein, which in turn activates adenyl cyclase and increases the levels of cellular cyclic adenosine 3',5'-monophosphate (cAMP), responsible for tyrosinase and tyrosinase-related protein-1 and -2 activity.[116,117]

The photoprotective role of eumelanin is commonly accepted however this not restricted to a radiation filtering action, but includes scavenging of free radical species by the pigment itself or its precursors resulting in an antioxidant effect.[60,85,118–124]

Photoprotection and antioxidant properties are closely related biological aspects: actually, oxidative stress, especially if UV induced, is one of the main determinants in carcinogenesis. MC1R and its ligand are also involved in regulation of homeostatic skin function,[117] redox equilibrium[74,125,126] and conservation of genomic integrity.[127–130] In addition, α-MSH is able to decrease intracellular levels of H_2O_2,[74,131,132] to repair DNA photoproducts[10,74,125,133,134] and to phosphorylate p53 in UVR-irradiated melanocytes. Phosphorylation activates p53 reducing the generation of ROS that could damage the DNA and regulating the expression of enzymes involved in base excision repair (BER).[127,129]

The supramolecular structure of eumelanin has been investigated by several studies[87,135–141] and determines the features of this pigment, including the already mentioned photoprotective and antioxidant properties but also the UV energy dissipation mechanism,[120,142] the water dependent ionic-electronic conductivity,[143] and the stable paramagnetic state resulting in a signal in the EPR spectroscopy.[2,144,145]

Most importantly, eumelanins display a broadband absorption spectrum with monotonic wavelength dependence and are able to absorb light and to convert the energy of the absorbed photon in non-photochemical processes. However, the molecular and cellular mechanism of action is not fully explained.[60,146]

The pigment is generally regarded as a heterogeneous polymer of DHI and DHICA linked through diverse bonding patterns[147,148] that confers the pigment a degree of disorder that extends to various levels (Figure 11).

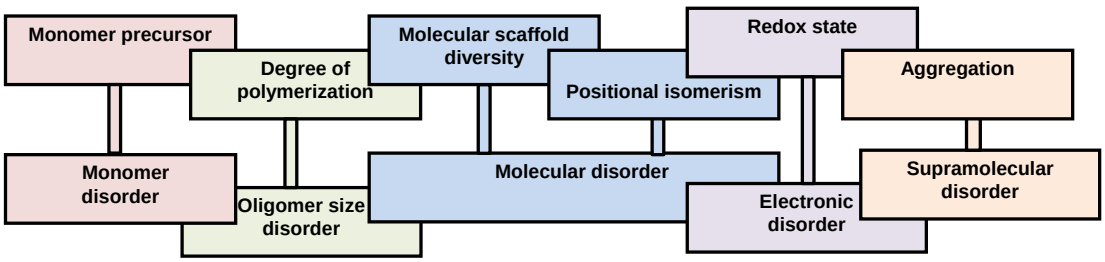

Figure 11. *Main levels of eumelanins disorder.*

The first level is the chemical disorder[149] related to the different coupling mode of DHI and DHICA leading to a variety of oligomeric species that can develop complex ensembles of chromophores spanning the entire UV-visible range.

Electronic disorder instead derives from the coexistence of oxidized and reduced moieties that is essential for the broadband visible-light absorption spectrum, as suggested by data from glycated water soluble eumelanin.[150] According with this study, black color would depend not only on the overlap of π-electron conjugated chromophores[151,152] but even on oxidation state- and aggregation-dependent interchromophoric interactions.

The use of poly(vinyl alcohol) (PVA) to prevent eumelanin precipitation[135] allowed to disentangle absorption properties due to chromophore from scattering effects, pointing out that beside the intrinsic chromophore component there is an extrinsic contribute that depend on intermolecular perturbation[153] of π-electron systems and that is dominant in DHICA melanin, because of the lack of planar conformation.[144,154]

These intrinsic and extrinsic contributes (Figure 12), together with the interaction of geometric order and disorder, would cooperate to generate the absorption spectrum of eumelanin.[155–158]

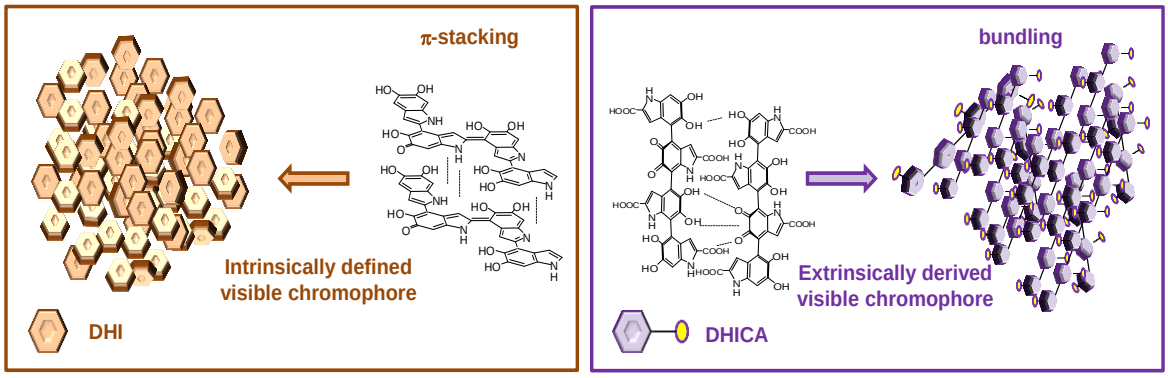

Figure 12. *Intrinsic and extrinsic contributions to eumelanin absorption properties.*

Computational studies suggested that the monotonic spectrum of eumelanin is due to delocalization of excitons over stacked DHI melanin.[156,157] The current view is that the optical eumelanin properties can be mimicked only by including catechol, semiquinone and quinone building blocks.[159]

In order to provide structure-properties relationships underlying the band broadening spectrum and to elucidate the contributions of the different levels of disorders, part of this thesis was directed to investigate and compare a broad collection of eumelanin precursors featuring different substituents, molecular size (monomers and dimers) and shape (isomeric dimers).

The dynamics of band broadening during eumelanin chromophore buildup and the role of chemical disorder were addressed by combining spectrophotometric experiments with computations. In particular, two contributions to chemical disorder were considered: *structural disorder*, reflecting the variety of σ-scaffolds, and *redox disorder*, as determined by catechol-semiquinone-quinone mixing and π-electron perturbations.

3.1.1 The dynamics of eumelanin chromophore evolution

The shielding effect of eumelanin is achieved by its ability to serve as a physical barrier against UVR that reduces the penetration of UV through the epidermis.[1]

On this basis, the development of a picture of the nature and interaction mechanism of individual chromophores underlying eumelanin UV-visible spectrum is of general interest because of its relevance to dissect crucial structure-properties-function relationships.

In order to reach this aim, preliminary experiments were directed at comparing the generation and evolution of chromophores from DHI in the presence and in the absence of 1% PVA, a hydrophilic polymer able to prevent melanin precipitation.

Three oxidizing systems have been used:

- potassium ferricyanide in phosphate buffer at pH 7.0, $K_3[Fe(CN)_6]$, operating by an outer sphere one-electron transfer mechanism (2 molar eq.)
- sodium periodate in phosphate buffer at pH 7.0, $NaIO_4$, operating by the induction of two –electrons oxidations via cyclic esters with catechols (1 molar eq.)
- ceric ammonium nitrate (CAN) in phosphate buffer at pH 3.0, $(NH_4)_2[Ce(NO_3)_6]$, operating by a one-electron transfer mechanism (2 molar eq.)

Oxidant concentration was based on a two-electron oxidation stoichiometry relative to the monomer, formally corresponding to *o*-quinone formation. Monomer consumption was checked by HPLC and was complete under these reaction conditions.

Ferricyanide and periodate induced similar chromophoric changes and evolution kinetics while CAN induced a less intense chromophore, possibly ascribable to the inhibition of deprotonation at acidic pH (Figure 13).

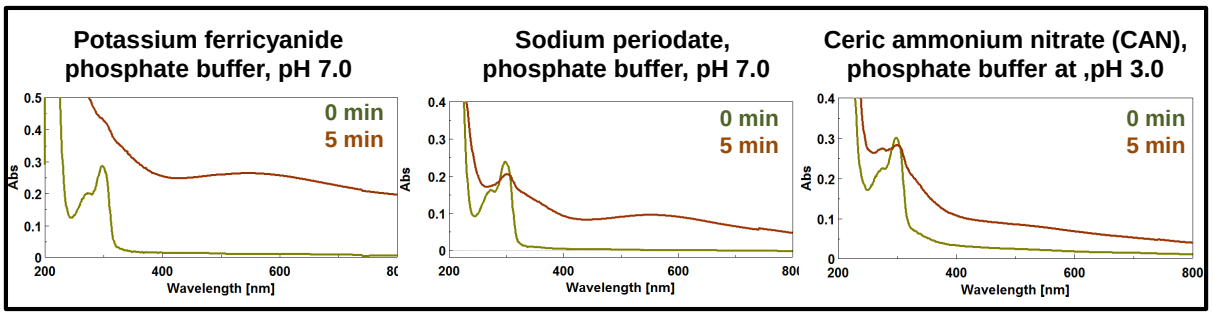

Figure 13. *Generation of chromophores from DHI (50 μM) using different oxidizing systems: potassium ferricyanide in phosphate buffer, pH 7.0, sodium periodate in phosphate buffer at pH 7.0 or ceric ammonium nitrate (CAN) in phosphate buffer at pH 3.0.*

Ferricyanide was selected as the oxidant and oxidations were carried out with DHI and other selected monomers and dimers (Figure 14) at 50 μM concentration.

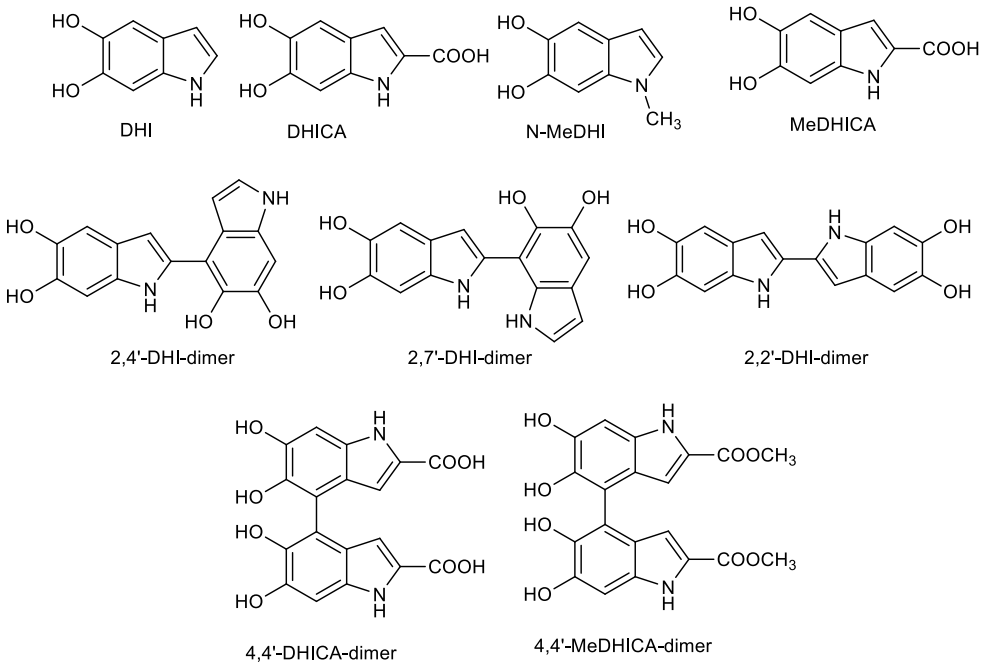

Figure 14. *Structures of monomers and dimers investigated in this thesis.*

Data from DHI oxidation over 24 hours reaction time showed the generation of a broad visible chromophore around 560 nm, named melanochrome, according to an old nomenclature (Figure 15).[16]

Further addition of 2 molar equivalents of potassium ferricyanide did not affect the maximum intensity and the persistence of the chromophore suggested the occurrence of oxidation processes unrelated to chromophoric species.

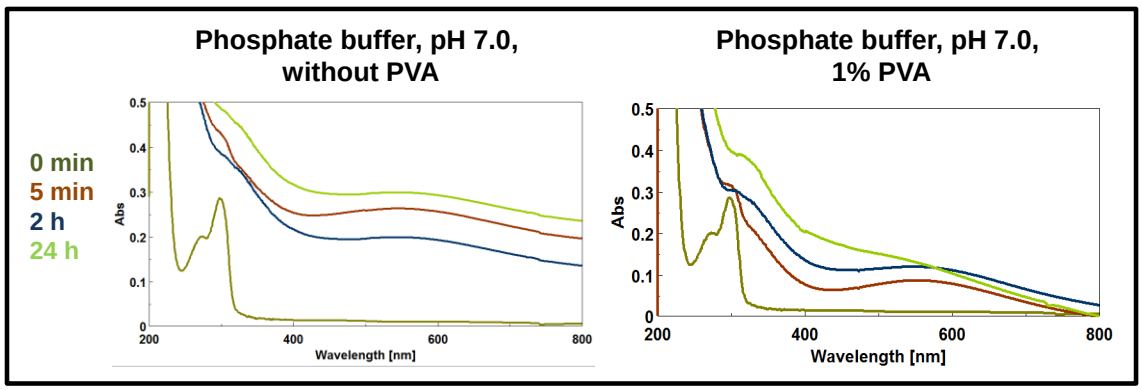

Figure 15. *Generation and evolution of chromophores from DHI (50 μM) oxidation by ferricyanide (2 molar equivalents) in the absence or the presence (b) of 1% PVA.*

In order to quantify scattering contributions to the final spectra, spectra were recorded before and after filtration through a 0.45 micron nylon membrane. Spectra showed that at 5 min the maximum was not detectable in the spectrum of the filtrate.

The oxidation mixtures slowly darkened both in air and under an argon atmosphere due to broadening of the absorption band accompanied by extensive precipitation, as measured by filtration at 24 h. In the presence of 1% PVA melanin precipitation was inhibited at least in part, but melanochrome formation proceeded in a similar manner (Figure 16).

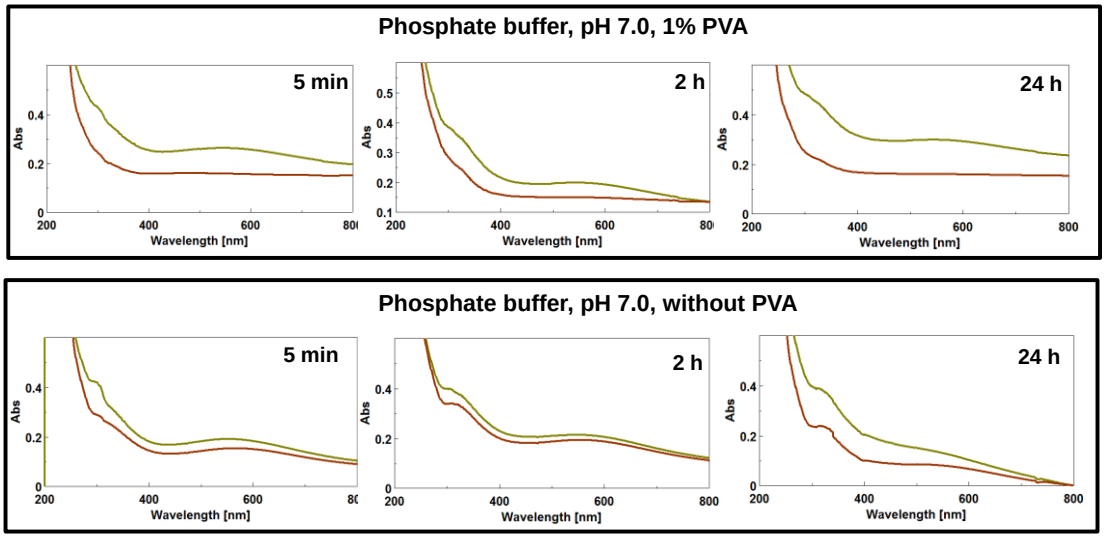

Figure 16. *UV-vis spectra of DHI (50 μM) oxidation mixtures by ferricyanide (2 molar equivalents) in the absence and in the presence of 1% PVA.* ***Green*** *traces were recorded before filtration,* ***brown*** *traces were recorded after filtration.*

We can identify three phases of the chromophore generation and evolution:

I) Fast generation of the melanochrome, whose absorption is mainly due to intrinsic chromophores.[160]

II) Slow band broadening process, mainly due to extrinsic contributions (i.e. intermolecular chromophore perturbations)

III) Melanin precipitation and consequent scattering.

While Phase I depends on the presence of the oxidant, phase II is oxygen independent. PVA allowed to disentangle contribution from phases II and III that would be otherwise superposed.

Digital pictures in Figure 17 show the gradual darkening of the oxidation mixtures and the deposition of melanin pigment. At 5 min, it was possible to observe the development of a bluish coloration due to the melanochrome. These comparative pictures allow to evaluate the effects of the presence of PVA on phase III.

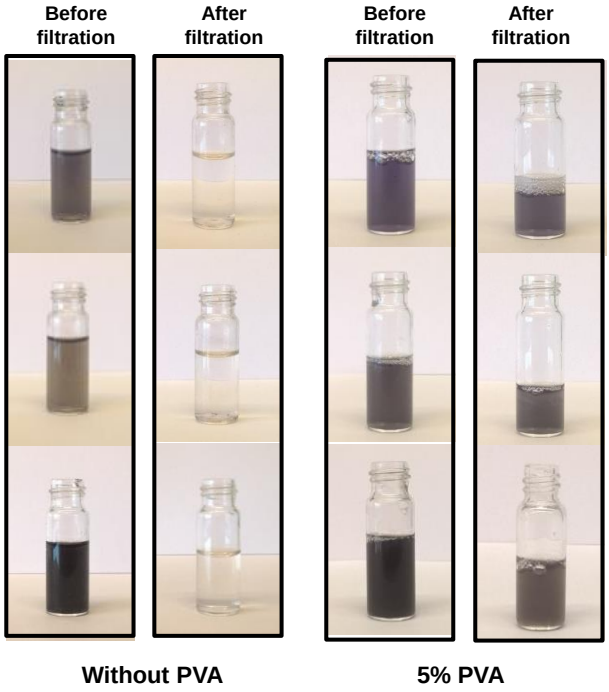

Figure 17. *Digital pictures of the oxidation mixtures obtained by ferricyanide oxidation of DHI (500 μM) over 24 h in the absence and in the presence of 5% PVA.*

In order to examine the effect of ring substituents on the dynamics of DHI polymerization, the same experiment was performed on N-methyl derivative of DHI (N-MeDHI), DHICA and MeDHICA..

The effect of the methyl group is negligible and the spectra are similar in case of DHI and N-MeDHI (Figure 18).

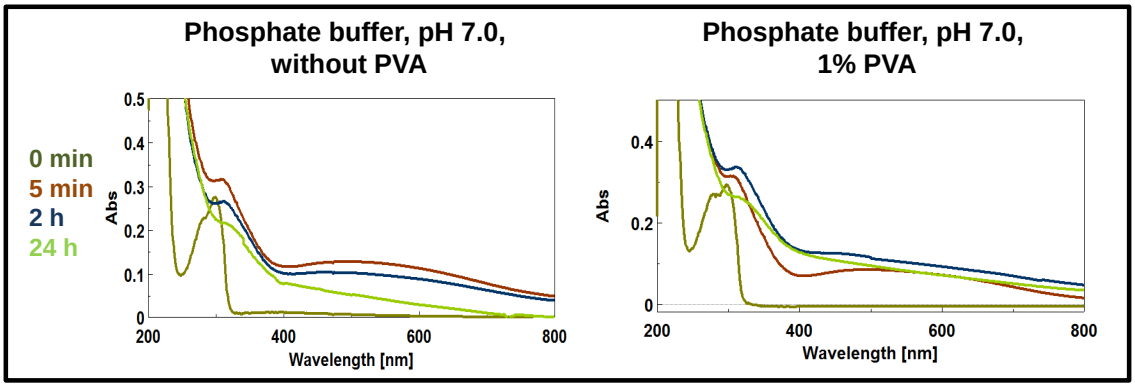

Figure 18. *Generation and evolution of chromophores from N-MeDHI (50 µM) oxidation by ferricyanide (2 molar equivalents) in the absence or in the presence of 1% PVA.*

In the case of DHICA a deep violet chromophore broadly centered between 500-550 nm and a well-defined UV absorbing band around 330 nm were observed both in the presence and in the absence of PVA (Figure 19). Spectra recorded at 5 min and 2 h showed that the inhibition of aggregation due to PVA delayed the decay of melanochrome.

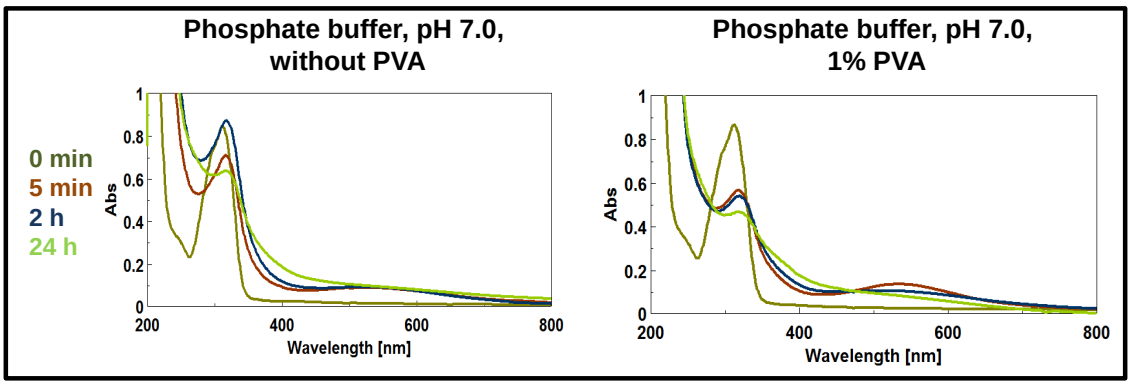

Figure 19. *Generation and evolution of chromophores from DHICA (50 µM) oxidation by ferricyanide (2 molar equivalents) in the absence or in the presence of 1% PVA.*

Digital pictures before and after filtration, in the presence and in the absence of PVA, confirmed the role of aggregation in color development (Figure 20).

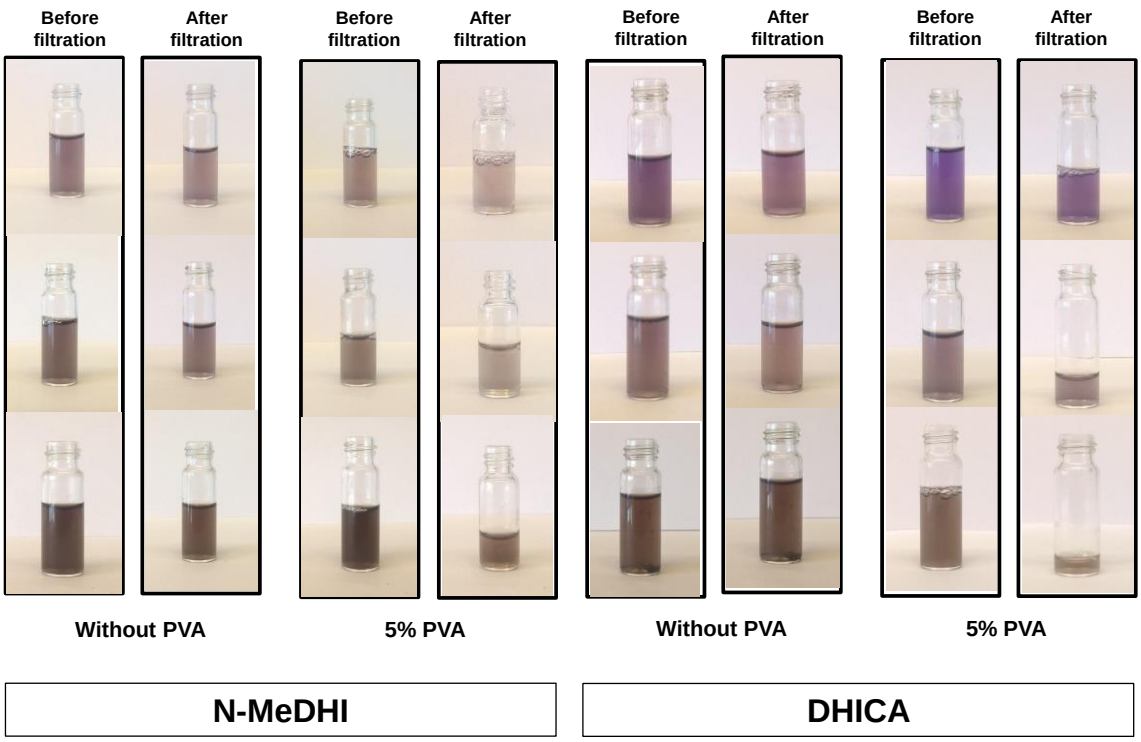

Figure 20. *Digital pictures of the oxidation mixtures obtained by ferricyanide oxidation of N-MeDHI or DHICA (500 μM) over 24 h in the absence and in the presence of 5% PVA.*

Differently from what observed in the case of DHICA, ferricyanide oxidation of MeDHICA did not lead to chromophores in the visible region nor appreciable rise of scattering (Figure 21).

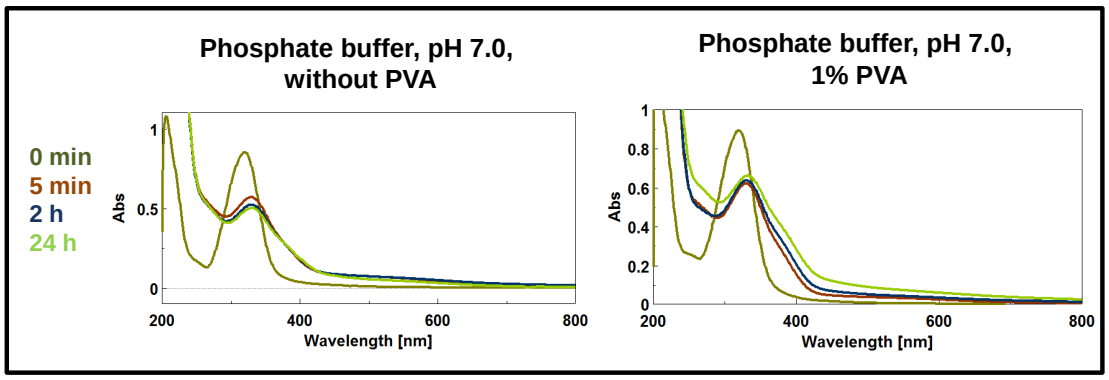

Figure 21. *Generation and evolution of chromophores from MeDHICA (50 μM) oxidation by ferricyanide (2 molar equivalents) in the absence or in the presence of 1% PVA.*

The lack of aggregated unsoluble materials was also confirmed by filtration that did not induce substantial modification of the chromophore intensity (Figure 22).

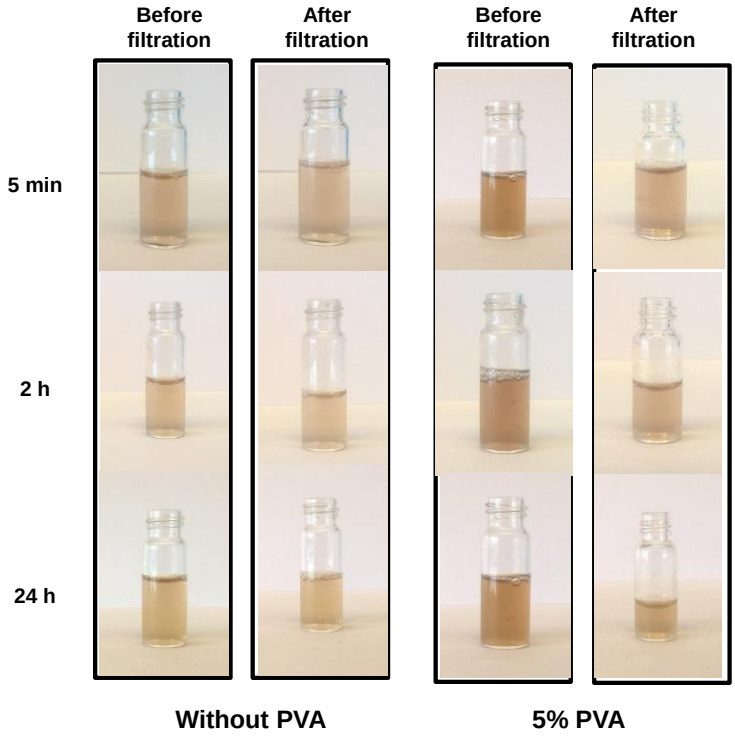

Figure 22. *Digital pictures of the oxidation mixtures obtained by ferricyanide oxidation of MeDHICA (500 μM) over 24 h in the absence and in the presence of 5% PVA.*

A complete set of the UV spectra recorded for N-MeDHICA, DHICA and MeDHICA is shown in Figure 23-25.

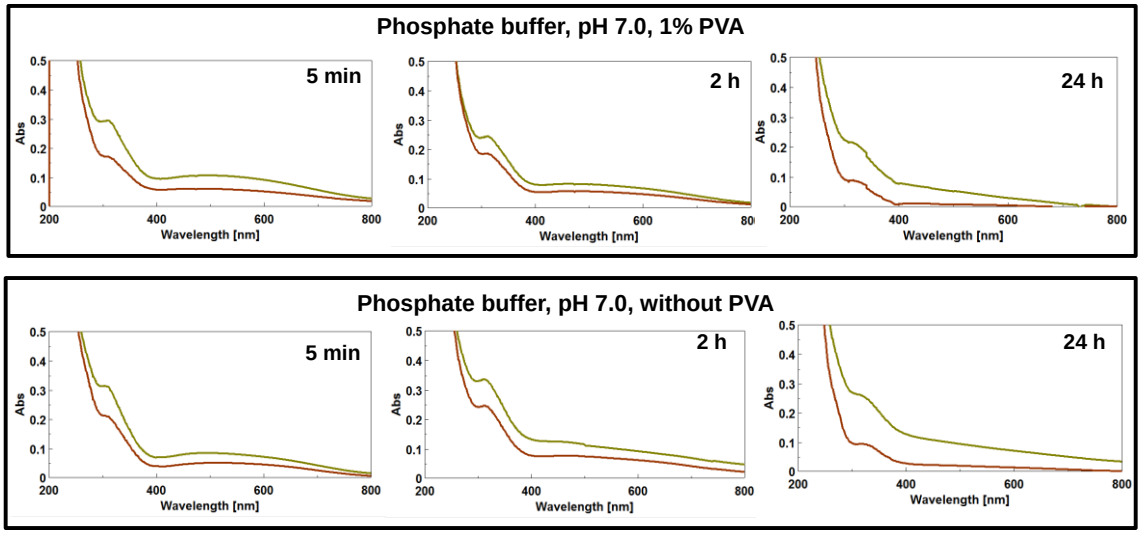

Figure 23. *UV-vis spectra of N-MeDHI (50 μM) oxidation mixtures by ferricyanide (2 molar equivalents) in the absence and in the presence of 1% PVA.* ***Green*** *traces were recorded before filtration,* ***brown*** *traces were recorded after filtration.*

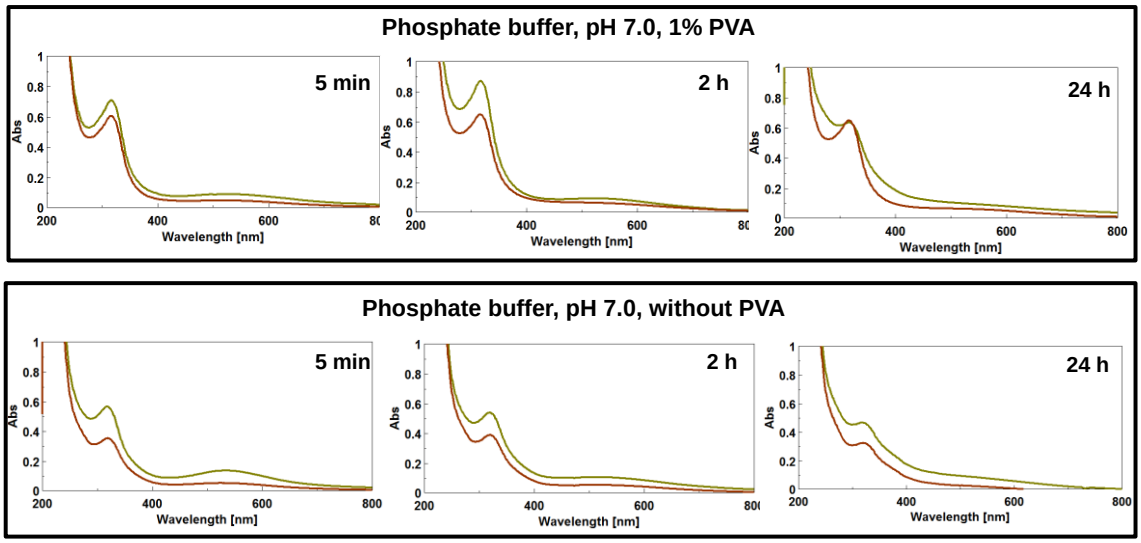

Figure 24. *UV-vis spectra of DHICA (50 μM) oxidation mixtures by ferricyanide (2 molar equivalents) in the absence and in the presence of 1% PVA.* ***Green*** *traces were recorded before filtration,* ***brown*** *traces were recorded after filtration.*

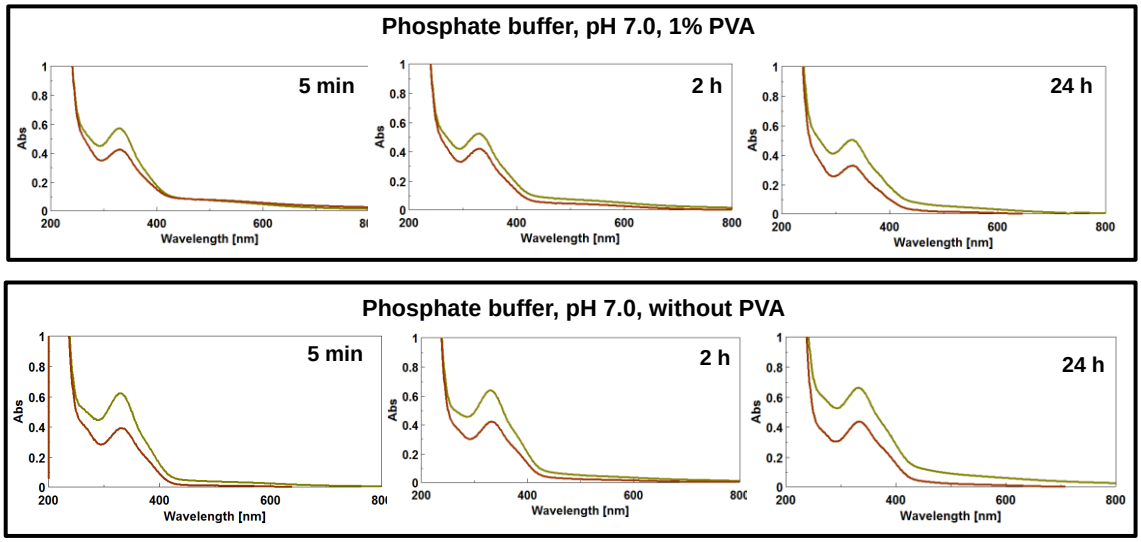

Figure 25. *UV-vis spectra of MeDHICA (50 μM) oxidation mixtures by ferricyanide (2 molar equivalents) in the absence and in the presence) of 1% PVA.* ***Green*** *traces were recorded before filtration,* ***brown*** *traces were recorded after filtration.*

3.1.2 The role of structural disorder

In order to assess the effect of molecular disorder, depending on molecular weight dispersion and molecular diversity, the course of oxidation of dimers was examined and compared to that of the corresponding monomers.

The molecular weight dispersion was decreased by the use of dimers as substrate, as only even-numbered oligomers are possible under these conditions.

The variety of scaffolds produced within each oligomer population was lower because of the inherent constraint posed by the interring bond.

The chromophores generated in the first phase by the isomeric 2,4'-, 2,7'- and 2,2'-dimers of DHI both in the presence and in the absence of PVA were different (Figure 26).

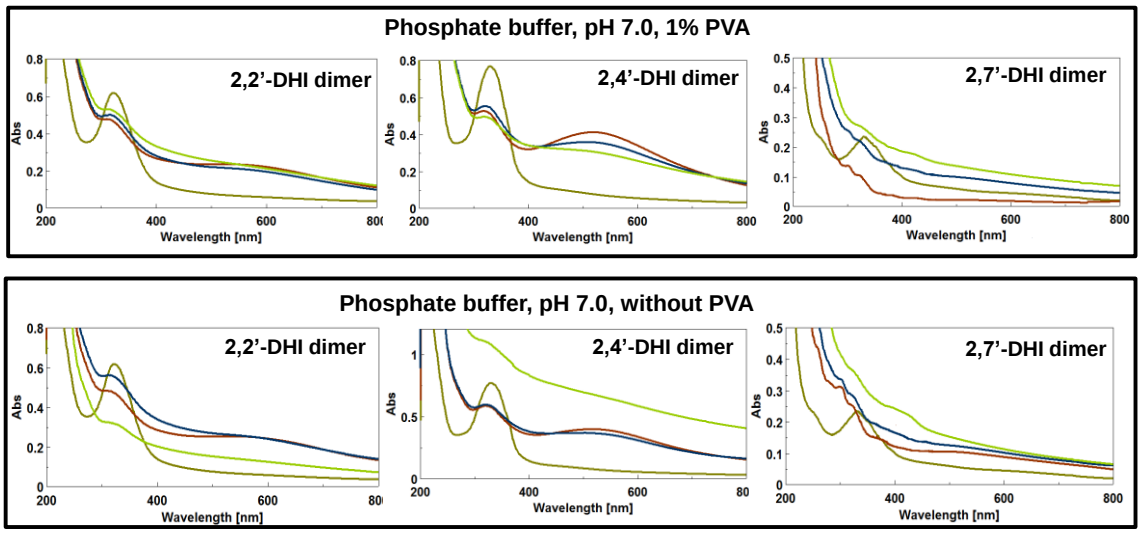

Figure 26. *UV-vis spectra of 2,2'-, 2,4'- and 2,7'-dimers of DHI (50 μM) oxidation mixtures by ferricyanide (2 molar equivalents) in the absence and in the presence of 1% PVA.*

The almost overlapping traces recorded at 5 min, 2 h and 24 h in the absence of PVA, suggest that the evolution of the melanochrome is faster in the case 2,2'- dimer. It is so reasonable that the way the indole units are bound is more important than the decrease of molecular weight dispersion and this influence is stronger in the first phase of the chromophore evolution.

Comparing the spectra of the oxidation mixture of 4,4'-DHICA dimer with those of the relative monomer, it appears that the melanochrome evolution is faster (Figure 27). Similar was also the course of the oxidation of the 4,4'–dimer compared to the monomer (not shown).

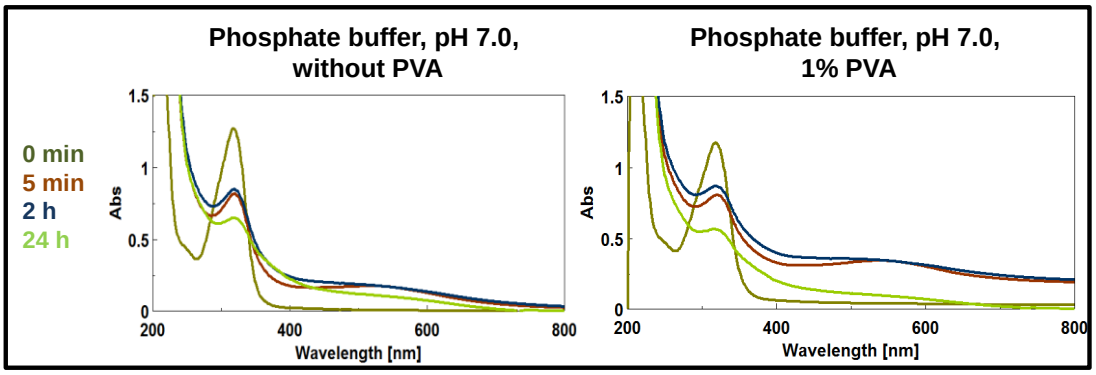

Figure 27. *Generation and evolution of chromophores from 4,4'-DHICA (50 μM) oxidation by ferricyanide (2 molar equivalents) in the absence or in the presence of 1% PVA.*

A complete set of the UV spectra recorded for 2,4'-, 2,7'- and 2,2'-dimers of DHI and for the 4,4'-dimer of DHICA is shown in figures 28-31.

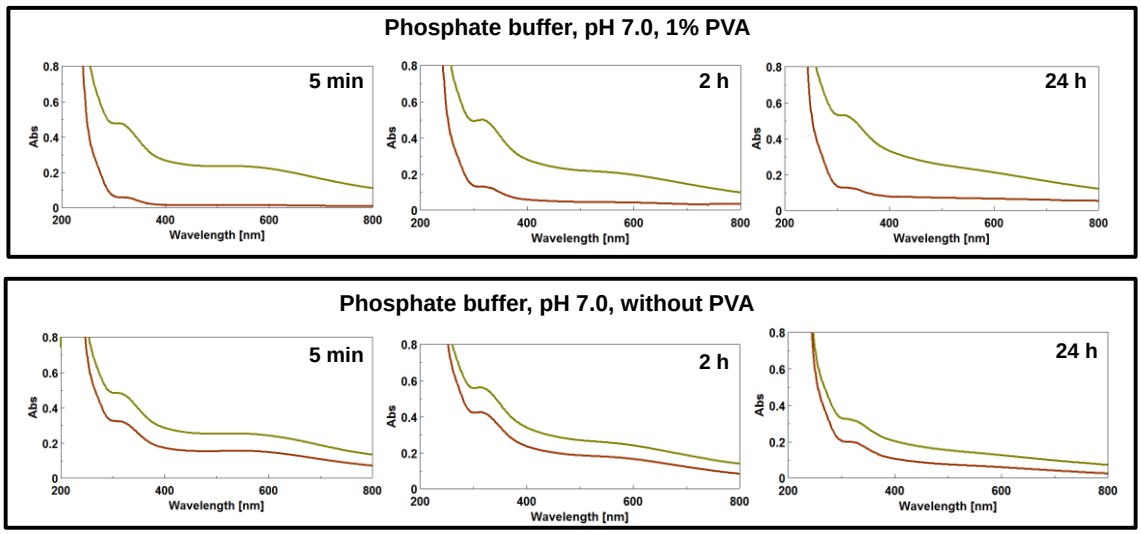

Figure 28. *UV-vis spectra of 2,2'-dimers of DHI (50 μM) oxidation mixtures by ferricyanide (2 molar equivalents) in the absence (a) and in the presence (b) of 1% PVA.* ***Green*** *traces were recorded before filtration,* ***brown*** *traces were recorded after filtration.*

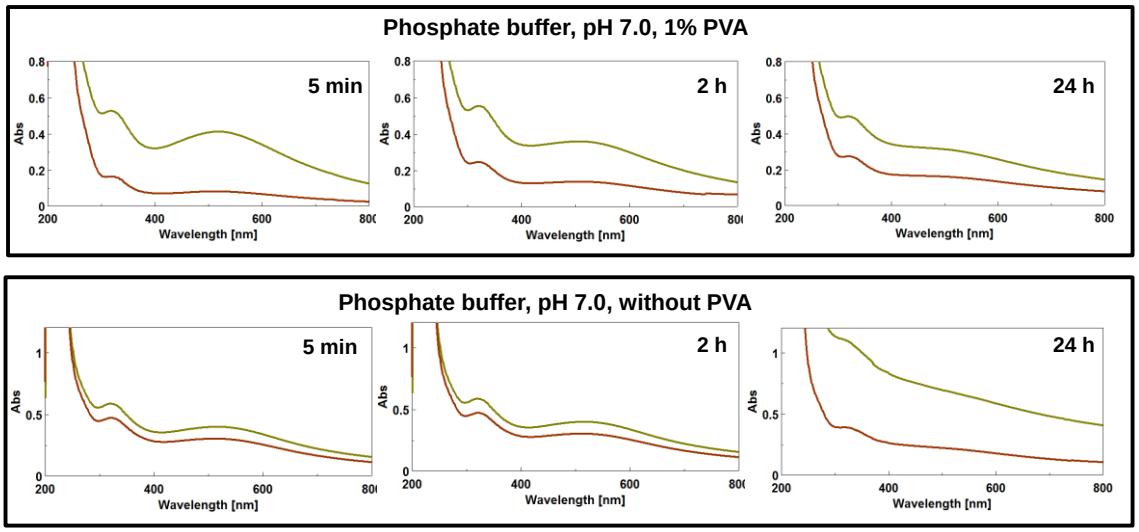

Figure 29. *UV-vis spectra of 2,4'-dimers of DHI (50 μM) oxidation mixtures by ferricyanide (2 molar equivalents) in the absence (a) and in the presence (b) of 1% PVA.* ***Green*** *traces were recorded before filtration,* ***brown*** *traces were recorded after filtration.*

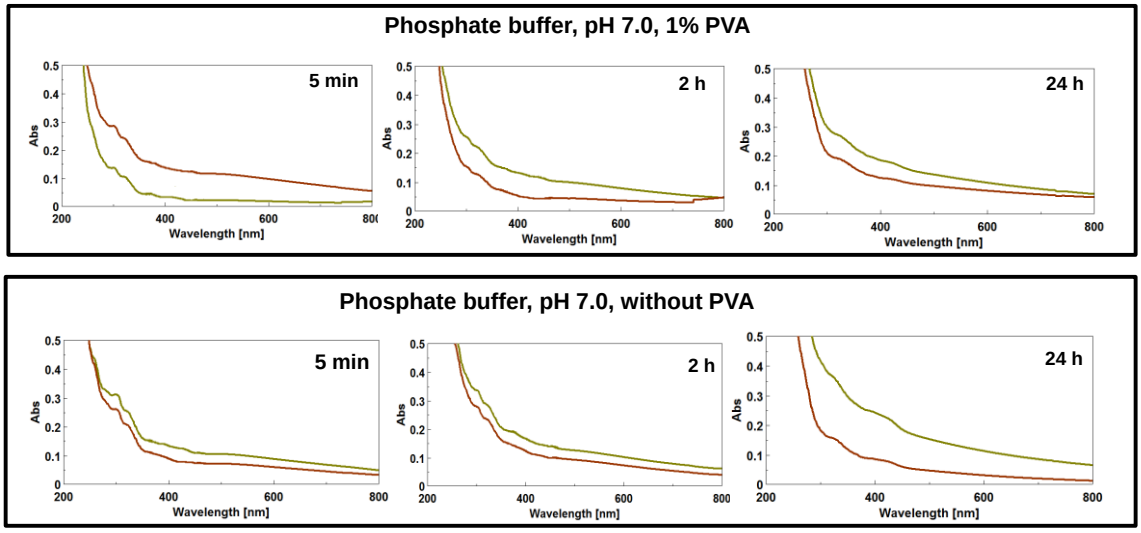

Figure 30. *UV-vis spectra of 2,7'-dimers of DHI (50 μM) oxidation mixtures by ferricyanide (2 molar equivalents) in the absence and in the presence of 1% PVA.* ***Green*** *traces were recorded before filtration,* ***brown*** *traces were recorded after filtration.*

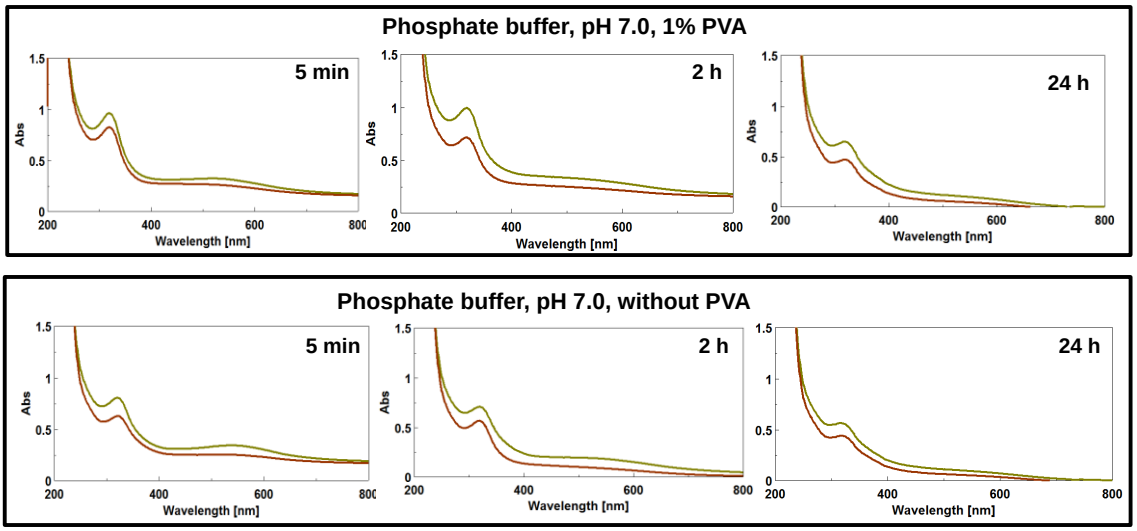

Figure 31. *UV-vis spectra of 4,4'-dimer of DHICA (50 μM) oxidation mixtures by ferricyanide (2 molar equivalents) in the absence (and in the presence of 1% PVA. **Green** traces were recorded before filtration, **brown** traces were recorded after filtration.*

To compare the shapes of the final spectra of the dimers with those of the monomers, absorbance data at fixed visible wavelengths were normalized against the UV band at 300 nm and the resulting traces were matched against the theoretical monotonic profile (Figure 32).

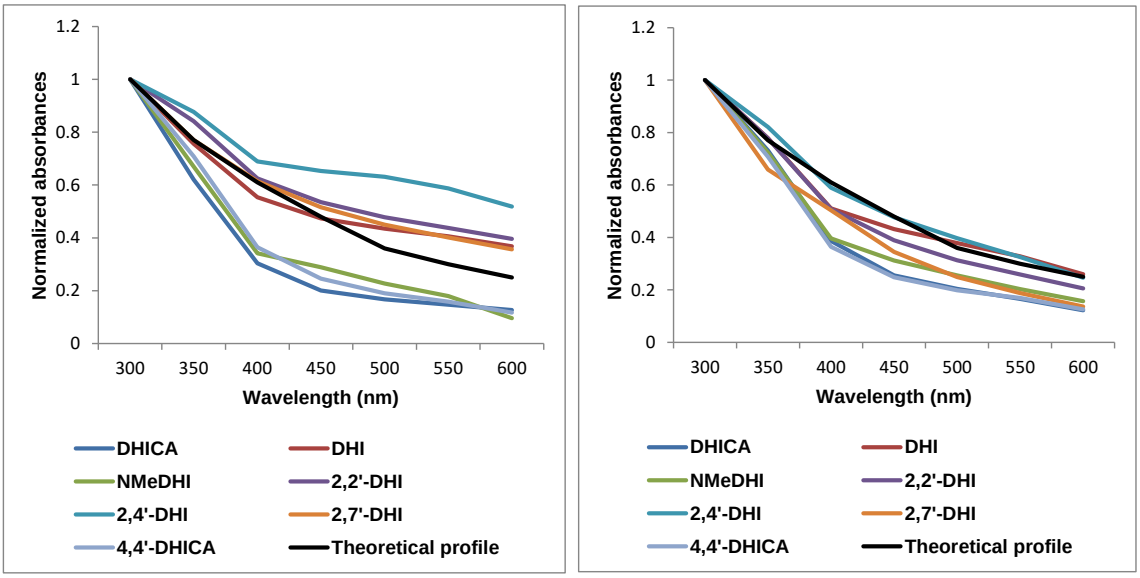

Figure 32. *Relative absorbance of the oxidation mixtures of the indole compounds at 24 h over the UV-visible region in the absence (left) and in the presence of 1% PVA (right). Values normalized against the absorbance at 300 nm for each mixture.*

DHICA and its dimer show a similar trend while the traces for DHI and its dimers are different, with more marked differences in the presence of PVA. The intensity of the visible chromophore decrease in the order 2,4'- > 2,2'- > 2,7'-isomers.

To complete the picture of eumelanin formation, the course of oxidation mixtures of 3,4-dihydroxyphenylalanine (DOPA) and dopamine (DA) were investigated. Since DHI and DHICA are produced from these catecholamines precursors by a 4-electrons oxidation process, 6 molar equivalent of potassium ferricyanide were used (Figure 33). These absorption profiles substantially lack the maximum due to melanochrome formation. The absorption in the visible range for DA is lower compared to DOPA, on account of its lower tendency to cyclize. The absorption maximum at around 420 nm observed in the spectra taken at 5 min is due to residual ferricyanide.

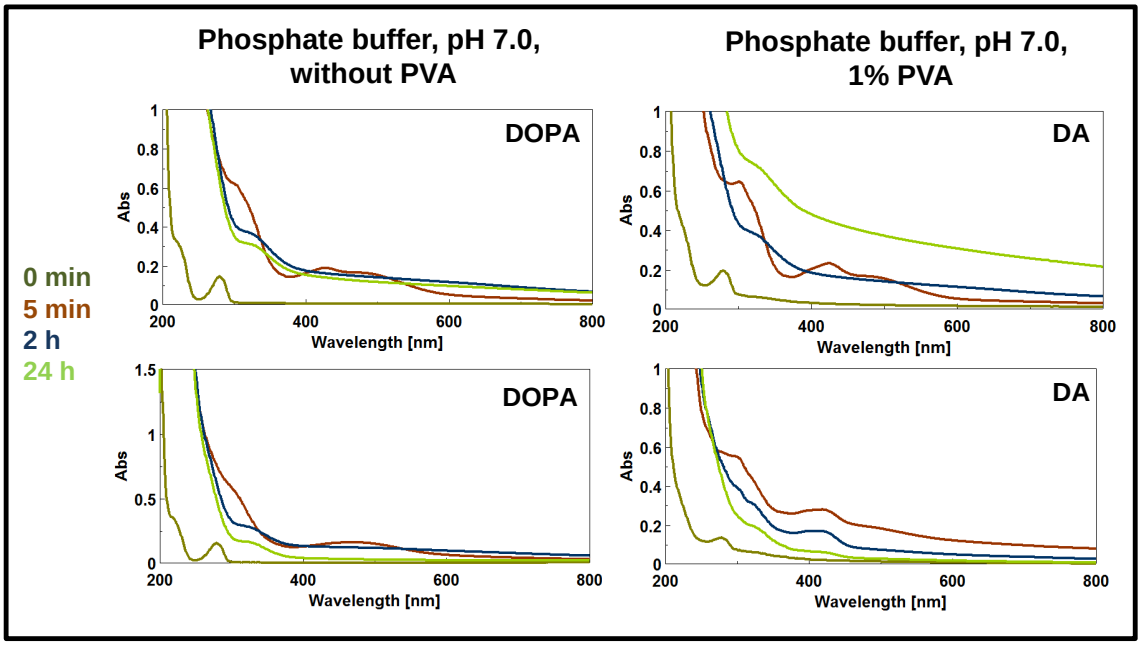

Figure 33. *Generation and evolution of chromophores from DOPA or DA (50 μM) oxidation by ferricyanide (6 molar equivalents) in the absence or in the presence of 1% PVA.*

Formal extinction coefficients (ε_f), were determined at 450, 550 and 650 nm for the chromophores produced at different reaction times in the presence of PVA.

$$\varepsilon_f = A/lc$$

(A is the absorbance, c is the initial monomer concentration and l is the optical path in cm)

Table 1. *Formal extinction coefficients at different wavelengths and reaction times of the eumelanin chromophores investigated.*					
Precursor (50 μM)	ε_f (450)	ε_f (550)	ε_f (650)	**ε_f ratio** 550/450	**ε_f ratio** 650/550
5 min					
DHI	2460	2909	2343	1.18	0.81
DHICA	1788	2618	1176	1.46	0.45
DOPA	3059	1267	256	0.41	0.20
DA	2589	1419	440	0.55	0.17
2 h					
DHI	3210	3369	2787	1.05	0.83
DHICA	1957	1990	1212	1.02	0.61
DOPA	3106	2478	1956	1.62	0.79
DA	1529	661	306	0.43	0.20
24 h					
DHI	3423	2603	1467	0.76	0.56
DHICA	2304	1493	705	0.65	0.47
DOPA	4042	2441	1316	0,60	0.54
DA	1915	967	344	0.50	0.36

a) DHI melanin exhibits higher formal extinction coefficients than those of DHICA melanin at 650 nm.

b) 650/550 nm coefficient ratios for DHICA are invariably lower than for DHI at each time;

c) 550/450 nm and 650/550 nm ratios at 5 min, show respectively higher and lower values in the case of DHICA compared to DHI. This can be considered an index of melanochrome intensity and it is consistent with a more defined band shape.

d) The 550/450 nm coefficient ratio decreases passing from 5 min to 2 h while 650/550 nm ratio increases. This can considered an index of band broadening.

Lower extinction coefficient at 5 min at 550 nm than DHI confirms the important role of the carboxyl group in DHICA in inhibiting the development of the visible chromophore at all three phases. Moreover, DHICA chromophore is more defined than that of DHI.

3.1.3 The role of redox disorder

The possible occurrence of each structural component at different oxidation levels would imply a redox disorder. If we consider a dimer, each isomer can exists in the entire gradational range of redox states comprised between the fully reduced (4 H) species and the oxidized fully quinonoid species (0 H), so n+1 redox species (with n = number of OH groups) are possible.

Experiments aimed at probing susceptibility of eumelanin final chromophore to modification by oxidant or reducing oxidant, can give indirect information about the average redox state

The addition of sodium dithionite or sodium borohydride to eumelanin samples produced in the presence of PVA caused a detectable decrease in the visible absorption (Figure 34).

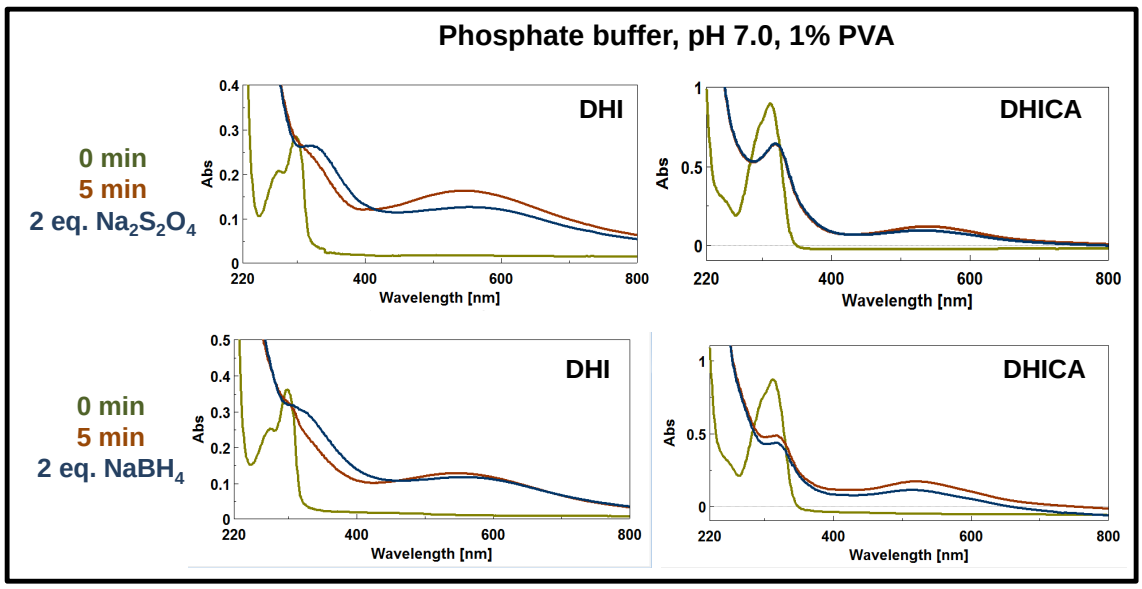

Figure 34. *Effect of addition of sodium dithionite or sodium borohydride to the oxidation mixtures of DHI or DHICA in the presence of 1% PVA.*

Despite the failure to attain complete color suppression, quinonoid species seem to be important determinants of the visible chromophores. It is worth noting that the PVA chain coin could hindered the action of the reductant so separate experiments carried out in the absence of PVA using an excess of reductant agents, showed comparable decrease of the absorption in the visible region.

Acidification to pH 2 caused a detectable ipsochromic shift of the visible chromophore of eumelanins and a bathochromic shift of the UV band (Figure 35). Alkalinization of the

oxidation mixtures induced no detectable change. Chromophoric species seem to be present in an ionized quinonoid form at neutral pH.

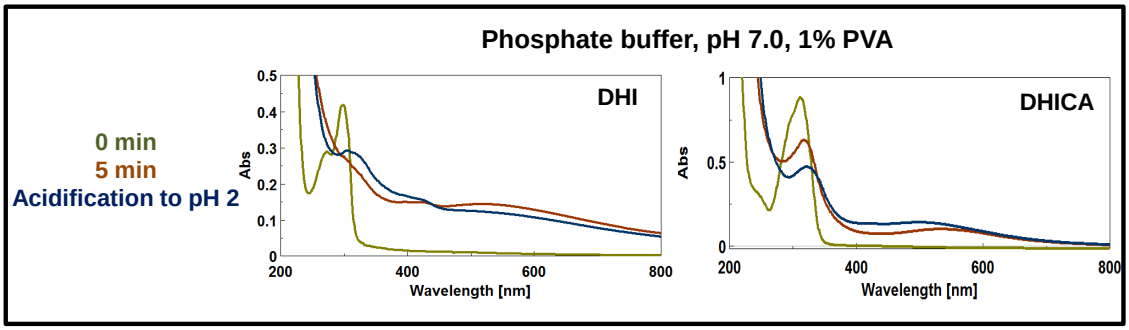

Figure 35. *Effect of acidification on the chromophores of DHI or DHICA oxidation mixtures (50 μM).*

These experiments overall confirmed the fundamental contribution of oxidized quinonoid units to eumelanin chromophore.

In a final set of experiments eumelanin samples prepared by ferricyanide oxidation of DHI or DHICA were exposed to the same concentration of the relevant monomer both in the presence or in the absence of PVA.

The addition of DHICA to the DHICA melanin and the addition of DHI to DHI melanin did not induce significant monomer conversion or chromophore change, suggesting the lack of redox activity for both the melanins (Figure 36).

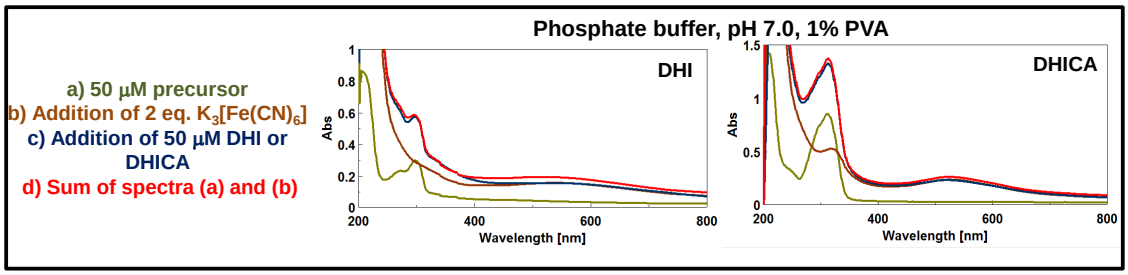

Figure 36. *Effect of addition of DHI and DHICA at 50 μM to the respective melanin generated in the presence of 1% PVA.*

In order to confirm the hypothesis that DHICA generates a poorly delocalized intrinsic chromophore and to prove the generation of extrinsic visible chromophores via intermolecular interaction of dimers from DHI and DHICA at different oxidation levels, computational studies were carried out in collaboration with the Institute of Chemistry of Organometallic

Compounds (ICCOM-CNR) and the Department of Chemistry and Industrial Chemistry of University of Pisa (Italy).

Preliminary calculations agree with experimental data[154,160] and confirm lack of visible absorption both in the case of DHI and DHICA monomers and dimers in the reduced catechol form (**HQ**), while the calculated spectra of the 2-electron oxidation products (**Q**) of DHI and DHICA dimers are different.

To consider the possible role of non-covalent intermolecular interactions between the intrinsic chromophores[157,161] a number of stacked configuration were assembled, for each of the investigated dimers, taking into account the coexistence[150,160] and the approach to each other of reduced and oxidized forms.

Three stacked conformers for each investigated species were selected after evaluating the reliability and accessibility of the possible conformations and their absorption spectra computed at TD-DFT level.

All **Q** forms of DHI dimers exhibit intense visible bands, that is particularly evident in the case of the planar 2,2' dimer (according with the evolution of chromophore in the absence of PVA), suggesting a strong influence of the stacking with a red-shift of main bands accompanied, especially at short stacking distances, by broadening and increased low-energy absorption. The same effect of band broadening was observed in the case of optimized geometry of the 2,4'-dimer.

A remarkable effect due to stacking was predicted for the DHICA dimer. The spectrum of the **HQ**/**Q** complex obtained by approaching the dimers is different from the spectra of separated **HQ** and **Q** forms (virtually superimposable) and displays a marked bathochromic shift in the UV band.

These data support the existence of stabilizing intermolecular interactions causing the appearance of low energy transitions in the visible range.

As a further insight in the chromophore development from oxidation of the indoles so far investigated and their dimers in a further series of experiments autooxidation was run in the presence of some biologically relevant metal ions. The oxidation was carried out in (4-(2-hydroxyethyl)-1-piperazineethanesulfonic acid) (HEPES) buffer at pH 7.5 in the presence of equimolar amounts of zinc, copper and iron ions. The course of the oxidation reaction was followed spectrophotometrically using the substrate at 50 μM concentration (Figure 37-40).

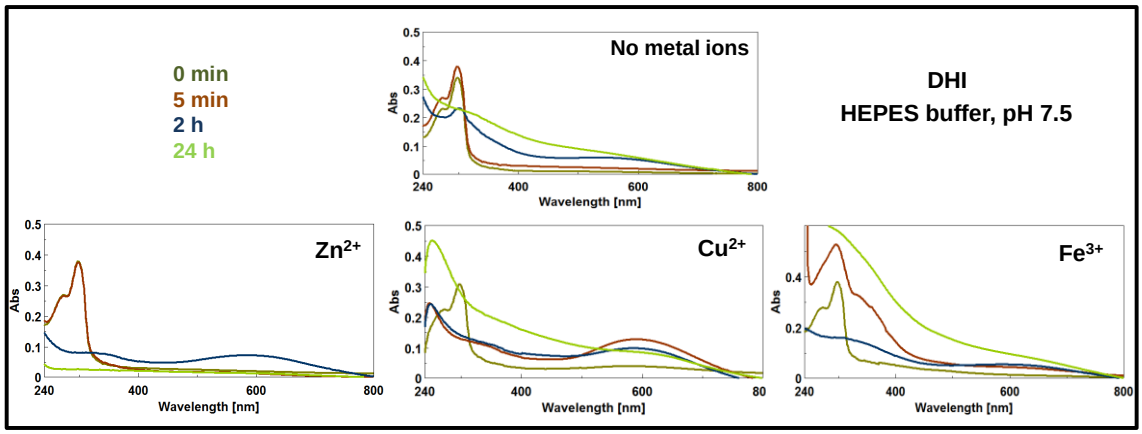

Figure 37. *Generation of chromophores from DHI in the presence and in the absence of 1 molar equivalent of* Zn^{2+} *or* Cu^{2+} *or* Fe^{3+}.

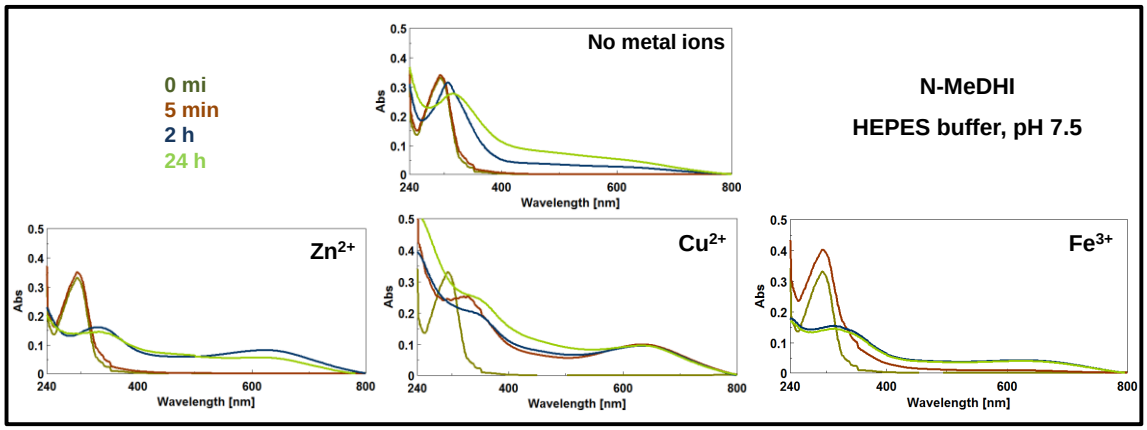

Figure 38. *Generation of chromophores from N-MeDHI in the presence and in the absence of 1 molar equivalent of* Zn^{2+} *or* Cu^{2+} *or* Fe^{3+}.

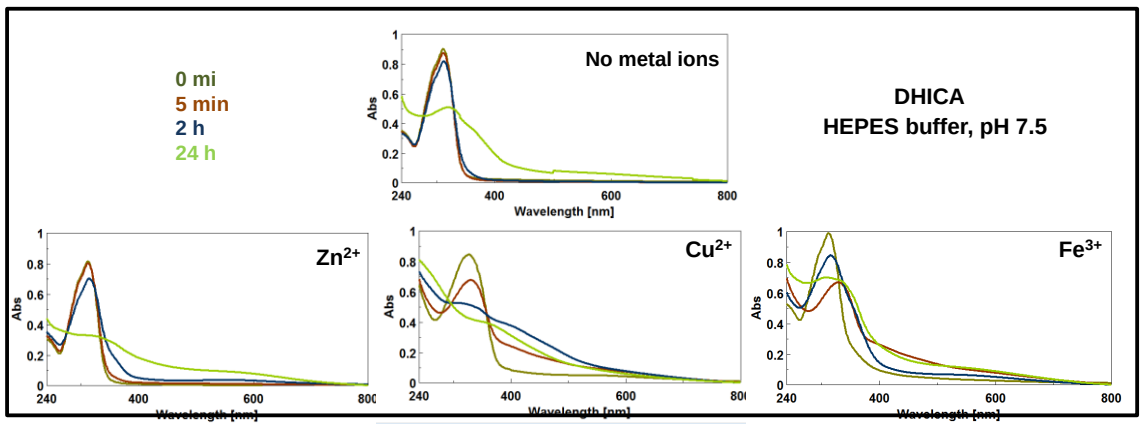

Figure 39. *Generation of chromophores from DHICA in the presence and in the absence of 1 molar equivalent of* Zn^{2+} *or* Cu^{2+} *or* Fe^{3+}.

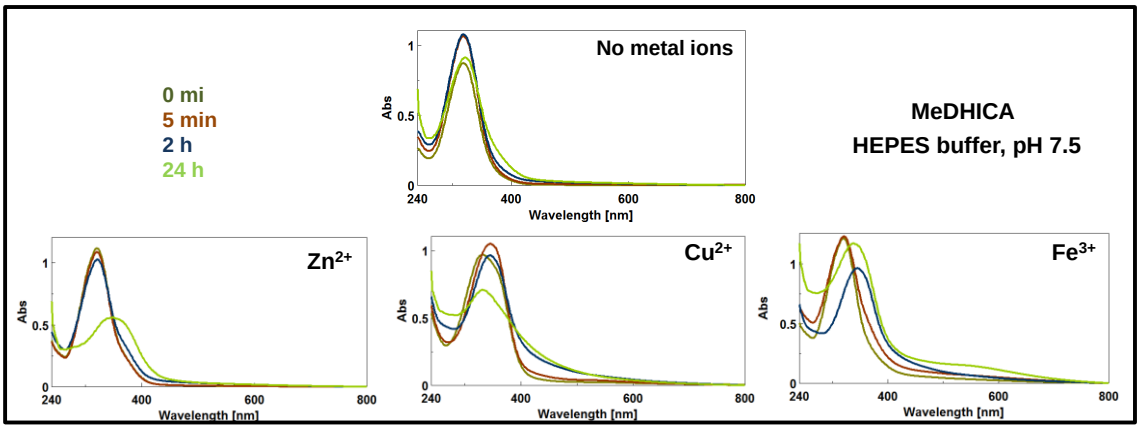

Figure 40. *Generation of chromophores from MeDHICA in the presence and in the absence of 1 molar equivalent of* Zn^{2+} *or* Cu^{2+} *or* Fe^{3+}.

Intense chromophores in the visible region are associated to the oxidation catalyzed by metal ions. DHI and Me-DHI gave rise to more intense absorptions in the visible range under all the oxidation conditions. DHICA developed a visible chromophore only in the metal catalyzed oxidation whereas MeDHICA did not under any oxidation condition. Differently from what observed with zinc, copper and iron proved able to induce the decay of all the monomers within a few minutes suggesting a redox exchange rather than aerobic oxidation. Purple to blue colors were observed for the reaction in the presence of copper in the case of both DHI and N-MeDHI, that are likely to arise from chelates of dimers or higher oligomers. By contrast in the presence of iron a brownish color prevailed. This is also well apparent in Figure 41 showing the colors of the oxidation mixtures in the presence of copper and iron ions at 10 min reaction time with the substrates at 100 μM. When treated with a reducing agent as sodium dithionite a complete discharge of the visible chromophore was observed for both DHI and DHICA with either metal ions suggesting that the chromophore derive from quinonoid forms of dimers or oligomers possibly stabilized by the metal ions.

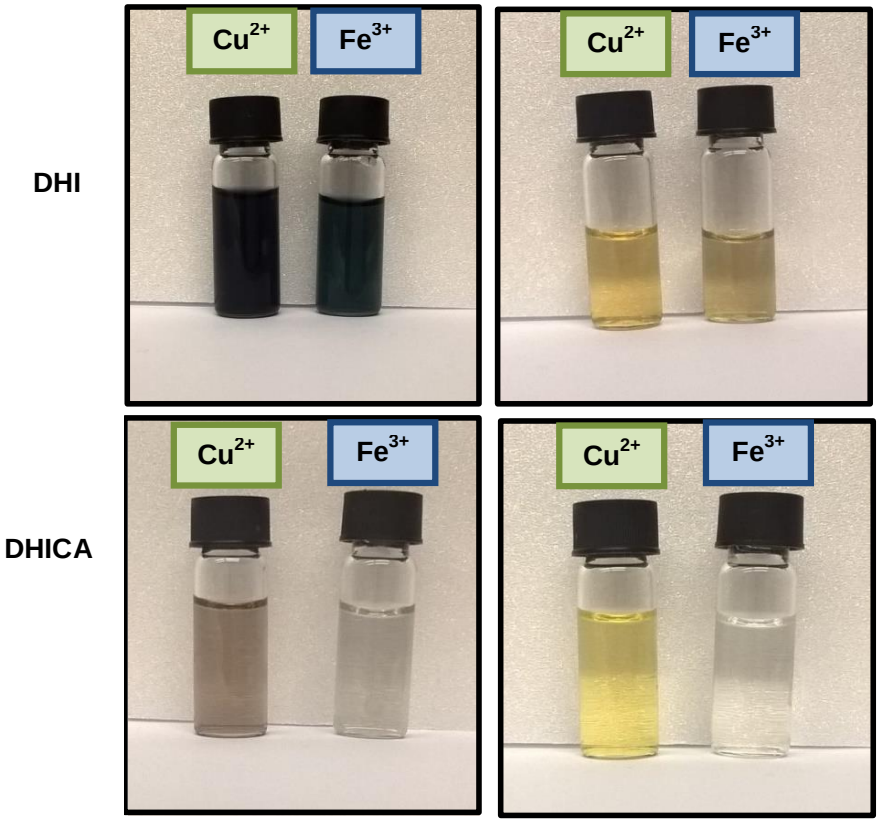

Figure 41. *Color of the oxidation mixtures of DHI or DHICA in the presence of equimolar metal ions with the substrate at 100 µM Left: at 10 minutes reaction time; Right: soon after addition of excess dithionite.*

A comparison of the course of the oxidation of monomers versus dimers for N-MeDHI, DHI and MeDHICA is shown in Figure 42. As representative dimers, the 2,2'- and 2,7'-biindolyl were chosen for DHI and the 4,4'-isomer for Me-DHICA.

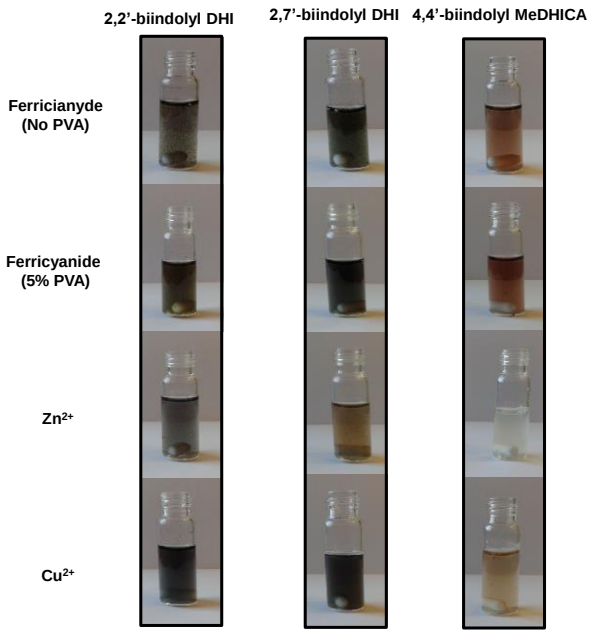

Figure 42. *Oxidation mixtures of 0.25 mM dimers of DHI and Me-DHICA under different reaction conditions, namely 1 min ferricyanide oxidation in the presence or in the absence of 5% PVA and metal catalyzed 10 min oxidation.*

These experiments indicate that the presence of metal ions is an important determinant of transient and final chromophores and color properties. Redox active metals can induce rapid formation of visible chromophores likely due to quinonoid dimer/oligomer species that survive in the reaction mixture thanks to the stabilization provided by metal chelation.

3.2 Antioxidant and other biological properties of indole precursors with special reference to DHICA

Besides eumelanin pigments, the entire eumelanogenic pathway is relevant to melanocyte function.[162] While *in vitro* eumelanin synthesis envisages the spontaneous decarboxylation of dopachrome to DHI,[163] *in vivo* the intervention of the enzyme dopachrome tautomerase (Dct or tyrosinase-related protein Tyrp 2) directs eumelanin synthesis to the formation of DHICA.[35,154,164] The outcome is that while synthetic eumelanin contain about 10% of DHICA-derived units, natural eumelanin is made up of more than 50% of DHICA-derived units,[165] as estimated by the ratio of 2,3-dicarboxylic acid (PDCA) to PTCA upon alkaline hydrogen peroxide oxidation (markers of DHI- and DHICA-derived units, respectively).

Dct is an enzymatic protein displaying significant homology with tyrosinase and together with tyrosinase-related protein Tyrp 1 is involved in melanogenesis in animals.

This enzyme modulates melanocyte response to oxidative stress. Its expression is involved in increase of GSSH levels in WM35 cells, with concomitant protection from free-radical induced DNA damages,[166]

Dct overexpression is associated with an increased resistance of melanoma cells to radiation and conventionally used chemotherapeutics drugs[167,168] and is related with the almost complete inhibition of DNA-damage induced apoptosis,[169] representing an interesting for therapeutic strategies.

Dct plays a role in the regulation of cell growth and survival of melanocytes exposed to UVB protecting melanoma cells from UVB-induced apoptosis. [170]

Moreover investigating the effect of this tyrosinase-related protein on skin photoprotection and ROS scavenging capacity it has been demonstrated that Dct inactivation increases the level of ROS and the number of sunburn and apoptotic cells and decreases the amount of eumelanin in the epidermis after UV exposure.[171]

DHICA is less oxidizable than DHI and generate a less dark pigment[35,154] so it is difficult to understand why Dct causes this deviation in eumelanogenesis, increasing the ratio DHICA/DHI in eumelanin, suggesting that DHICA could play other roles than mere eumelanin precursor.

Actually, DHICA and its main metabolite 6-hydroxy-5-methoxyindole-2-carboxylic acid (6H5MICA, 0.07-2.15 ng⁄mL in normal plasma)[172] have antioxidant properties and play a critical role in melanocyte response to oxidative stress and inflammation.[17]

DHICA is able to inhibit lipid peroxidation in vitro decreasing malondialdehyde (MDA) formation by lipid peroxidation and inhibits Fe(II)/EDTA-induced oxidation of arachidonic acid and MDA formation by iron-promoted degradation of 15-hydroperoxy-5,8,11,13-eicosatetraenoic acid (15-HPETE).[121]

Data from 2,2-diphenyl-1-picrylhydrazy radical (DPPH) assay show that both DHICA and its main metabolite are stronger antioxidant than trolox in the H-donor activity, while comparing the efficiency of the two indoles in reducing Fe(III) ions to Fe(II) ions using the ferric reducing anti- oxidant power (FRAP) assay, both DHICA and 6H5MICA proved to be better antioxidant than trolox (2.4 and 1.8 trolox equivalents for DHICA and its methoxy derivative, respectively).[17]

Nanomolar concentrations of DHICA and 6H5MICA can inhibit H_2O_2-Fe(II)/EDTA (Fenton)-induced oxidation processes (IC_{50} = 4.3 and 6.0 nM for DHICA and 6H5MICA, respectively).[122,123]

DHICA displays an absorption maximum in the UVB erithematogenic region (λ_{max} = 313 nm) and can act as triplet state quencher.[120,124]

When treated with increasing concentrations of the DHICA normal human keratinocytes (NHKs),[173] undergo an inhibition of growth with no increase in mortality at any dose and time point tested. Quantitative real-time reverse transcriptase–PCR (qRT–PCR) shows that DHICA significantly enhances the expression of keratinocyte differentiation marker (namely involucrin, loricrin, and filaggrin), while its main metabolite 6H5MICA does not. Moreover it induces activity and expression of antioxidant enzymes, namely superoxide dismutase (SOD) and catalase, the main enzymes involved in the maintenance of the intracellular redox equilibrium during an oxidative stress.[174] This same study shows that DHICA protects keratinocytes against the free-radicals–mediated damages resulting from UVA exposure.

All these data point out that DHICA exerts an antioxidant and protective function *per se* unrelated to pigment synthesis, suggesting that the indole and/or its derivatives could play an important role in preventing and treating inflammatory skin pathologies related to oxidative stress, such as acne, atopic dermatitis and melanoma.[104,175]

Moreover, it could represent a useful tool to recover the antioxidant defense pool in individual exhibiting red hair phenotype (RHP) who lack the protecting eumelanin pathway and suffer from chronic oxidative stress.[81]

3.2.1 Development of bioinspired sunscreen formulations: synthesis of dioleoyl-MeDHICA

Excessive UVB and UVA exposure is related to sunburns, skin aging, DNA damage and tumorigenesis.[1] On the other hand UV protection plays an important role in reducing the risk of squamous cell carcinoma, actinic keratosis and probably also the risk of melanoma.[176]

One of the main mechanisms of photoprotection is the absorption of the UV radiation with release of less harmful energy. An effective sunscreen formulation should be able to absorb and scatter UV radiation, to resist to photodegradation and limit photochemical damage acting like an antioxidant.

Inorganic and organic components are successfully used to protect skin from UV induced damages resulting in high Sun Protection Factor (SPF). Usually inorganic components, such as titanium dioxide (TiO_2), a mineral prepared as ultra-fine nanoparticles, act as physical sunscreen agents by absorbing, reflecting and scattering UV radiation while organic compounds, such as conjugated aromatic molecules, act as a chemical sunscreen absorbing radiation rather than reflecting or causing it to scatter.[177]

Unfortunately, adverse secondary effects deriving from sunscreen formulations were described, suggesting that their application can induce contact and photocontact dermatitis and photoallergic reactions.[177–180] Moreover some sunscreen ingredients can be absorbed into deep layers of the skin inducing local and systemic toxicity.[181]

Following the current trend that considers natural products the future of cosmetics, considerable efforts in research have been directed to the discovery and exploitation of all natural functional ingredients so to warrant customers safety and sustainability of the product.
In the quest for new natural and bioinspired agents of photoprotection, DHICA, a human metabolite known for its anti-inflammatory and antioxidant properties (see previous paragraph), is suitable to be used as a protective tool against sun induced damages.
UV radiation can penetrate deeply into the skin so topically applied photoprotective agents should be able to reach deeper cutaneous layers to afford the skin an effective photoprotection.
In order to be able to incorporate this compound in a formulation for topical administration, its lipophilicity has been increased by preparing a methyl ester at the carboxyl group and by the conjugation of the phenolic hydroxyl groups with a fatty acid, namely oleic acid, thus yielding a prodrug.
According to the IUPAC definition, a prodrug is a "compound that undergoes biotransformation before exhibiting pharmacological effects".[182] The use of a conjugate of an active compound with a lipophilic substituent, is a good way of improve its bioavailability and skin permeability.[183]
Prodrugs are often modified by esterification reactions and are more easily adsorbed into the outer layer of the skin, *stratum corneum* (the main obstacle against the penetration of exogenous substances through the skin), reaching the epidermis where they are hydrolyzed to more polar active metabolites by esterases such as carboxylesterase (CES; EC 3.1.1.1) and arylesterase, present both in rat and human skin.[184,185]

Oleic acid (OA) was chosen as derivatizing agent. Triglycerides of this monounsaturated omega-9 fatty acid compose the majority of olive oil. OA is commonly used as permeation enhancer and is known to increase skin permeability,[186,187] acting on extracellular lipids that regulate the penetration of small molecules interacting with the lipid matrix of the stratum corneum. Moreover this unsaturated fatty acid can modulate inflammatory and immune responses in case of cutaneous wounds accelerating healing.[188]

On this basis the synthesis of the highly lipophilic ester of DHICA methyl carboxylate with oleic acid was performed, adapting an already developed procedure.[189] Oleoyl chloride was used instead of free OA as a more reactive acylating agent.

Spectral characterization of the product confirmed the expected structure.

The lipophilic product was incorporated in Vaseline (5% w/w) by standing at room temperature under vigorous stirring overnight.

In order to examine the role of the acyl substituent in the photoprotection activity to be tested, an O-acetyl derivative of DHICA (DAICA) was also prepared by acetylation of the indole with acetic anhydride-pyridine overnight at room temperature.

3.2.2 In vivo evaluation of efficacy of dioleoyl-MeDHICA as photoprotective agent

UVB erythema is considered as one of the most suitable models for studying in vivo skin damage after acute UV exposure.[190,191] The extent of UVB-induced skin erythema may be monitored by means of reflectance spectrophotometry.

The ability of dioleoyl-MeDHICA to reduce UVB-induced skin erythema was tested in healthy human volunteers. 10 healthy volunteers (both sexes) of skin types II and III, with a mean age of 35 ± 13 years were selected. All the volunteers were informed in detail of the nature of the study and the procedures involved and gave their written consent. The subjects did not suffer from any ailment and were not on medication at the time of the study.

Skin erythema was induced by UVB irradiation using an ultraviolet lamp (Skin-tester Kit, Cosmedico Medizintechnik GmbH, Scwennigen, Germany) which emitted in the range of UVB. The lamp is equipped with a six grid-containing square opening through which UVB-light is emitted. The grids have different abilities to attenuate the UVB-light so that the percentages of UVB-light let through the opening are different.

For each subject, the minimal erythema dose (MED) was preliminarily determined. MED is defined as the lowest time interval or dosage of UV light irradiation sufficient for producing a minimal, perceptible erythema (sunburn or redness caused by engorgement of capillaries) on unprotected skin within a few hours following exposure.

Three sites on the ventral surface of one forearm of each subject were chosen using a square template (1 cm^2) and demarcated with permanent ink. The creams were applied for three days on two of three sites, while a site was left untreated (control). On the fourth day the induced erythema was monitored by means of a reflectance visible spectrophotometer (X-rite mod.158- 964, Michigan, USA) having 45° illumination and 0° viewing angle.

Spectrophotometers provide measures of the three coordinates of CIELAB: L*, a* and b*.

The lightness, L*, represents the darkest black at L* = 0, and the brightest white at L* = 100 while a* and b* represents the position of the color between red/magenta and green ($a^* < 0$ indicates green while $a^* > 0$ indicates magenta) and yellow and blue ($b^* < 0$ indicates blue while $a^* > 0$ indicates yellow)

Preliminary results showed that oleoyl-MeDHICA afforded a significant protection to the skin against UVB-induced erythema, with significant differences with respect to the controls. On the other hand DAICA gave erythema values that were not significantly different with respect to the control.

The higher lipophilicity of oleoyl-MeDHICA may explain the fact that it permeates through the *stratum corneum* better than DAICA, being more effective.

3.2.3 Effects of carboxyl group substituents of indole precursors on eumelanin properties

Understanding the relationships between structure, properties and function in melanin can elucidate its role in skin (photo) protection and UV-susceptibility.

One of the main variation that can be observed and that strongly affects melanin properties, is the presence or the absence of the carboxyl group in the precursors.[192]

The rearrangement of dopachrome to DHI or DHICA[17] constitutes an important branch in melanogenesis as carboxyl retention results in essential biological consequences such as antioxidant eumelanin properties that are enhanced in the case of DHICA melanin.[144]

In vitro and at neutral pH, dopachrome spontaneously decomposes to give DHI and DHICA in a 70:1[193] ratio but in the presence of dopachrome tautomerase (Dct, also called tyrosinase-related protein-2, Tyrp2) or of metal cations, the formation of DHICA is favored.[35,194–196]

Metal ions can also affect the course of pheomelanogenesis directing the synthesis towards generation of carboxylates moieties.[22]

Oxidative polymerization of DHI and DHICA produces eumelanin via a wide range of oligomers, mainly coupled through 2,2'-, 2,4'- and 2,7'-bonding in the case of DHI,[197–199] through 4,4'-, 4,7'- and 7,7'-bonding in the case of DHICA (Figure 43). This different reactivity is due to the electron-withdrawing carboxylic acid group that decreases the nucleofilicity of the pyrrole moiety and the reactivity of the 3- position.[197,199]

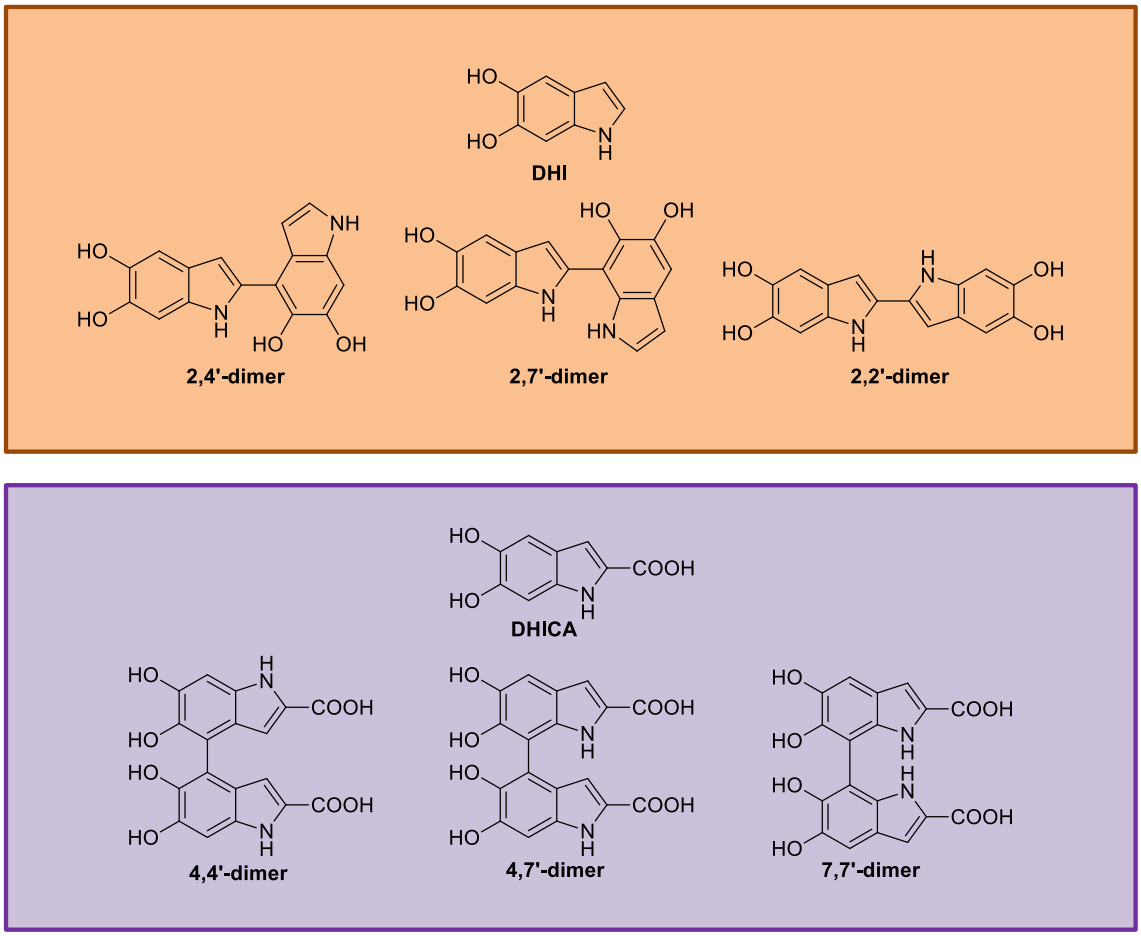

Figure 43. *DHI and DHICA dimers.*

While DHI oligomers exhibit a planar conformation with π-stacked supramolecular aggregates, DHICA mainly polymerizes through biphenyl-type bond, adopting a non-planar conformation with a hindered rotation at the inter-ring bonds, giving reason to atropisomerism (Figure 44).[200,201] Negative charges on the carboxylate groups reinforces this deviation from planarity, so while DHI oxidation produces planar species absorbing visible radiation, DHICA oligomers do not absorb above 400 nm because a significant interruption of π-electron delocalization.[154,160]

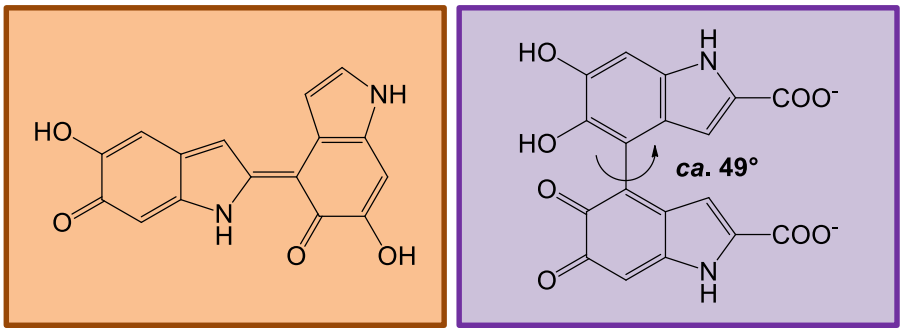

DHI dimer quinone
- p-stacked supramolecular aggregates
- **Planar conformation**
- **Monotonic absorption profile**

DHICA dimer quinone
- **Biphenyl-type bond**
- **Twisted conformation**
- **Atropisomerism**
- **Intense absorption at *ca.* 320 nm**

Figure 44. *Predicted structures of DHI and DHICA dimers quinones.*

As already illustrated in paragraph 3.1 of this chapter dealing with the melanin chromophore, DHI melanin displays a monotonic profile,[155] DHICA melanin shows an intense absorption at about 320 nm,[144] suggesting the presence of both reduced monomer-like chromophoric components and quinonoid units. This is confirmed by the observation that the addition of $NaBH_4$, a reducing agents, decreases the absorption in the visible range but does not affect the absorption at 320 nm due to the reducible quinonoid moiety.

Comparing the spectra of DHI and DHICA melanin in the presence polyvinyl alcohol (PVA), that is able to prevent melanin precipitation,[135,153] DHI but non DHICA melanin displays a broad band around 500 nm. Moreover, dilution in PVA containing buffer induce loss of visible absorption in DHICA melanin but not in DHI melanin (Figure 45).

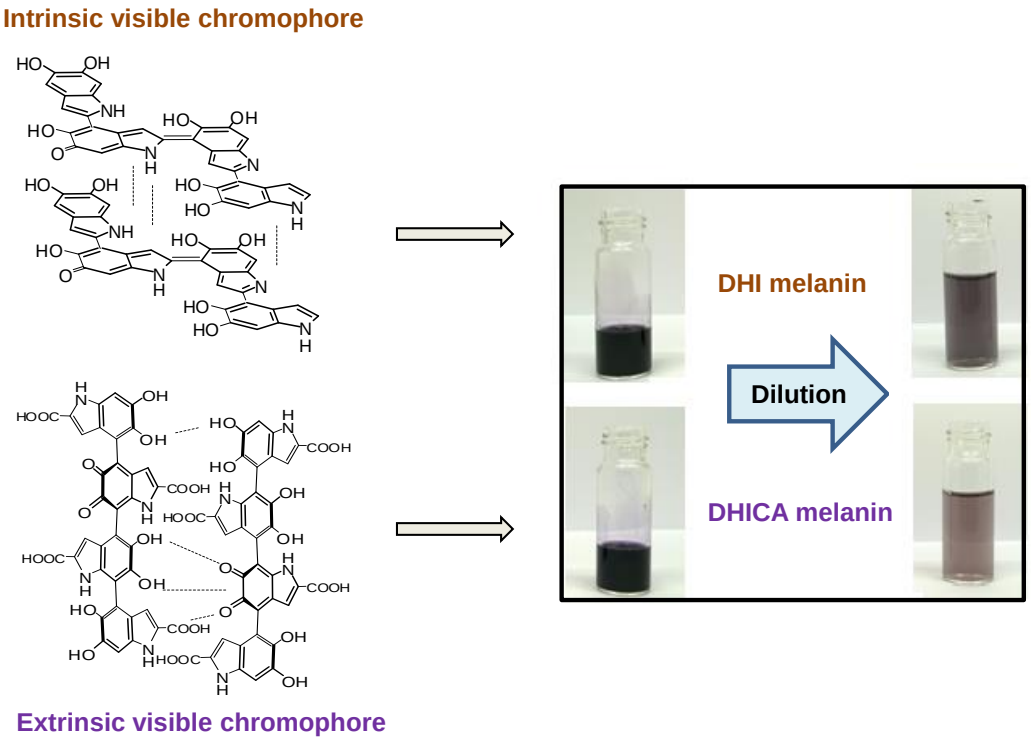

Figure 45. *DHICA and DHI melanin before and after 1:90 dilution in 1% PVA-containing buffer and intrinsic and extrinsic contributions to the chromophoric properties of DHI and DHICA melanin.*

These data suggested that DHI melanin chromophore derived from intrinsic effects due the π-delocalization while the DHICA chromophore is mainly determined by extrinsic contributes due to aggregation-dependent intermolecular perturbation of the π-electron system.

Both DHI and DHICA melanin are paramagnetic and display similar g-value in their EPR spectra but the DHICA melanin signal is significantly narrower than DHI one.[60,143,144,202]

Moreover, power saturation curves show that free radical components in DHICA melanin are more homogenous, suggesting spatially confined within restricted segments of this polymer. DHI melanin seems to be characterized by a broader variety of free radical species, possibly generated within the delocalized π-electron system of the DHI polymer.

The decrease of ΔB for DHICA melanin in the presence of 1% PVA suggests that the free radical population of DHICA melanin is markedly affected by intermolecular interactions. No differences were observed in the case of DHI melanin.[144]

The decrease of DHICA content in melanin is associated with Dct inactivation that is also related to the increase of ROS levels following UVA exposure and the number of sunburn and apoptotic cells in epidermis.[171]

Antioxidant properties can be extended from monomer to melanin as also DHICA melanin is

a hydroxyl radical-scavenger in the Fenton reaction in a dose-dependent manner.[144] DHI-melanin, instead, acts as a pro-oxidant generating ROS, whose levels are decreased by DHICA melanin suggesting that the naturally occurring mix of DHI and DHICA unit in eumelanins is necessary to minimize ROS generation and protect skin cells from oxidative damage.

Investigation of the excited-state dynamics of DHICA by ultrafast time-resolved fluorescence spectroscopy showed deactivation of the excited state that is mediated by inter-unit interactions within the oligomeric molecular scaffold.[120]

DHICA melanin is a stronger hydroxyl radical–scavenger *in vitro* with respect to DHI melanin, as confirmed in three different tests (Table 2), suggesting that Dct could regulate antioxidant properties.

Table 2. *Free radical scavenging properties of DHI and DHICA melanins.*[144]

	DHI melanin	**DHICA melanin**
DPPH (%)	29±1	100±4
ABTS (%)	4±1	46±2
NO (%)	26±1	64±3

These antioxidant properties could be ascribed to the destabilizing effects of non-planar structures on electron delocalization and aggregation, imparting monomer-like behavior to the polymer. Weak aggregates would make free radicals more accessible than in the case of DHI melanin.

All these data suggest that retention of carboxyl group play a key role in controlling pigment properties in eumelanins (Table 3).

Table 3. *Comparison of the properties of eumelanins from carboxylated/non-carboxylated precursors.*		
	DHI	**DHICA**
Monomer characteristics		
Reactive sites	At least 4	Usually 2
Oxidizability	High	Low
Polymer properties		
Solubility (neutral pH)	Nihil	Very slight
EPR signal intensity	Strong	Weak
Visible absorption	Intense	Poor
Photophysical properties	Efficient excited state decay	More efficient excited state decay
Chemical properties	Antioxidant	More potent antioxidant

Three features could account for differences in carboxylated or non carboxylated rich units in melanin:

- Lower number of reactive sites available for polymerization and cross-linking
- Lower oxidation potential
- Negative charge

This last characteristic can affect the structural properties of oligomers and their susceptibility to post-synthetic modifications.

The role of carboxyl group is only partially elucidated in the case of pheomelanin while in the case of eumelanin it explains why an enzymatically-controlled pathway to produce a poor pigment precursor like DHICA instead of exploiting the spontaneous production of

DHI. Although caution must be exercised before extending conclusion from in vitro to in vivo situation, this latter point may be taken as an additional indirect argument against a merely pigmentation role of melanin in nature.

3.2.4 The impact of esterification on 5,6-dihydroxyindole-2-carboxylic acid antioxidant activity and oxidative polymerization

In order to understand the role of the carboxyl group as determinant of the chemical properties of the 5,6-dihydroxyindole system, DHICA and MeDHICA were compared. Their conversion to eumelanin chromophore and their antioxidant properties were investigated.

Comparing the autoxidation behavior of DHICA and MeDHICA (50 μM) in phosphate buffer (pH 8.5), a progressively decrease of the maximum of the indole at 320 nm was observed, replaced by the featureless broadband absorption typical of melanins. A similar course was observed in the case of both the indoles, but in the case of MeDHICA the autoxidation seemed to be slower and the indole was still partially visible at 48 h (Figure 46).

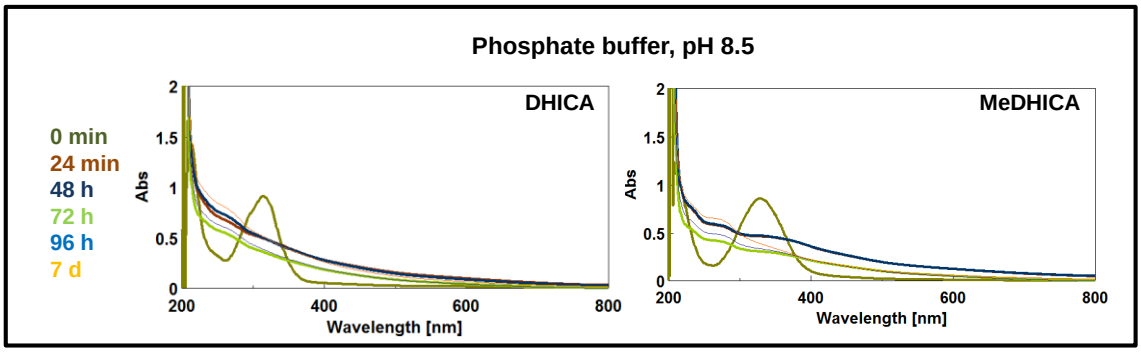

Figure 46. *Spectrophotometric course of the autoxidation mixture of DHICA or MeDHICA (50mM) in 0.1 M phosphate buffer, pH 8.5.*

Monitoring the course of the oxidation by reverse phase HPLC, a complete consumption of the monomer was observed at 72 h, while at 48 h the decay of the starting indole was about 40%. The elutographic profile showed other more retained components the first eluted of which clearly predominant (Figure 47). A similar product pattern is obtained using potassium ferricyanide as oxidant, while the addition of metal ions like copper or cobalt to the autooxidation mixture, markedly accelerated the process, favoring the formation of the first eluted component, that was isolated by preparative HPLC from the oxidation mixture of the indole at 10 mM concentration in the presence of equimolar cobalt sulphate in 0.2 M HEPES buffer pH 7.5 over 15 min reaction time.

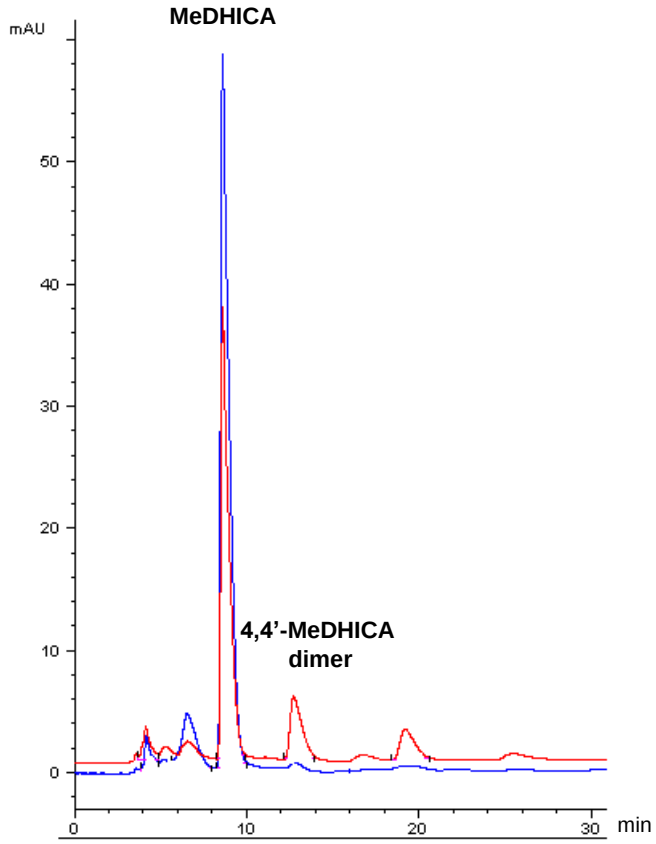

Figure 47. *HPLC profile of the MeDHICA oxidation mixture with UV detection (280 nm).* ***Blue trace: t = 0; red trace: t = 48h.***

The product was identified as the 4,4'-biindolyl based on NMR analysis in comparison with data reported for DHICA dimers.[203] Since also in the case of DHICA the autoxidation in the presence of metal ions gives 4,4' dimer as the major oligomer, it can be concluded that the regioselectivity of the oxidative coupling observed for DHICA is not affected by derivatization of the carboxyl group.

Melanin from MeDHICA (and from DHICA, for comparative analysis) were prepared using different oxidizing condition including autooxidation in phosphate buffer at pH 8.5 and chemical oxidants like ferricyanide, running the reaction until complete consumption of the indole as determined by HPLC analysis. The oxidation mixtures were acidified and the melanin pigment was separated by centrifugation.

The solubility properties of MeDHICA and DHICA melanins prepared by autoxidation were assayed in different organic solvents selected among those with high miscibility in water, using a test concentration of 0.3 mg/mL and stirring the materials in the appropriate solvent for 15 min.

Digital pictures of the solution/suspension in methanol or dimethyl sulfoxide (DMSO) chosen as representative solvents are shown in Figure 48.

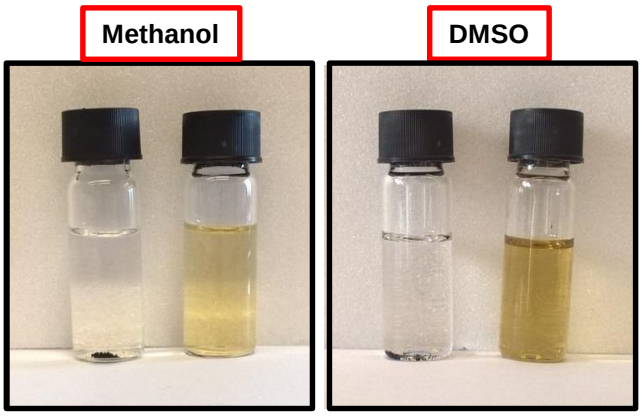

Figure 48. *Digital pictures of 0.3 mg/mL DHICA (left) or MeDHICA (right) melanin prepared by autoxidation and stirred in methanol or DMSO for 15 minutes.*

In the case of DMSO, MeDHICA melanin was completely solubilized whereas DHICA melanin is not, while in methanol as well as in other solvents only a partial solubilization was obtained. Absorption spectra of the supernatants after discarding the solid materials and appropriate dilution showed absorption at around 330 nm in the case of MeDHICA melanin whose intensity correlated fairly well with the observed solubility in the solvents examined (Figure 49).

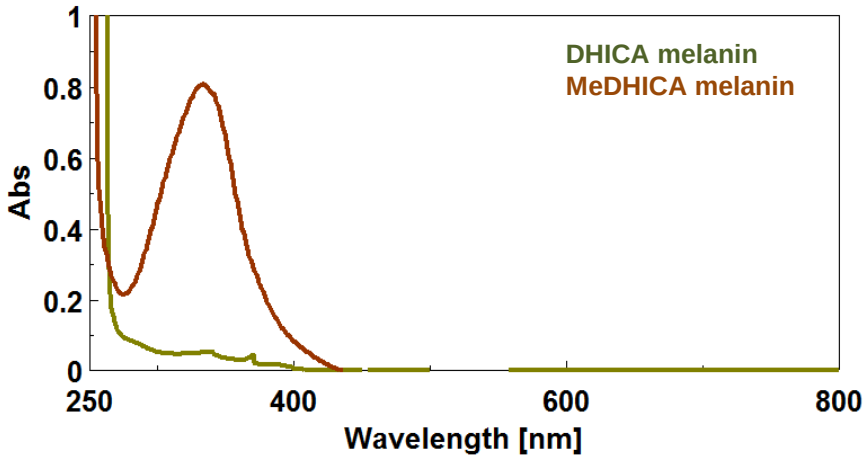

Figure 49. *Uv-vis spectra of **DHICA** and **MeDHICA** melanin in DMSO.*

Mass spectrometric analysis in the MALDI mode was run using 2,5-dihydroxybenzoic acid as the matrix and the melanin applied to the plate from a fine suspension in ethanol obtained by homogenization in a glass to glass potter.

The spectrum of the MeDHICA melanin prepared by aerobic oxidation displays a well distinct pattern of signals corresponding to oligomers from the dimer to the octamer, peaking at the trimer (Figure 50). Though it can not be ruled out that other high molecular weight components are not detected by this methodology, the spectrum provides evidence for a clean collection of intact oligomers as constituents of MeDHICA melanin. A similar though less defined spectrum was obtained for MeDHICA melanin prepared by ferricyanide oxidation (data not shown).

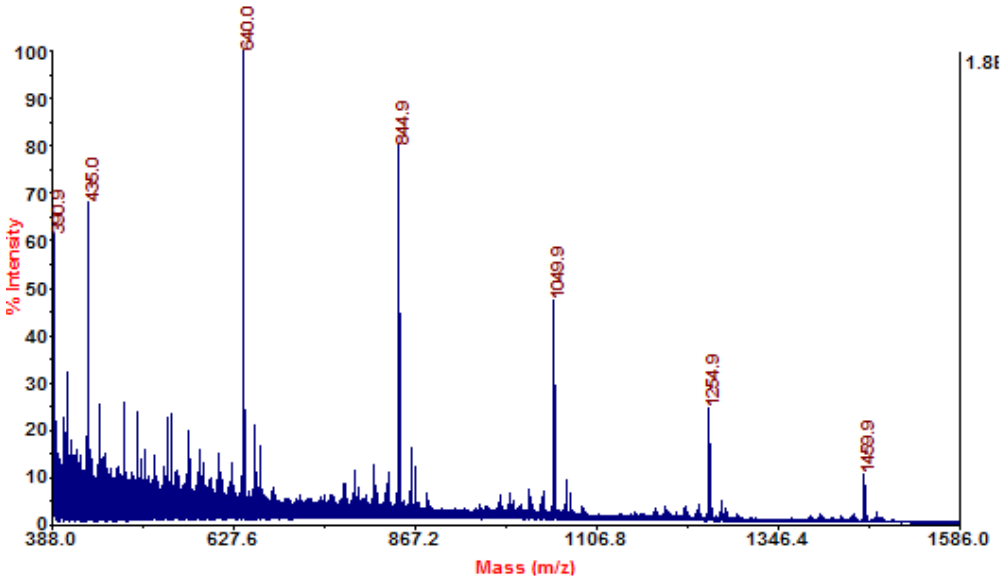

Figure 50. *MALDI spectrum of the MeDHICA melanin prepared by aerobic oxidation.*

EPR spectra of different MeDHICA melanins in comparison with one representative DHICA melanin were recorded. Almost identical g-values were exhibited by all melanins and signal amplitudes (ΔB) were comparable and relatively narrower (see Table 4) compared with those reported for DHI and other melanins.[144]

Table 4. *EPR spectral parameters for MeDHICA and DHICA melanin prepared under different conditions.*			
Sample	**ΔB (G)**	**spin/g**	**g-factor**
MeDHICA autooxidation melanin	4.4 ± 0.2 G	6.2×10^{18}	2.0029 ± 0.0002
MeDHICA ferricyanide melanin	4.0 ± 0.2 G	2.4×10^{18}	2.0029 ± 0.0002
DHICA autooxidation melanin	4.5 ± 0.2 G	8.2×10^{17}	2.0029 ± 0.0002

These data coupled with analysis of the power saturation curves (Figure 51) would confirm a similar free radical character of these melanins showing a good degree of homogeneity and low dispersion of the free radical components in full agreement with previous observations.

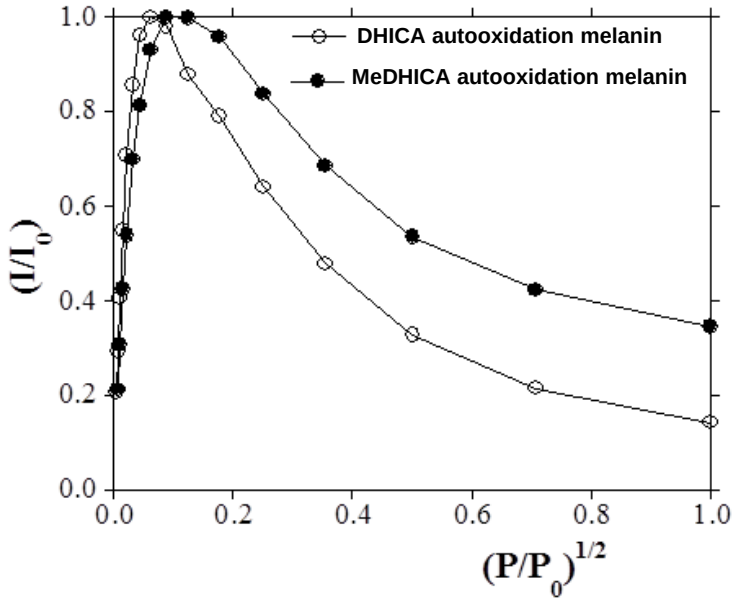

Figure 51. *Power saturation curves for MeDHICA and DHICA melanin prepared by autooxidation.*

The spin density of MeDHICA melanins are of magnitude higher with respect to DHICA melanin, suggesting the presence of radical centers likely of semiquinone-type arising from disproportionation *equilibria* of localized quinone and indole units inside the pigment backbone, differently from what observed for DHI-melanin[144] featuring extensively delocalized π-electron systems with strong π–stacking interactions, in which the carbon centered component localized in the center of stacked units provides seemingly the predominant contribution.[143]

Antioxidant properties of MeDHICA melanins (in comparison with respective monomers and 4,4' dimers) were assayed by two chemical tests, namely the 2,2-diphenyl-1-picrylhydrazy (DPPH),[204] an assay that measures the H-donor ability of a given species and the ferric reducing antioxidant power (FRAP),[205] which measures the ability of the antioxidant to reduce a Fe^{3+}-tripyridyltriazine complex to a dark blue Fe^{2+} complex with absorption maximum at 593 nm.

In the case of DPPH (Figure 52) the EC_{50} *i.e.* the dose of the material at which a 50% DPPH reduction is observed, were determined. Very low and similar values were obtained for both monomers, whereas for the dimer the values were comparable and as low as 2.4 μg/mL. This is in line with the high antioxidant potential of DHICA as reported in previous work by different assays which is substantially unaltered in the ester.

In the case of melanins, a fine suspension was obtained by homogenization in a glass/glass potter. MeDHICA melanin obtained by autoxidation is a very effective antioxidant to an extent comparable or even higher with respect to DHICA melanin, but either pigments are less potent that their respective monomer or 4,4'-dimer.

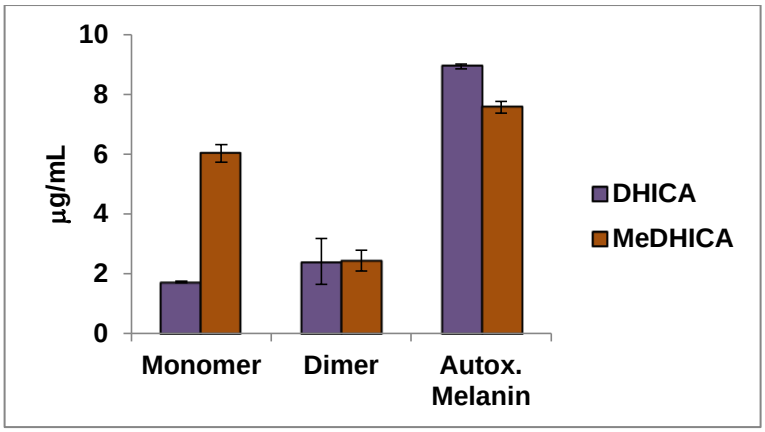

Figure 52. *EC_{50} values from DPPH assay on DHICA and MeDHICA monomers, dimers, and melanin prepared by autooxidation. Data are expressed as mean ± SD of three independent experiments, each performed in duplicate.*

In the case of FRAP (Figure 53), results were expressed as trolox equivalents and show comparable values in the case of the monomer and of the dimer, while MeDHICA melanin proved to be a stronger antioxidant than DHICA melanin.

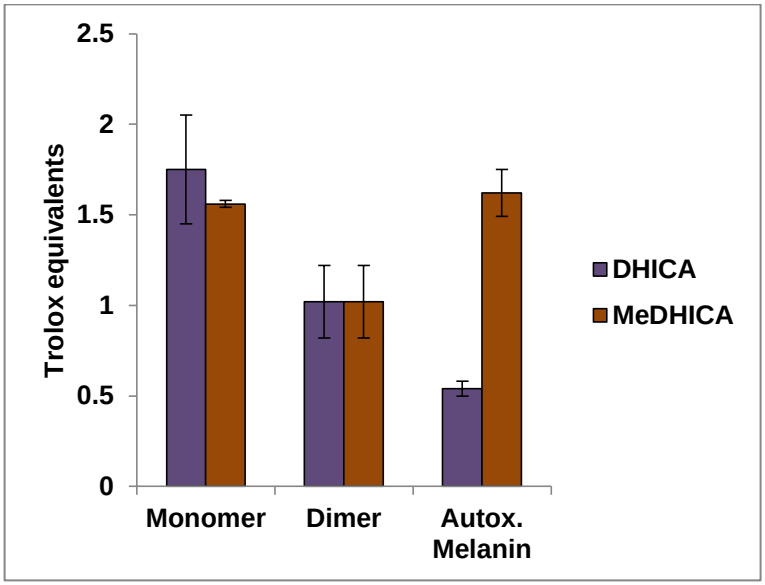

Figure 53. *Ferric reducing power of DHICA and MeDHICA monomers, dimers, and melanin prepared by autooxidation, expressed as trolox equivalents. Data are expressed as mean ± SD of three independent experiments, each performed in duplicate*.

These results suggest that the role of the carboxyl group in melanogenesis from DHICA is more complex than simply blocking the 2-position of the indole ring, and can be modulated through the control of ionization of carboxylate anion. Based on the behavior of the ester, it is suggested that suppression of carboxylic acid ionization under the acidic conditions of melanosome interior enhances antioxidant properties while hindering dark melanin formation. However, data presented in this paragraph are only preliminary and still underway.

CHAPTER 4

4.1 Mechanism of control of pigmentation

Local excess of pigmentation (hypermelanosis) is one of the most common pigmentary disorder and can be the result of inflammatory responses or local abnormal melanocyte function.[2] Several hyperpigmentary disorders are associated with the overproduction or accumulation of melanin, for example melasma or lentigo.[206]

The aesthetically impact of such disorders have urged the search for non-toxic skin depigmenting agents.[207] In the investigation of the mechanism of action of newly designed molecules or natural extracts the mechanisms of regulation of skin complexion were analyzed in detail. As a result several processes involved in the control of pigmentation were highlighted including inhibition of tyrosinase and related enzymes, regulation of melanocyte homeostasis, alteration of constitutive and facultative pigmentation, down-regulation of melanosome transfer to the keratinocytes, melanogenesis signalling proteins, tyrosinase expression and stability.[208]

The key regulatory enzyme of melanogenesis is tyrosinase (EC 1.14.18.1), a copper containing complex whose structure is highly conserved among different species and widely distributed in the biosphere. This enzyme shows high homology with two tyrosinase-related protein, namely tyrosinase-related protein 1 (TRP1 or TYRP1) and tyrosinase-related protein 2 (TYRP2 or Dct).[2]

Tyrosinase can catalyzes two different reactions:[209]

- hydroxylation of monophenol to *o*-diphenol (cresolasic or monophenolasic activity)
- dehydrogenation of catechol to *o*-quinone (catecholasic or diphenolasic activity)

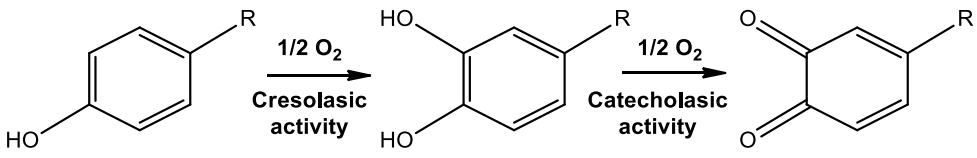

Scheme 3. *Reaction catalyzed by tyrosinase.*

In particular, tyrosine oxidation catalyzes the hydroxylation of the monophenol L-tyrosine to the *o*-diphenol L-3,4-dihydroxyphenylalanine (DOPA) and the oxidation of DOPA to the o-quinone Dopaquinone. The binding site for L-tyrosine and L-DOPA is the same and the reactions involve an electrons exchange with copper atoms[210,211]

Oxidation rates depend on several factors, like tyrosinase concentration, oxygen availability, pH and temperature.

Moreover, tyrosinase activity and stability are strictly connected to redox conditions, having four possible oxidation states (Figure 54).[212] Inactive enzyme ([$Cu(II)_2$], met-tyrosinase) is activated by reduction of its two Cu^{2+} to Cu^{+} giving the fully active form deoxytyrosinase, [$Cu(I)_2$], that is able of binding dioxygen to form oxy-tyrosinase [$Cu(II)_2O_2$]. The most efficient electron donor is L-DOPA even if other reducing agent can activate the enzyme, acting on the oxidation products of tyrosinase and inducing accumulation of DOPA.[2] Oxidation of catechols can lead to reductive elimination of one of the active-site copper ions and conversion to the inactive deact-tyrosinase [Cu(II)Cu(0)].[212]

O-quinones generated by tyrosinase oxidation of catechols are of great importance in biochemistry, being able to form a wide range of pigments widespread in animals and plants.

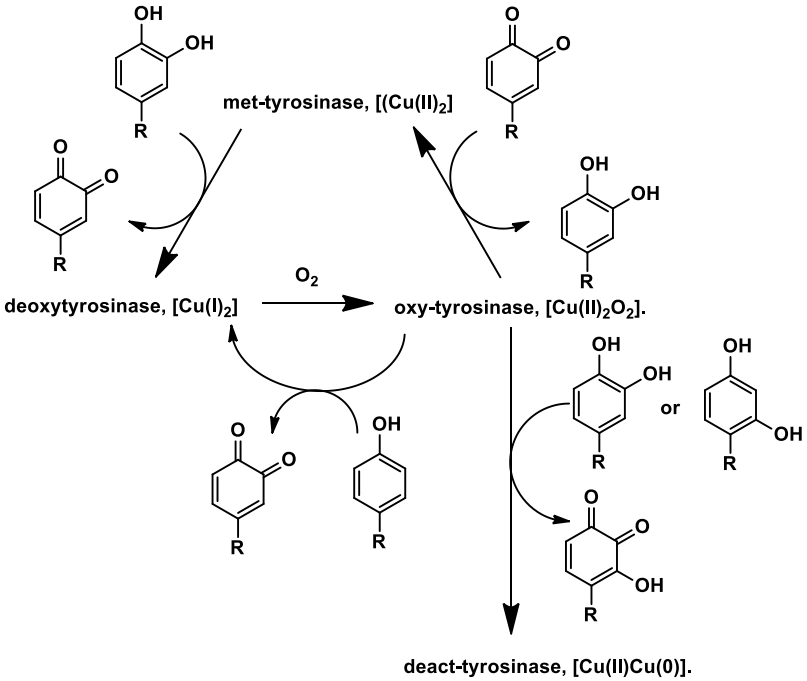

Figure 54. *The four oxidation states of the active site of tyrosinase.*

Presently skin depigmenting and melanogenesis regulators acting through different mechanisms have been developed and are commercially available.[208]

The first level that can be controlled to modulate the activity of tyrosinase and related enzymes is transcription. The microphthalmia-associated transcription factor (MITF) is the factor that regulates melanocyte cellular differentiation and the transcription of melanogenic enzymes (tyrosinase, TYRP1 and TYRP2) and melanosome structural proteins.[213–215]

The binding of α-melanocyte stimulating hormone (α-MSH) to the melanocortin 1 receptor (MC1R) stimulates the activation of adenyl cyclase and the consequent production of cAMP that in turn activates the protein kinase A (PKA) pathway to phosphorylate cAMP-responsive element binding protein (CREB) transcription factors. This one activates MITF-M promoter that induces melanogenesis.

Lowering of the expression of tyrosinase mRNA acting on this pathway is one of the mechanism used by some efficient melanogenesis inhibitors, such as 2-aryl-1,3-thiazolidines.[216–218] An example is MHY384, an inhibitor synthesized from 2,4-dihydroxybenzaldehyde and cysteine,[218] whose action has been attributed to its intervention in the NO-induced melanogenic pathway:[219] UV-exposed keratinocytes produced NO that activates guanylate cyclase (GC), which produces cGMP, that in turn activates protein kinase G (PKG).[220,221] According to a mechanism proposed, MHY384 would scavenge NO being reduced to nitroxyl (HNO) by H atom donation from the phenolic group of thiazolidine, decreasing cGMP levels and the phosphorylation of cAMP response element binding (CREB) protein via the PKG/cGMP signaling.[219] As proposed in a commentary[222] prepared on invitation by Experimental Dermatology, the species involved in the redox reaction could rather be NO_2 (produced by NO under aerobic conditions)[223] capable of generating a nitrophenol derivative by reaction with the phenoxyl radical.[224,225] Otherwise, the –SH group derived from the cleavage of the thiazolidine could react with the dopaquinone generated by the tyrosinase catalyzed oxidation of tyrosine. The hydrolysis of the thiol conjugated immine product would lead to the 2,4-dihydroxybenzaldehyde and cysteinyldopa (a pheomelanin precursors) (Figure 55). The opportunity of acting through such a variety of mechanisms may represent an advantage allowing to improve the efficacy of these inhibitors, reducing the duration of therapy and the risk of adverse effects.

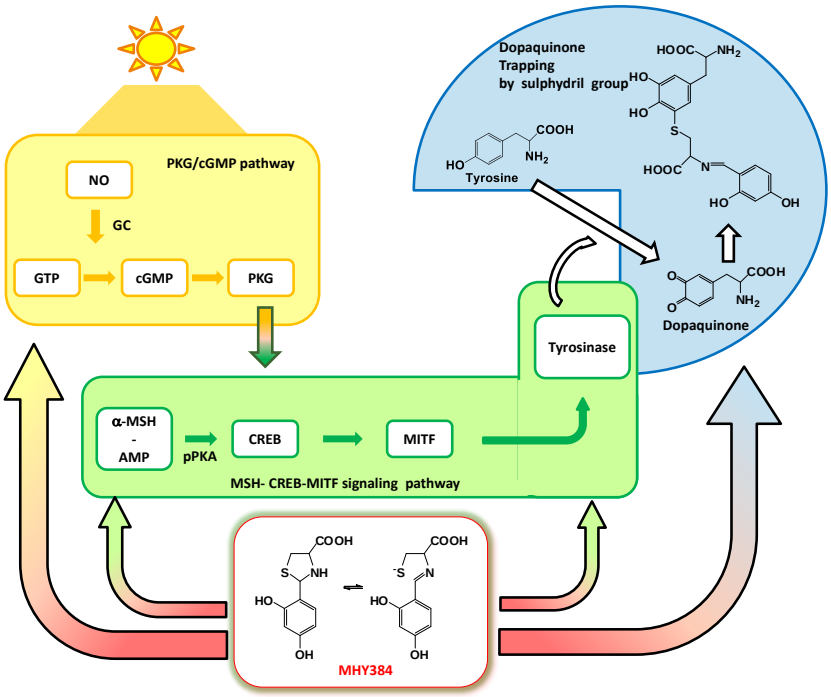

Figure 55. *Multiple mechanisms by which MHY384 and structurally related 2-aryl-1,3-thiazolidines control of melanin pigmentation in vitro and in vivo. Bent arrows indicate the sites of intervention. Adapted from Napolitano et al. 2016.*[222]

One of the most common approach for control of pigmentation involves the use of tyrosinase inhibitors like phenols, hydroquinones, flavonoids, stilbenes and coumarins.[226]Actually, only a few tyrosinase inhibitors have practical application as several factors should be considered, such as cytotoxicity, solubility, cutaneous absorption, and stability.

Moreover, further to the case of rhododendrol (RD),[227] a skin whitening agent that has been reported to cause leukoderma, an increasing attention is paid to the toxicity of depigmenting agent *in vitro* and *in vivo*. Tyrosinase catalyzes the production of toxic metabolites of RD[228] whose toxicity in melanocytes is exerted by mediation of ROS. These species, identified as RD-quinone, which is quickly converted to RD-cyclic quinone through an intramolecular addition of the hydroxy group, irreversibly bind to nucleophilic site of the enzyme causing melanocytes apoptosis.[229,230] Tyrosinase phenolic inhibitors should therefore be tested as substrates in order to ensure their safety.

Many simple phenolic compounds have been demonstrated to show inhibitory effects on melanogenesis through inhibition of the enzymatic activity of tyrosinase. For example, hydroquinone has been extensively used in the treatment of melasma.[231] However, because of its side effects, its use has important legal restrictions.

Dermatologic research has been encouraged to seek for new safe tyrosinase inhibitors for dermocosmetic applications to reduce skin hyperpigmentation. An increasing attention has been focused on the evaluation of the effect of structural modifications on the properties of phenolic systems from natural sources.

An investigation of the electronic and hydrogen bonding effects of the *ortho* and *para* substitution of phenols with alkylthio groups showed that the chain-breaking antioxidant activity of these derivatives is enhanced by decreasing the bond dissociation enthalpy of the OH group and affecting the reaction rate with peroxyl radicals.[232]

Among thioalkyl substituents, a particular attention was directed to dihydrolipoic acid (DHLA) a carboxylic acid featuring a pair of thiol groups.

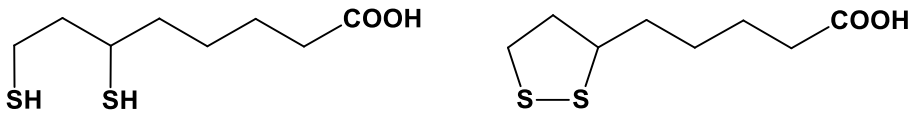

Dihydrolipoic acid (DHLA) **Lipoic acid (LA)**

DHLA is the reduced form of lipoic acid (LA, also known as vitamin N) and together with its oxidized form fulfills two main functions:[233]

- It is a cofactor of numerous enzymes involved in oxidative decarboxylation of pyruvate and other ketoacids, being continuously regenerated.[234,235]
- The LA/DHLA system possesses one of the lowest standard biological redox potentials (E0 = -0.29 V), being able to reduce not only ROS but also the oxidized forms of other antioxidants. It is able of scavenging hydroxyl radical, hypochlorous acid and peroxynitrite, and chelating Fe^{2+} ions.[236] Moreover, LA and DHLA are easily soluble both in fats and water, and can exert their functions both at membrane level and in aqueous phases of cytoplasm.

Lipoic acid administration has been shown to be beneficial in the treatment of diabetes,[237] cataract formation,[238] and in the prevention of neurodegenerative pathologies.[239–241]

Lipoyl-conjugates with L-DOPA and dopamine (DA) were prepared and tested for their antioxidant and iron-chelating properties, as a premise to assess their potential in treating pathologies such as Parkinson's disease.[242]

The free sulfhydryl groups of DHLA can react with dopaquinone to form lipoyl DOPA conjugates[243] and indeed lipoyl derivatives have been shown to affect melanin production by formation of DOPA conjugate products.[244]

On this basis the research activity developed was aimed at the preparation of a conjugate of DHLA with caffeic acid, a hydroxycinnamate compound widely diffused at relatively elevated levels in various agricultural products as pears.

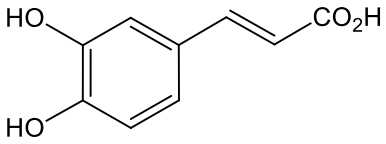

Caffeic acid

Caffeic acid is involved in immunoregolation and in a variety of diseases, including allergic conditions and asthma. Moreover it is a strong and selective transcription inhibitor of matrix metalloproteinase, that are directly involved in human hepatic tumorigenesis and metastasis.[245]

Caffeic acid linked to aminoacid residues such as the caffeoyl-prolyl-hydroxamic acid (CA-Pro-NHOH) proved an excellent tyrosinase inhibitor,[246] while CA alone, that is known to be a substrate for tyrosinase like L-DOPA,[247] was not. It is possible that this derivative has the appropriate structure for binding to the active site of tyrosinase due to its hydrophobicity. Actually, amino acids containing hydrophobic aliphatic group like Leu are known to play an important role in tyrosinase inhibition, and amino acids containing a hydrophobic aromatic ring like Phe can interact with tyrosinase being similar to tyrosine, the natural substrate of the enzyme.[248] Also amidic derivatives of caffeic acid with serine ore lysine, in particular N-Caffeoyl-O-acetylserine methyl ester showed strong tyrosinase inhibition activity.[249]

4.2 Preparation of a conjugate of caffeic acid with dihydrolipoic acid

The synthesis of the conjugate of caffeic acid (CA) with dihydrolipoic acid (DHLA) was carried out adapting a procedure previously reported for hydroxytyrosol, using *p*-coumaric acid as the starting product.[30]

A strategy was adopted that involved the generation of the *o*-quinone of caffeic acid from *p* -coumaric acid, followed by in situ addition of DHLA.

Regioselective hydroxylation of coumaric acid was achieved by reaction with 2-iodoxybenzoic acid (IBX)[250] affording to the *o*-quinone of caffeic acid.

The reaction mechanism,[251] not fully elucidated, should involve the reaction of coumaric acid with the IBX with elimination of a molecule of water from the intermediate A, that rearranges to B via oxygenation of the ortho-position of the phenolic group and concomitant reduction of the iodine from I (V) to I (III). Tautomeration of B gives the intermediate C that breaks down into the *o*-quinone and 2-iodobenzoic acid, while iodine (III) is reduced to iodine (I) (Figure 56).

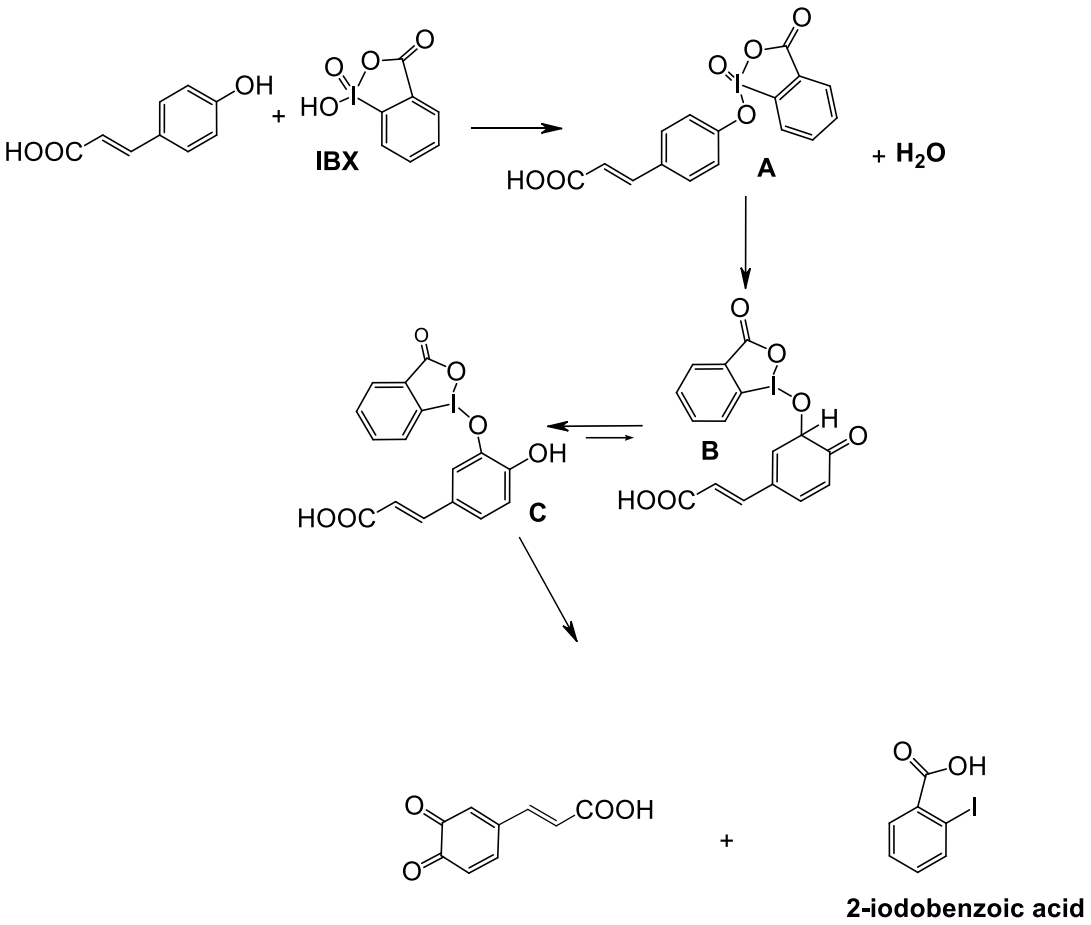

Figure 56. *Proposed mechanism for the generation of o-quinone of caffeic acid.*

IBX was prepared oxidizing 2-iodobenzoic acid with oxone® in water at 70° C, following a reported procedure.[250]

DHLA was prepared by reduction of lipoic acid with sodium borohydride, according to a previously reported procedure.[252]

Briefly, to an aqueous solution of a racemic mixture of LA (0.25 M) in 0.25 M $NaHCO_3$, $NaBH_4$ (1.0 M) at 0°C was added. After 2h the mixture was acidified to pH 1 and extracted with toluene (89%).

Solid IBX (1.5 eq.) was added to a methanolic solution of *p*-coumaric acid (70 mM) at room

temperature. After 4 min, DHLA (4 eq.) was added drop by drop to promote the nucleophilic addition instead of redox exchange between the *o*-quinone and DHLA, giving as byproduct caffeic acid.

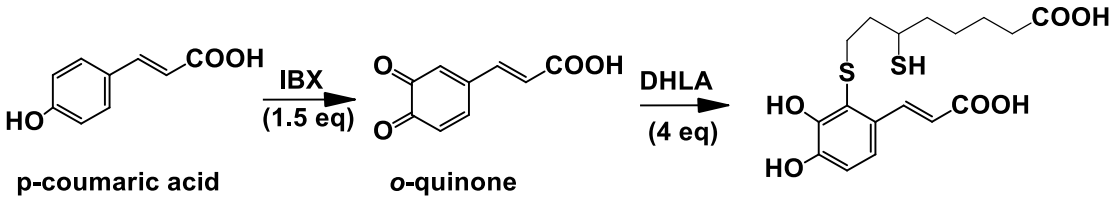

In order to isolate the conjugate, the mixture was diluted with water, acidified until pH 1 and extracted with solvents at increasing polarity. A hexane/toluene (8:2, v/v) mixture allowed to remove 2-iodobenzoic acid, LA and DHLA, while chloroform extracted the lipoylcaffeic adduct isolated in 20% yield. It is possible to recover the more polar caffeic acid remained in solution by ethyl acetate extraction.

The identity of the product was confirmed by ^{1}H and ^{13}C NMR (Figure 57) that allowed to elucidate the regiochemistry of the addition, as the spectrum displays two doublets at δ 6.86 and 7.22 with a J of 8.4 Hz typical of an *ortho* relationship indicating that the conjugation as occurred at position 2 in line with what observed in previous studies for the reaction of thiols to hydroxycinnamate.[253,254]

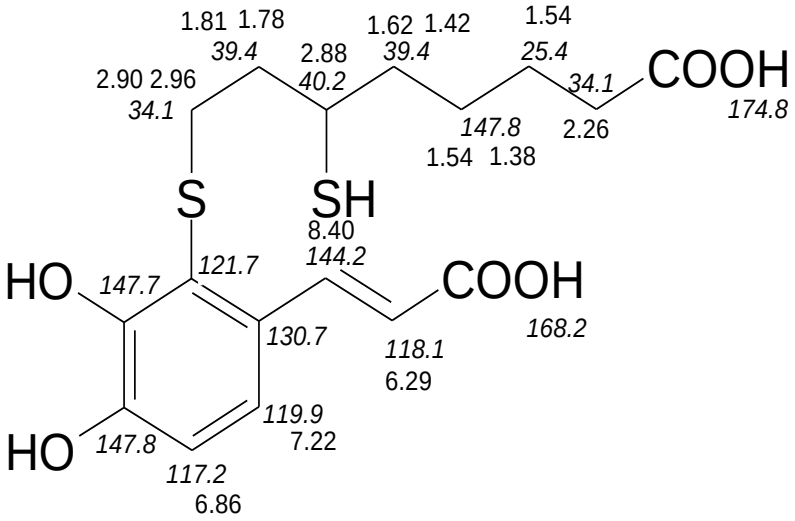

Figure 57. *^{1}H and ^{13}C resonances of 2-S-lipoylcaffeic acid.*

4.3 Inhibition of mushroom tyrosinase activity by 2-S-lipoylcaffeic acid

The tyrosinase inhibitory activity of 2-S-lipoylcaffeic acid was investigated using mushroom tyrosinase that is routinely used for assessment of the activity of potential tyrosinase inhibitors (Figure 58).[255–259]

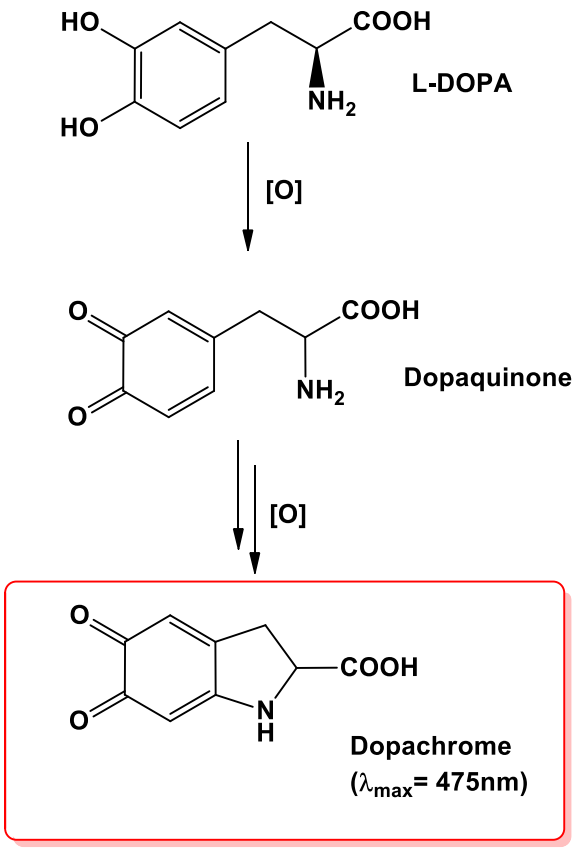

Figure 58. *Simplified scheme of enzymatic reaction that is monitored in the mushroom tyrosinase assay.*

The compound was incubated in 50 mM phosphate buffer (pH 6.8) in the presence of mushroom tyrosinase (20 U/mL) at room temperature for ten minutes. Following incubation, L-DOPA was added (1mM final concentration) and the amount of dopachrome production in the reaction mixture was determined spectrophotometrically at 475 nm after further 10 minutes (Figure 59).

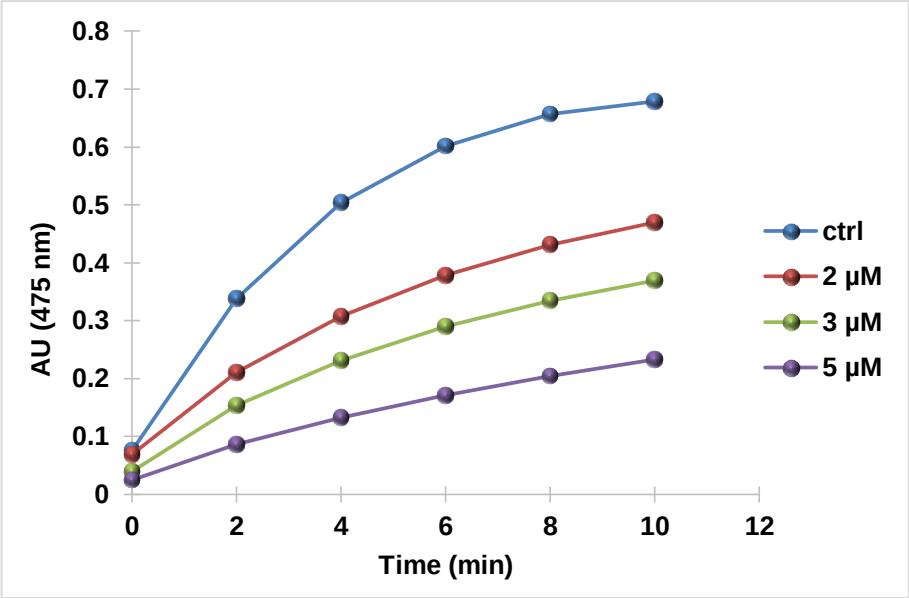

Figure 59. *Course of the oxidation of L-DOPA with mushroom tyrosinase in the presence of different concentrations of 2-S-lipoylcaffeic acid Data are expressed as mean of three independent experiments, each performed in duplicate (SD ≤ 5%).*

Percent of inhibition was calculated as follow:

$$\%\ \boldsymbol{inhibition} = \left(1 - \frac{\Delta A_{475/\min} \text{ in the presence of the inhibitor}}{\Delta A_{475/\min} \text{ in the absence of the inhibitor}}\right) \text{x } 100$$

Figure 60 shows that the lipoyl conjugate of caffeic acid is able to induce a maximum inhibition of more than 80% at a concentration of 7 µM.

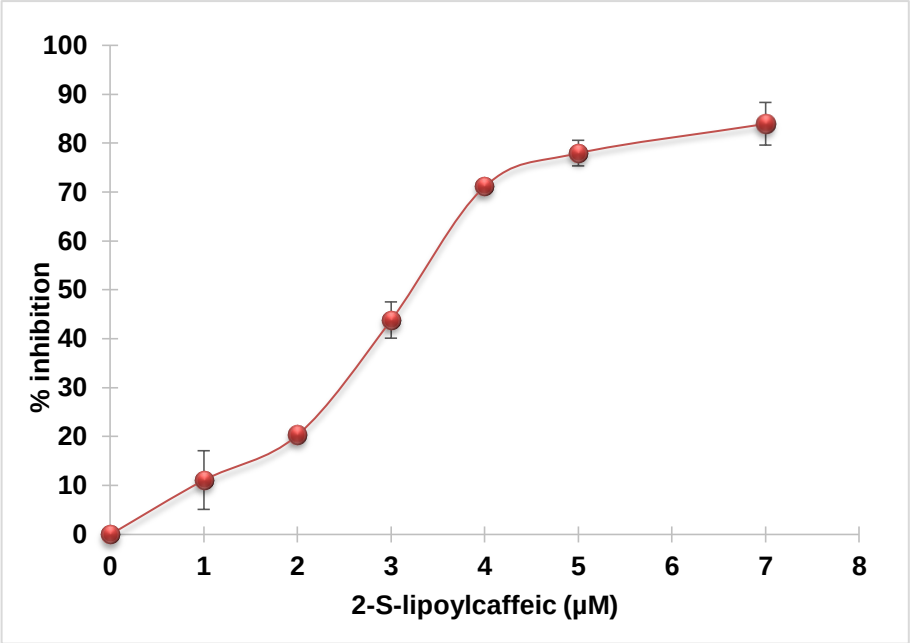

Figure 60. *Percent of inhibition of mushroom tyrosinase activity versus 2-S-lipoylcaffeic acid concentration using L-DOPA as substrate. Data are expressed as mean ± SD of three independent experiments, each performed in duplicate.*

The strength of an inhibitor is usually expressed as the inhibitory IC_{50} value, which is the concentration of an inhibitor needed to inhibit half of the enzyme activity in the tested condition. IC_{50} value was determined by linear interpolation between two points limiting the range including 50% inhibition (Figure 61). This value was 3.22 ± 0.02 µM.

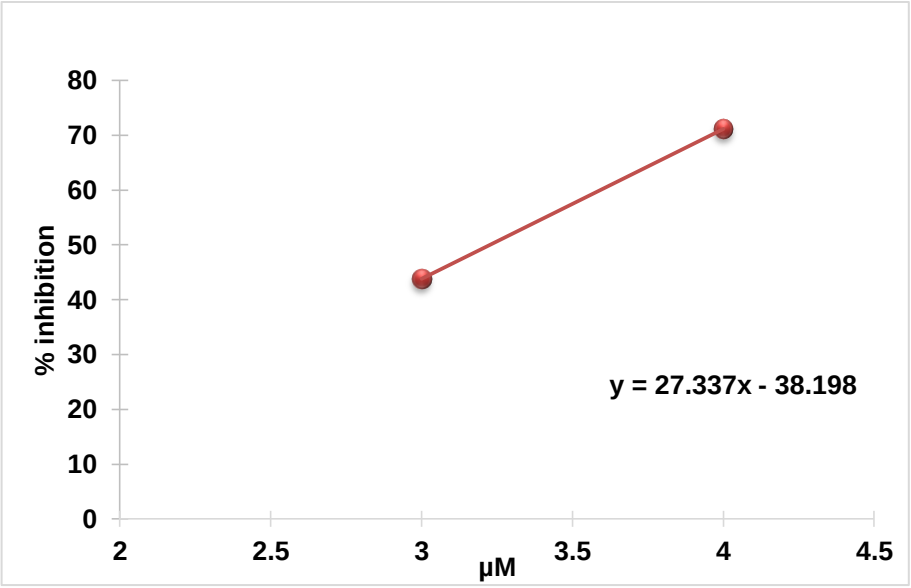

Figure 61. *Plot used for IC_{50} determination by linear interpolation using L-DOPA as substrate.*

Since the IC_{50} values for the tyrosinase inhibitors are usually incomparable due to the varied assay conditions, kojic acid (KA) that is thought to inactivate tyrosinase by chelating copper atoms.[260] is often used as a positive control.[261] KA is a fungal metabolite currently applied as a cosmetic skin-lightening agent even if its use has been limited because of some side effects such as sensitization, contact dermatitis and erythema. IC_{50} for KA under the same conditions used for 2-S-lipoylcaffeic acid was 340 µM.

Figure 62 shows oxidation mixtures of L-DOPA in the presence and in the absence of 10 µM 2-S-lipoylcaffeic acid after 10 minutes: the inhibition effect on the formation of the melanic pigment was well apparent. At the same concentration, caffeic acid and KA did not induce any inhibition.

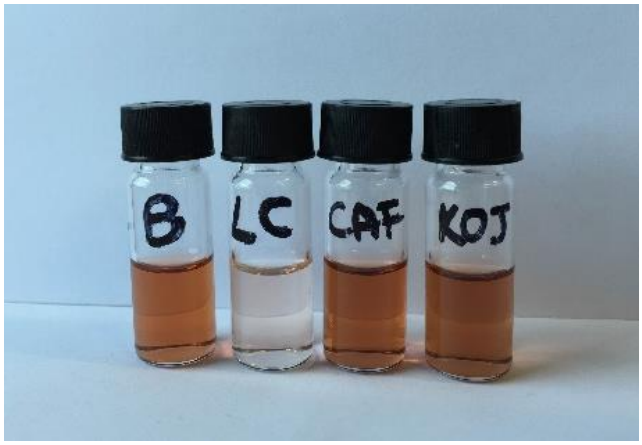

Figure 62. *L-DOPA oxidation mixtures in the absence (vial B) or in the presence of inhibitor (LC: 2-S-lipoylcaffeic acid; Caf: caffeic acid; Koj: kojic acid).*

The mechanism of inhibition of the lipoyl conjugate was then investigated. The bases of enzymatic kinetic rely on the theory by Michaelis and Menten, involving the following points:

- The rate of a reaction depends both on the substrate and enzyme concentration. When the substrate has completely saturated the enzyme giving the complex enzyme-substrate, the rate reaches a maximum and an increase of the substrate concentration does not increase the rate of the reaction.
- The enzyme (E) reacts with the substrate (S) to give the ES complex with a reversible reaction

$$E + S \underset{k_{-1}}{\overset{k_1}{\rightleftharpoons}} ES$$

Where

k_1 = Forward rate

k_{-1} = Reverse rate

ES releases final product P regenerating the original enzyme. The inverse reaction is neglected since its rate is minimum because the amount of the starting product is very low.

$$ES \xrightarrow{k_2} E + P$$

The global process consists of two consecutive reactions:

$$E + S \underset{k_{-1}}{\overset{k_1}{\rightleftharpoons}} ES \xrightarrow{k_2} E + P$$

During the reaction the concentration of ES complex reaches a constant value (hypothesis of stationary state): this value determines the rate of formation of the final products.

The rate of formation of the ES complex will be:

$$\mathbf{V_{formation} = k_1[E][S]}$$

While the rate of dissociation will be:

$$\mathbf{V_{dissociation} = k_{-1}[ES] + k_2[ES] = (k_{-1} + k_2)\,[ES]}$$

Under steady-state condition the rate of formation and the rate of dissociation of the ES complex will be the same.

$$\mathbf{k_1[E][S] = (k_{-1} + k_2)\,[ES]}$$

Since [E] is the concentration of the free enzyme and [ES] is the concentration of the enzyme-substrate complex, from the enzyme conservation law we have that their sum will give the total concentration of the enzyme, E_0:

$$\mathbf{[E] + [ES] = [E]_o}$$

So:

$$\mathbf{[E] = [E]_o - [ES]}$$

Combining with the previous expression:

$$\mathbf{k_1\,([E]_o - [ES])\,[S] = (\,k_{-1} + k_2)\,[ES]}$$

$$\mathbf{k_1\,[E]_o[S] - k_1\,[ES][S] = (\,k_{-1} + k_2)\,[ES]}$$

Multiplying both the side of the equation by -1**:**

$$\mathbf{-k_1\,[E]_o[S] + k_1\,[ES][S] = -\,(k_{-1} + k_2)\,[ES]}$$

$$\mathbf{k_1\,[ES][S] + (\,k_{-1} + k_2)\,[ES] = k_1\,[E]_o[S]}$$

Solving the equation for [ES], we get:

$$\mathbf{[ES] = k_1\,[E]_o[S]/\,(k_1[S] + k_{-1} + k_2)}$$

So the rate of formation of the product will be:

$$\mathbf{V = k_2[ES] = k_2\,k_1[E]_o[S]/\,(k_1[S] + k_{-1} + k_2)}$$

Dividing by k_1:

$$\mathbf{V = k_2[E]_o[S]/\,((k_{-1} + k_2)/k_1 + [S])}$$

The quantity $k_{-1} + k_2/k_1$ is indicated as K_M (Michaelis-Menten constant), so it is possible to write the so called Michaelis-Menten equation:[262]

$$\mathbf{V_0 = k_2[E]_o[S]/(K_M + [S])}$$

This equation allows to calculate the rate of the reaction as a function of the concentration of the substrate [S] for a given concentration of the enzyme. The trend of the function is hyperbolic (Figure 63).

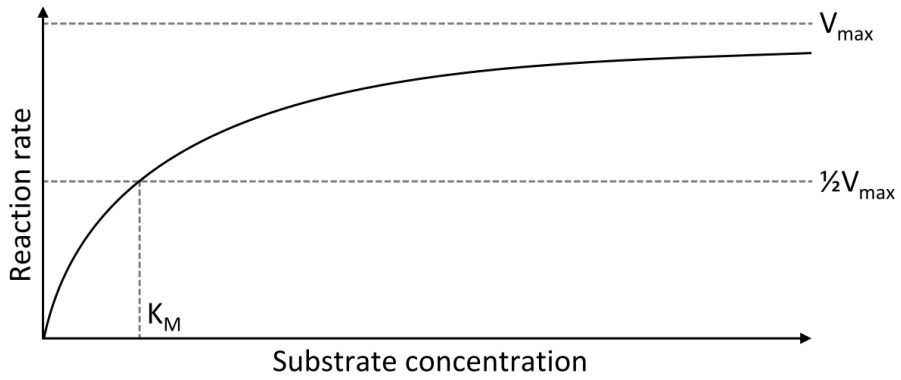

Figure 63. *"Saturation curve for an enzyme reaction showing the relation between the substrate concentration and reaction rate." by Thomas Shafee. The image is licensed under a creative common attribution CC BY 4.0 (https://creativecommons.org/licenses/by/4.0/) and it is available on Wikipedia.*

- At low substrate concentration, [S] << K_M. Under these conditions the reaction rate increases proportionally to the increase of substrate concentration (first order kinetic). Because the enzyme is in excess with respect to S, its concentration can be considered constant.

- When the concentration of the substrate is high, [S] >> K_M, V asymptotically approaches its maximum rate (V_{max}), indicating that all the enzyme is bound to substrate. The reaction becomes independent of [S] and further addition of substrate does not affect the rate of the reaction (zero-order kinetics). V_{max} only depend on the total concentration of the enzyme (E_0) and describe the maximal rate of decrease of substrate's concentration or growth of the product concentration in a specified time unit.

. $$\boldsymbol{V_{max} = k_2[E]_0}$$

The equation of Michaelis-Menten can be written as follows:

$$\mathbf{V = V_{max}\,[S]/(\,K_M + [S])}$$

If we consider the reaction rate being half of V_{max}

$$\mathbf{V = V_{max}/2}$$

Substituting V with $V_{max}/2$ in the previous equation we have:

$$\mathbf{V_{max}/2 = V_{max}\,[S]/\,(K_M + [S])}$$

So:

$$\mathbf{1 = 2\,[S]/\,(K_M + [S])}$$

Multiplying both the sides of the equation by (K_M+ [S]) we have:

$$\mathbf{K_M + [S] = 2\,[S]}$$

Or

$$\mathbf{K_M = [S]}$$

K_M constant represents the substrate's concentration for which the initial enzymatic conversion rate is equal to ½Vmax and depends not only on the enzyme and the substrate but also on reaction conditions such as pH and temperature.[263] It is an inverse measure of the affinity of the substrate for the enzyme: small k_M means high affinity as the rate will approach V_{max} with a lower substrate concentration.

K_M is characteristic for each enzyme and indicates the affinity of the enzyme to its substrate: the lower is K_M the lower is the S concentration that allows to have half of V_{max}, showing that enzyme and substrate tend to react. An high value of K_M indicates that an high concentration of S is needed to reach half of V_{max}.

A useful tool for the analysis of the kinetic behavior during the oxidation of L-tyrosine or L-DOPA is the Lineweaver–Burk double reciprocal plot, obtained from the reciprocal of the Michaelis-Menten kinetics equation.

$$\mathbf{1/V = K_M/(}\boldsymbol{V}_{\mathbf{max}}\mathbf{[S]) + 1/}\boldsymbol{V}_{\mathbf{max}}$$

The data are displayed as a plot of 1/V versus 1/[S] giving a straight line whose slope is K_M/V_{max} and whose intersection with the X-axe is $1/V_{max}$ (Figure 64).

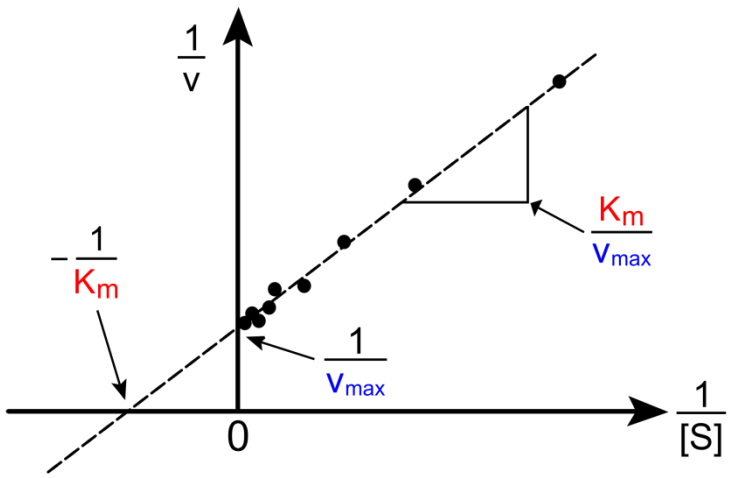

Figure 64. *An example of Lineweaver–Burk plot by Pro bug catcher. The image is licensed under a creative common attribution CC BY 3.0 (https://creativecommons.org/licenses/by-sa/3.0/) and it is available on Wikipedia.*

The kinetic of enzymatic reaction can be altered by the presence of inhibitor that are classified into three main groups:[260]

- The **competitive inhibitors** bind to unoccupied enzymes' active sites competing with the substrate and altering the formation of ES complexes, but cannot bind to ES. The affinity of this substrate to the enzyme molecule decreases with a consequent increase of the K_M, since an higher concentration of S is needed to reach half of V_{max} that remains unchanged because the competition between substrate and inhibitor may be surpassed when the substrate's concentrations dramatically exceeds the concentration of the inhibitor (Figure 65).

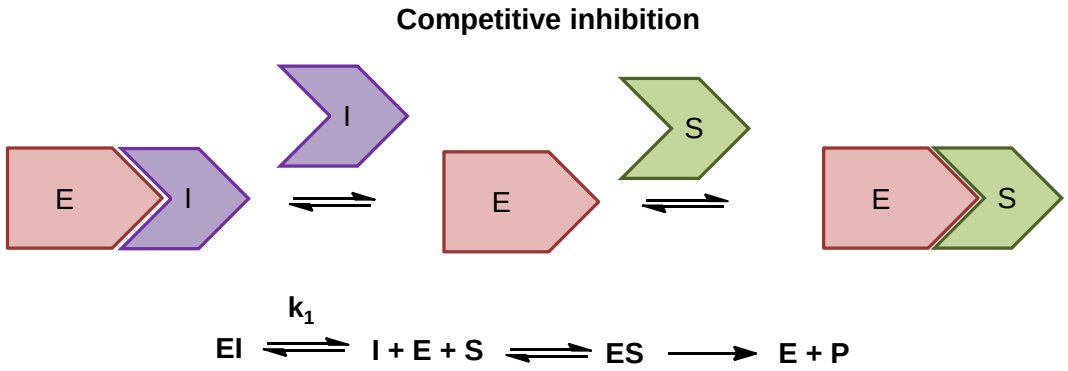

Figure 65. *Diagram showing competitive inhibition.*

- The **non-competitive inhibitors** have the same affinity to free enzyme (E) and to enzyme-substrate complex (ES), so they can bind to the enzyme without blocking substrate's access to enzyme's active site but altering the enzyme structure. For this reason, catalytic properties of enzyme are modified and V_{max} decreases but K_M remains the same (Figure 66).

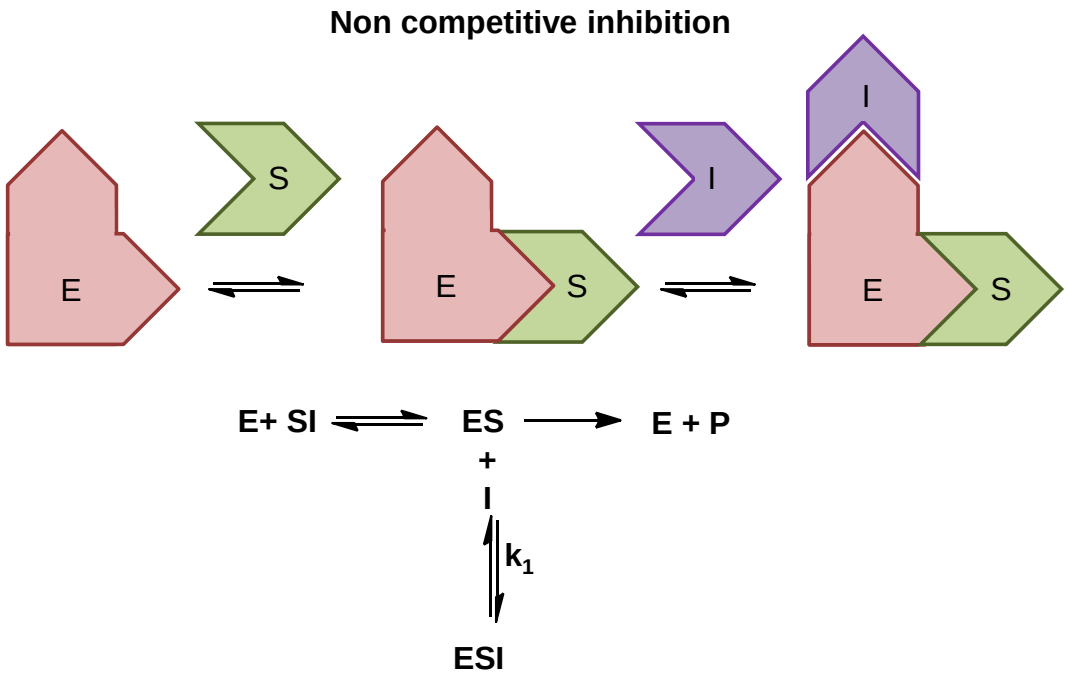

Figure 66. *Diagram showing non-competitive inhibition.*

- **Mixed inhibitor** binds to both E and ES partially blocking an access of substrate to enzyme's active site. The effect on kinetic constants depends on the affinity of E and ES to the inhibitor. It leads to an increase of K_M value and a decrease of V_{max} value (Figure 67).

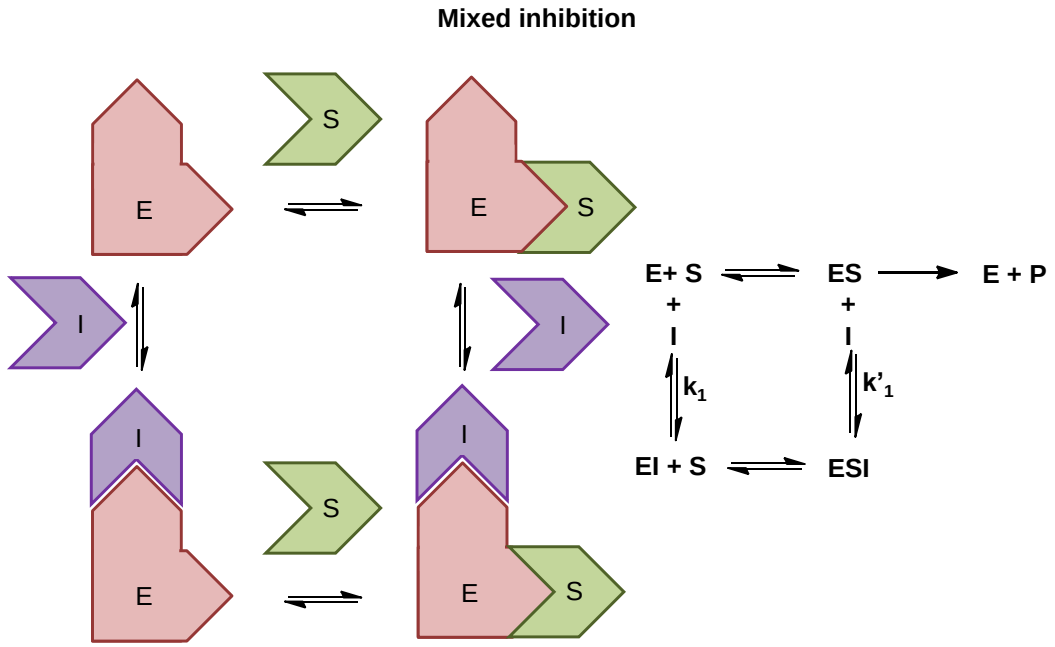

Figure 67. *Diagram showing mixed inhibition.*

Figure 68 shows the Lineweaver-Burk plots of the different kinds of inhibition.

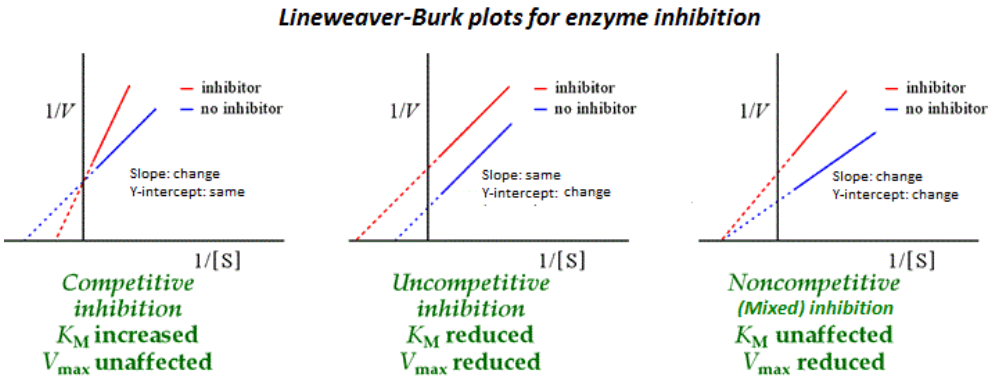

Figure 68. "Double reciprocal plots for competitive, uncompetitive, and noncompetitive (mixed) inhibitions." *by Bizz11. The image is licensed under a creative common attribution CC0 (https://creativecommons.org/publicdomain/zero/1.0/deed.en)and it is available on Wikipedia.*

The inhibition kinetics of the enzyme by the of 2-S-lipoylcaffeic acid was analyzed by the Lineweaver–Burk plots compared to data obtained in the absence of inhibitor (control). Experiments were carried out using the same protocol described above, except for varying concentrations of L-tyrosine or L-DOPA.

The plots for tyrosinase activity in the presence of increasing concentrations of L-DOPA yield a family of straight lines with different slopes intersecting one another in the fourth quadrant (Figure 69).

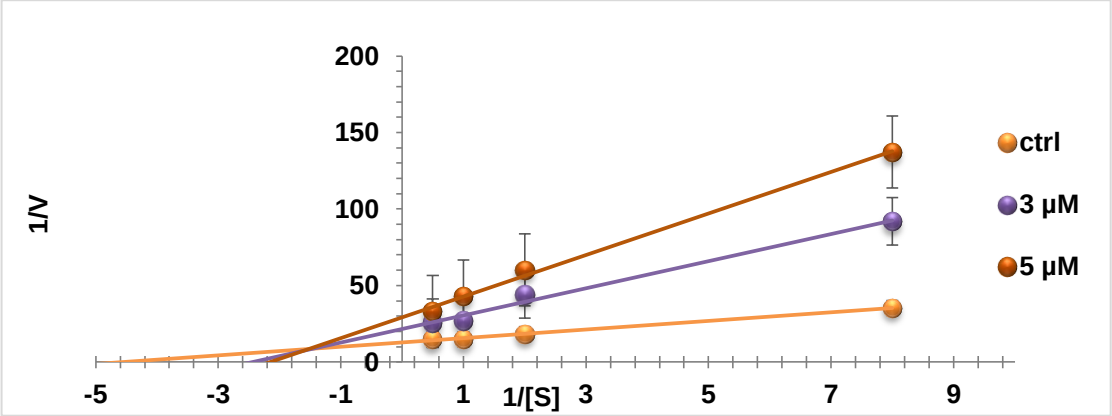

Figure 69. *Lineweaver–Burk plots for inhibition of mushroom tyrosinase in presence of 2-S-lipoylcaffeic acid. Data are expressed as mean ± SD of three independent experiments, each performed in duplicate.*

While the concentration of the 2-S-lipoylcaffeic acid increased, V_{max} decreased and K_M increased. These results suggest a mixed type of inhibition inhibitor. When L-DOPA was added as a substrate, increasing concentrations of the inhibitor increases the K_M of tyrosinase, while it produced a decrease of V_{max}, as observed in the family of lines with different slopes and intercept on the X-axe.

Figure 70 shows that in the presence of 2-S-lipoylcaffeic acid both the rate of the reaction and V_{max} decrease.

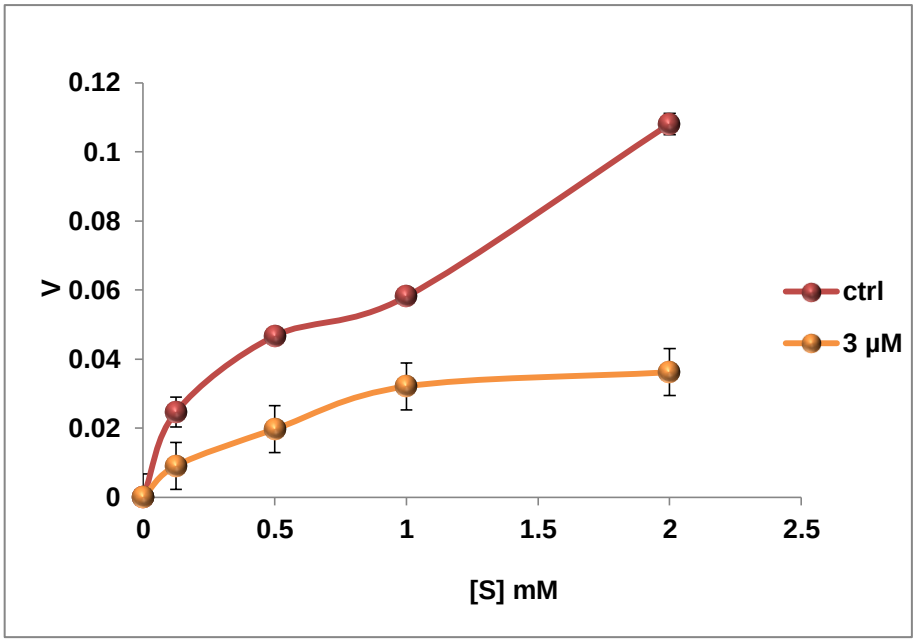

Figure 70. *Course of enzymatic kinetic of the tyrosinase induced oxidation of L-DOPA in the presence and in the absence of 2-S-lipoylcaffeic acid. Data are expressed as mean ± SD of three independent experiments, each performed in duplicate.*

The effect of the mushroom tyrosinase on the inhibitor was examined to verify if 2-S-lipoylcaffeic acid was oxidized by the enzyme. The inhibitor (250 µM) was incubated in the presence of the enzyme under the same conditions of the spectrophotometric assay. HPLC analysis of the oxidation mixture after 10 minutes does not show any consumption of the inhibitor suggesting that it is not an alternative substrate of the enzyme. The same result was obtained in the presence of L-DOPA.

The effect of preincubation of the enzyme was investigated performing the spectrophotometric assay by adding the inhibitor (3 µM final concentration) to the 50 mM phosphate buffer (pH 6.8) containing tyrosinase solution, after ten minutes. After further 10 minutes absorbance was registered (475 nm) and the values obtained was comparable those obtained without preincubation.

Another control experiment was run to rule out the possibility that the abatement of absorbance at 475 nm was due to a redox exchange or addition to dopachrome. The experiment was performed as above but the inhibitor was added to the reaction mixture after 10 minutes reaction between tyrosinase and L-DOPA.

The value of absorbance at 475 nm after 5 minutes did show not difference with respect to values registered before the addition of the inhibitor, excluding a possible reaction between 2-S-lipoylcaffeic acid and dopachrome.

In separate experiments the ability 2-S-lipoylcaffeic acid (100 µM final concentration) to inhibit the monophenolasic activity of mushroom tyrosinase was investigated, using L-tyrosine instead of L-DOPA.

Figure 71 shows the result when L-tyrosine is used as substrate. Also in this case, a strong inhibition activity was observed (>90%).

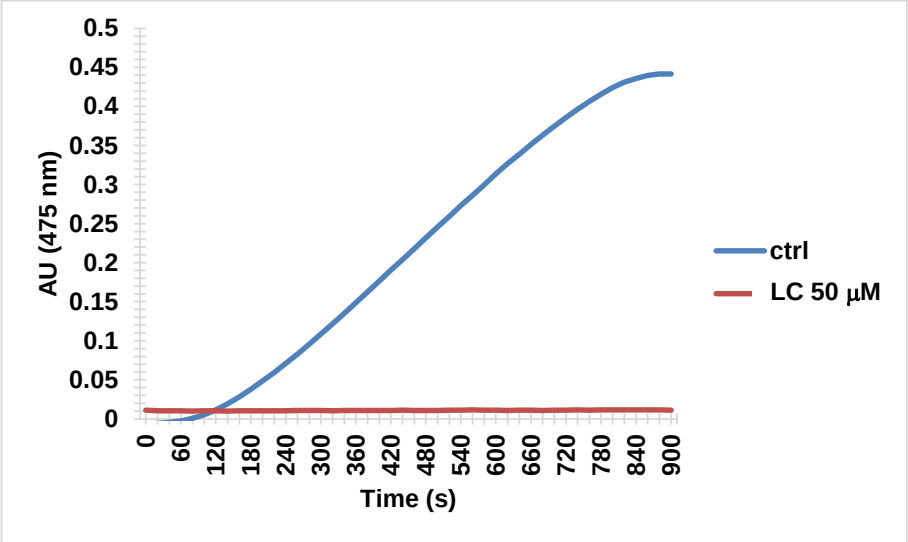

Figure 71. *Spectrophotometric course of tyrosinase induced oxidation of L-tyrosine in the presence and in the absence of 2-S-lipoylcaffeic acid (LC). Data are expressed as mean of three independent experiments, each performed in duplicate (SD $\leq$ 5%).*

The assay was performed at different concentrations of inhibitor. Figure 72 shows percent of inhibition *vs*. concentration, pointing out that 50 µM 2-S-lipoylcaffeic acid is able to induce a maximum inhibition of *ca.* 90%.

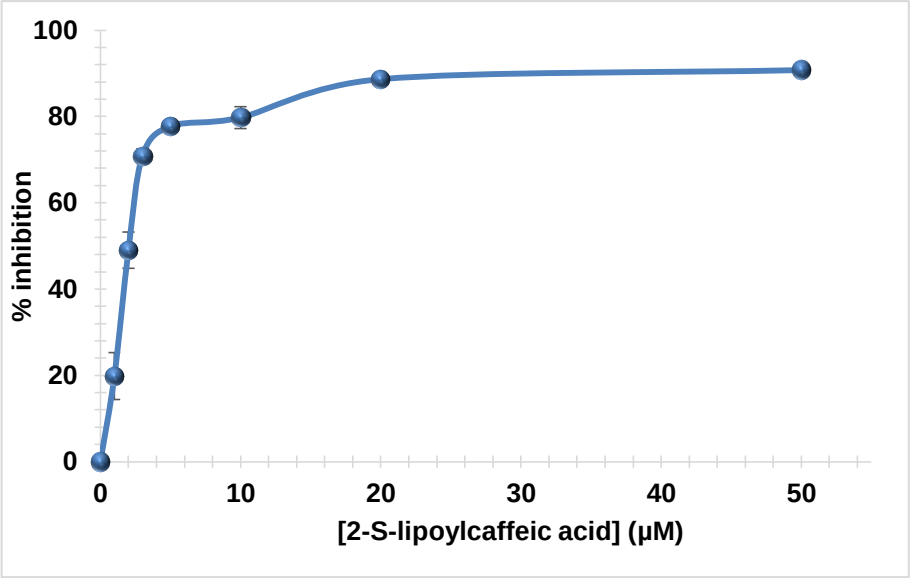

Figure 72. *Percent of inhibition of mushroom tyrosinase activity versus 2-S-lipoylcaffeic acid concentration using L-tyrosine as substrate. Data are expressed as mean ± SD of three independent experiments, each performed in duplicate*.

IC_{50} value was determined by linear interpolation between two points limiting the range including 50% inhibition (Figure 73). This value was 3.22 ± 0.02 µM. This values was 2.0 ± 0.1 µM.

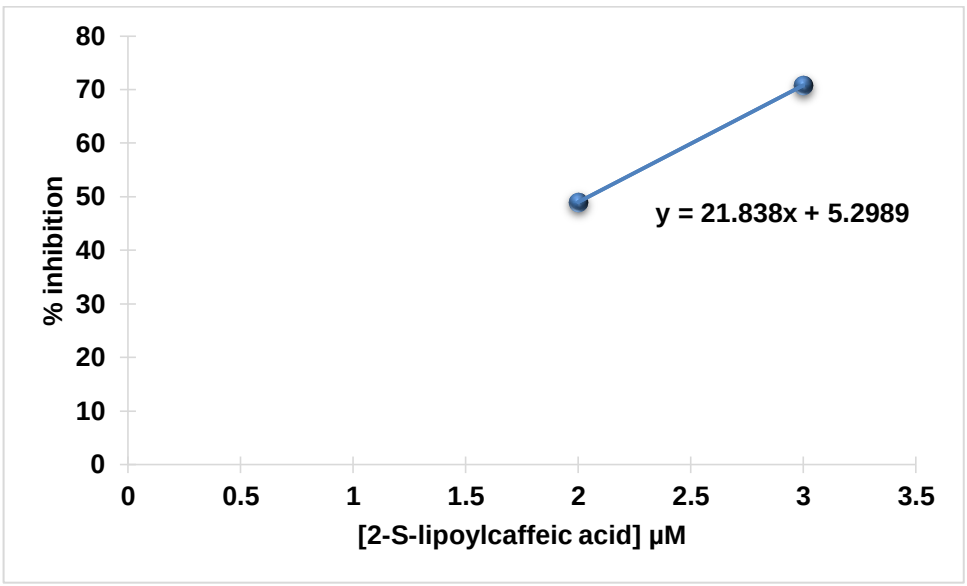

Figure 73. *Plot used for IC_{50} determination by linear interpolation using L-tyrosine as substrate.*

In conclusion these experiments highlighted the 2-S-lipoilcaffeic acid adduct as a potent non-competitive inhibitor of tyrosinase either in the tyrosine or in the DOPA oxidation with values of IC_{50} inhibition concentrations far lower those of the reference inhibitor kojic acid.

Further experiments on cell cultures will be essential to evaluate the actual toxicity of this compound on keratinocyte/melanocytes and to confirm the inhibitory activity. This will represent the premise to evaluate the potential of this compound as novel skin depigmenting agent.

CHAPTER 5

Conclusions

The results reported in this thesis provide important advances in the definition of the mechanism of toxicity of pheomelanic pigments in the absence of light, and the origin of the eumelanin broadband absorption spectrum. Following investigation of the properties of indole precursors with special reference to DHICA, a bioinspired photoprotective agent was synthesized and tested and the impact of esterification on 5,6-dihydroxyindole-2-carboxylic acid antioxidant activity and oxidative polymerization was studied. Moreover, a conjugate of caffeic acid with dihydrolipoic acid was prepared and its capacity of inhibiting mushroom tyrosinase activity was evaluated.

The main outcomes of this thesis can be summarized as follows:

- Red Hair Pheomelanin (RHP), and to a minor extent Black Hair Eumelanin (BHE), can exert a light-independent pro-inflammatory and pro-oxidant action in keratinocytes cultures, possibly being internalized by endocytosis.[264] RHP would lower endogenous antioxidant levels and produce ROS, thus accounting for a permanent abatement of the antioxidant defense. This chronic oxidative stress condition could favor a chronic pro-inflammatory status, underlying cause of melanoma development in red hair phenotypes.[105] Without excluding the recognized role of UV radiation, these data confirm that UV-independent events play an important function in carcinogenic processes pointing out that new strategies of prevention, other than sunprotection, could be necessary, with particular attention to the most susceptible individuals.

Results relative to this part of the project were reported in the following publication:

✓ "Light-indipendent pro-inflammatory and pro-oxidant effects of purified human hair melanins on keratinocyte cell cultures." (**2016**) S. Lembo , R. Di Caprio, **R. Micillo**, L. Panzella, A. Balato, A. Napolitano, G. Monfrecola *Exp. Dermatol.* 16, DOI:10.1111/exd.13122.

- Both eumelanin and pheomelanin can play a "catalytic" role promoting the shuttling of electrons between oxidants and reductants. Indeed melanin can be reduced accepting electrons from biological relevant antioxidant such as NAD(P)H and/or GSH and can be oxidized donating electrons to biological oxidant, *e.g.* O_2, generating ROS. In particular the reverse engineering experiments showed that pheomelanin has a higher oxidative potential compared to eumelanin and could disrupt cellular redox balances through a redox-buffering mechanism. The pro-oxidant properties of polycysteinyldopamine (pCDA), a red hair-inspired polydopamine-like polymer able to deplete GSH and NADH levels, further confirm the ability of this pigment to mediate electron exchange.

Results relative to this part of the project were reported in the following publications:

✓ "Reverse Engineering Applied to Red Human Hair Pheomelanin Reveals Redox-Buffering as a Pro-Oxidant Mechanism." (2015) E. Kim, L. Panzella, **R. Micillo**, W.E. Bentley, A. Napolitano, G.F. Payne *Sci Rep.* 5: DOI: 10.1038/srep18447.

✓ "Tailoring melanins for bioelectronics: polycysteinyldopamine as ion conducting redox-responsive polydopamine variant for pro-oxidant thin films." (**2015**) N. F. Della Vecchia, R. Marega, M. Ambrico, M. Iacomino, **R. Micillo**, A. Napolitano, D. Bonifazi, M. d'Ischia *J. Mater. Chem. C.* 3, 6525–6531.

- Experimental and computational data presented in this thesis represent a broad comparative investigation on the formation and evolution of eumelanin chromophores, a process involving three phases

PHASE I: the rapid melanochrome generation is due to the contributes of the intrinsic chromophores of the oligomers in a stable oxidation state. The presence of the 2-carboxyl group[192] influences the absorption properties of DHICA melanin decreasing the generation of melanochrome. Comparing spectrophotometric oxidation courses of monomers and dimers, it was observed that the spectra of 4,4'-dimer of DHICA are almost superimposable to those of the corresponding monomer, while in the case of DHI, monomer and dimers displayed marked differences, especially in this first phase.

PHASE II: the band broadening process is due to an intermolecular reorganization/equilibration of redox states. Acidification but not alkalization affects

the chromophores, suggesting that the chromophoric species could be present in an ionized quinonoid form at neutral pH. Both melanochromes and eumelanin final chromophores can be partially reduced with sodium dithionite but are not affected by further addition of oxidizing agents. The redox mixing would explain the resistance to oxidation and, at least in part, to reduction. Mutual perturbation would lead to the broadening of the absorption band, ascribable to extrinsic contributions (as suggested by the inhibitory effect of PVA). Computational data showed that the formation of a HQ/Q dimer is able to generate a large band in the visible region due to stacking processes between dimers pairs. These process are favored in DHI rather than in DHICA because of the twisted conformation of the carboxy-derivative.

PHASE III: the black color is a consequence a stronger π-electron stabilization in the solid state.

Overall, the data concur to point out the importance of intermolecular interaction between catechol and quinone moieties or related extended quinone moieties as one of the major determinant of the band broadening and the black color of eumelanin. The final visible chromophores are determined by both intrinsic and extrinsic contributions in the case of DHI melanin, while in the case of DHICA melanin the extrinsic contribute is predominant.

These results constitute a solid background for the design of eumelanin-inspired functional materials tailored to dermocosmetic applications,[147] such as hair dyes or photoprotective agents.

Results and concepts relative to this part of the project were reported in the following publication:

- ✓ "Eumelanin broadband absorption develops from aggregation-modulated chromophore interactions under structural and redox control." (**2017**) **R. Micillo**, L. Panzella, M. Iacomino, G. Prampolini, I. Cacelli, A. Ferretti, O. Crescenzi, K. Koike, A. Napolitano, M. d'Ischia, *Sci Rep*. DOI: 10.1038/srep41532.

- Oleoyl-MeDHICA, afforded a significant protection to the skin against the UVB-induced erythema. Further experiments will be essential to evaluate the mechanism of action of this DHICA derivative and investigate its antioxidant properties. Preliminary data presented in this thesis suggest its potential use as topical photoprotective agents.

Concepts relative to this part of the project were reported in the following publications:

- ✓ "A new light on the dark DNA damages." (**2017**) **R. Micillo**, S. Lembo, G. Monfrecola, *SKINmed Journal*, 15: 409-411.
- ✓ "A reappraisal of the biological functions of melanins and melanogens: The role of 5,6-dihydroxyindole-2-carboxylic acid (DHICA) in skin (photo)protection." (**2014**). **R. Micillo**, L. Panzella, G. Fabbrocini, F. Ayala, G. Monfrecola *Journal of Plastic Dermatology*, 101: 252-255.

- The impact of carboxyl group esterification on DHICA, structural properties and antioxidant activity were evaluated pointing out that combining the antioxidant properties of DHICA with the more favorable solubility properties in alcoholic or other common organic solvents of its methyl ester could be a good strategy to exploit this material in a variety of applications including dermocosmetic formulations.[265]

Results and concepts relative to this part of the project were reported in the following publications:

- ✓ ""Fifty Shades" of Black and Red or How Carboxyl Groups Fine Tune Eumelanin and Pheomelanin Properties." (**2016**) **R. Micillo**, L. Panzella, K. Koike, G. Monfrecola, A. Napolitano, M. d'Ischia *Int. J. Mol. Sci.* 17, 746.
- ✓ "Assessing the impact of carboxyl group esterification on the antioxidant activity, structural properties and stability of 5,6-dihydroxyindole-2-carboxylic acid melanins." **R. Micillo**, L. Panzella, M. Iacomino, O. Crescenzi, K. Koike, G. Monfrecola, A. Napolitano, M. d'Ischia (submitted).

- Mushroom tyrosinase inhibition assays and definition of enzyme kinetics of 2-S-lipoilcaffeic acid proved that this compound is a potent mixed inhibitor of the enzyme either using tyrosine or dopa as substrate, with values of the IC_{50} inhibition concentrations far lower those of the reference inhibitor kojic acid (2.0 μM and 3.22 μM vs. 340 μM in the case of kojic acid). Further experiments will be essential

to evaluate the cytotoxicity of this compound on keratinocyte/melanocytes and to confirm the inhibitory activity *in vitro* but preliminary results indicate a good potential of the compound for application as skin depigmenting agent.

Results and concepts relative to this part of the project were reported in the following publication:

- ✓ "Melanin pigmentation control by 1,3-thiazolidines: does NO scavenging play a critical role?" (**2016**) Napolitano, **R. Micillo**, G. Monfrecola *Exp Dermatol.* 25: 596-597.

Some of the results and the concepts relative to this PhD thesis were presented to the following international meetings:

- 19th European Society for Pigment Cell Research Meetings (Edinburgh, 2015)
  "Why are eumelanins black? A bottom-up approach to structure-absorption-color relationships." **R. Micillo**, L. Panzella , O. Crescenzi , K. Koike , G. Monfrecola , M. d'Ischia , A. Napolitano. Poster awarded with the ESPCR Travel award.
- 20th European Society for Pigment Cell Research Meetings (Milan, 2016)
  "The eumelanin carboxyl conundrum: unexpected impact of esterification on 5,6-dihydroxyindole-2-carboxlic acid antioxidant activity and oxidative polymerization." **R. Micillo**, L. Panzella, M. Iacomino, O. Crescenzi, K. Koike, G. Monfrecola, A. Napolitano, M. d'Ischia.

CHAPTER 6

6.1 Pheomelanin pigments: (photo)toxicity and pro-oxidant properties

6.1.1 Materials

Hydrogen peroxide (30% v/v), *threo*-1,4-dimercapto-2,3-butandiol (*d*,*l*-dithiothreitol), sodium metabisulfite, proteinase K from *Tritirachium album* (EC 3.4.21.64), polyethylene(10)isooctylphenyl ether (Triton X-100), L-glutathione (GSH), L-Glutathione oxidized (GSSG), nicotinamide adenine dinucleotide phosphate reduced form (NADPH), nicotinamide adenine dinucleotide reduced form (NADH), ethylenediaminetetraacetic acid disodium (EDTA-Na_2), 3,4-Dihydroxy-L-phenylalanine (L-DOPA), dopamine hydrochloride, horseradish peroxidase (HRP; donor: H_2O_2 oxidoreductase, EC 1.11.1.7), sodium *tert*-butoxide, thiobarbituric acid, trichloroacetic acid were commercially available and were used as obtained

5-*S*-cysteinyldopa (5SCD),[110] and 5-S-cysteinyldopamine (CDA)[266] were prepared as reported. All solvents were HPLC grade. Bidistilled deionized water was used throughout the study. CDA thin film prepared by Dr. M. Iacomino (University of Naples) allowing the polymer (10 mM) to autoxidize in bicarbonate buffer (50 mM, pH 8.5) in the presence of quartz and glass cuttings.

Biological samples. Red, black and white hair locks were donated from healthy volunteers. Informed consent was obtained from all subjects. Only hair samples that had not received dyeing or other chemical treatments were included in the present study. In particular, hair was collected from the nuchal region, as the proximal end was considered the less light exposed and selected for melanin extraction.

6.1.2 Methods

HPLC analyses were performed on a Agilent 1100 binary pump instrument equipped with and a SPD-10AV VP UV-visible detector and electrochemical detector (ESA Coulochem2) using a Synergi Hydro-RP 80A column (250 x 4.60 mm 4 μm).

For NADPH analysis, UV detection was used (wavelength set at 340 nm), with 0.2 M phosphate buffer (pH 6.0) /methanol 86:14 v/v as the eluent, at a flow rate of 0.7 mL/min.

For GSH analysis the EC detector was set at +500 mV *vs.* an Hg/Hg_2Cl_2 reference electrode. Phosphate buffer 0.01 M (pH 3.0) containing methanol 98:2 (v/v) was used as the eluent, at a flow rate of 0.7 mL/min

For thiazole-2,4,5-tricarboxylic acid (TTCA) and pyrrole-2,3,5-tricarboxylic acid (PTCA) analyses, 1% formic acid (pH altered to 2.8 with sodium hydroxide)/methanol 97:3 (v/v) as the eluent, at a flow rate of 0.7 mL/min. Detection wavelength was set at 254 or 280 nm.

UV spectra were recorded on a Jasco V-730 Spectrophotometer.

6.1.3 Isolation of hair melanin[32,90]

Pigment purification from red and black hair was carried out according to the following procedure.[84] Briefly, hairs (5.0 g) were washed with acetone/dichloromethane/diethyl ether (2:1:1), to remove sebum, and left to air dry overnight. Subsequently they were cut into short segments approximately 2 mm long and submerged with 0.1 M phosphate buffer (pH 7.4). The suspension obtained was homogenized with a glass/glass potter and *d,l*-dithiothreitol (625 mg) was added under a stream of argon; thereafter, the reaction mixture underwent vigorous stirring at 37°C for 18h. Proteinase K (40 mg) and *d,l*-dithiothreitol (600 mg) were added under an argon atmosphere and the mixture was stirred at 37°C for 18 h and centrifuged for 20 min (3000 rpm, 4°C). The precipitate was washed with 1% acetic acid (3×) and the supernatant was acidified to pH 3 with 4M. HCl, all stored at 4°C overnight and then centrifuged for 20 min (3000 rpm, 4°C). The new precipitate was washed with 1% acetic acid (3×) again, and the combined precipitates were suspended in 0.1 M phosphate buffer (pH 7.4) and treated with *d,l*-dithiothreitol (600 mg) and proteinase K (40 mg). After 18h the mixture was treated as above, and the combined precipitates were subjected to 3 further digestions: protease K (24 mg) and *d,l*-dithiothreitol (360 mg), protease K (2 mg) and *d,l*-dithiothreitol (8.4 mg), protease K (3mg) and *d,l*-dithiothreitol (12.6 mg). Finally, a pellet was generated, suspended in deaerated phosphate buffer (20 mL), and treated with Triton X-100 (500 µL). The suspension was allowed to stir for 4h at 37°C and then centrifuged. The pellet obtained was washed three times with 1% acetic acid and once with nanopure water (12000 rpm, for 20 min at 4°C). The supernatant was treated as above, acidified to pH 3 with 4M HCl, all stored at 4°C overnight and then centrifuged for 20 min (3000 rpm, 4°C). The combined precipitates were subjected to another digestion step with protease K (83 mg) and *d,l*-dithiothreitol (12.6 mg). The final pigment pellet collected by centrifugation was washed and lyophilized. The overall purification procedure afforded 157 mg of pigment from black hairs, 124 mg from red and 65 mg from white ones.

6.1.4 Preparation of synthetic melanins

Synthetic melanins were prepared by enzymatic oxidation of dihydroxyphenylalanine (DOPA),[88] 5-S-cysteinyldopa[75] and cysteinyldopamine[267] following previously reported procedures.

6.1.5 Oxidative degradation

Finely minced hair (10 mg) or purified hair melanins (5 mg) were suspended in 1 M NaOH (1mL) and treated with 30% H_2O_2 (50 µL, final concentration 1.5%) at room temperature and under vigorous stirring for 24h. The mixture was treated with 5% $Na_2S_2O_5$ (200 µL), taken to pH4 with 4 M HCl, filtered through nylon membranes (13 mm, 0. 45 µm) and analyzed by HPLC.[90] Melanin content of RHP and BHE was estimated by comparison of the yields of TTCA and PTCA, respectively, with those of reference synthetic pigment from 5- S-cysteinyldopa for pheomelanin[268] and 5,6-dihydroxyindole-2-carboxylic acid (DHICA) for eumelanin.[269] A value of 2.8% (w/w) for RHP and 2.6% (w/w) for BHE was obtained.

6.1.6 EDTA treatment

Integrative experiments with the 3 compounds (RHP*, BEH*, WHP*) previously washed with EDTA, a strong chelating agent, have been performed to ensure removal of drugs or other substances possibly derived from environmental contamination. Purified RHP or BHE (3 mg) were suspended in 40 mM EDTA-Na_2 solution (pH 5.8, 3 mL) and allowed to stir at room temperature overnight. Samples were centrifuged a 5000 rpm for 15 min at 20°C and the precipitates were washed six times with ultrapure water and lyophilized.[270]

6.1.7 Determination of cellular antioxidants (GSH and NADPH)

HaCat cells were suspended in 600 µl PBS and sonicated (Sonicator bath Seneco Science, Milan, Italy) with 3 short burst of 30 sec followed by intervals of 30 sec to allow cooling. Cell debris was removed by centrifugation at 4°C for 30 min at 7500 rpm, and the lysates were analyzed by HPLC.

6.1.8 Determination of cellular thiobarbituric acid reactive substances (TBARS)

Determination of thiobarbituric acid reactive substances (TBARS) was performed spectrophotometrically by an adapted procedure.[271,272] In brief, 300 µL of lysate was treated with 10% trichloroacetic acid (0.5 mL), the mixture was heated at 95 °C for 15 min with

stirring and then allowed to cool and centrifuged at 3000 rpm at 4 °C for 15 min. The supernatant was added to a 0.67% solution of thiobarbituric acid and taken at 95 °C for 15 min. After cooling the absorbance of the solution at 532 nm was measured and TBARS quantitated using a molar extinction coefficient of $1.56 * 10^5$ $M^{-1}cm^{-1}$.

6.1.9 GSH and NADH oxidation

A 150 μM solution of GSH or a 300 μM solution of NADH in 0.1 M phosphate buffer (pH 7.4) was allowed to stand at room temperature under vigorous stirring in the presence and in the absence of pCDA (1 mg) or pCDA thin film. Aliquots of the reaction mixtures were periodically withdrawn and analyzed by HPLC with UV and electrochemical detector.

6.2 Eumelanin pigments: (photo)protective and antioxidant properties

6.2.1 Material

3,4-Dihydroxy-L-phenylalanine (L-DOPA), dopamine hydrochloride, hydrogen peroxide (30% v/v), potassium ferricyanide, sodium periodate, nickel sulfate eptahydrate, copper acetate, zinc sulfate heptahydrate, cobalt sulfate, ferric chloride, 4-(2-hydroxyethyl)-1-piperazineethanesulfonic acid (HEPES), ceric ammonium nitrate (CAN), sodium dithionite, sodium borohydride, horseradish peroxidase (HRP; donor: H_2O_2 oxidoreductase, EC 1.11.1.7) and sodium *tert*-butoxide, oleoyl chloride, triethylamin (TEA), anhydrous tetrahydrofuran (THF) 1,1-diphenyl-2-picrylhydrazyl (DPPH), 2,4,6-tris(2-pyridyl)-s-triazine, and 6-hydroxy-2,5,7,8-tetramethylchroman-2-carboxylic acid (trolox) were purchased from Sigma-Aldrich. All solvents were HPLC grade. Bidistilled deionized water was used throughout the study.

The ability of dioleoyl-MeDHICA to reduce UVB-induced skin erythema was tested in healthy human volunteers. 10 healthy volunteers (both sexes) of skin types II and III, with a mean age of 35 ± 13 years were selected. All the volunteers were informed in detail of the nature of the study and the procedures involved and gave their written consent. The subjects did not suffer from any ailment and were not on medication at the time of the study.

6.2.2 Methods

HPLC analyses were performed on a Agilent 1100 binary pump instrument equipped with and a SPD-10AV VP UV-visible detector using an octadecylsilane-coated column, 250 mm x 4.6

mm, 5 μm particle size (Phenomenex Sphereclone ODS) at 0.7 mL/min. Detection wavelength was set at 280 nm.

Analysis of oxidation mixtures of melanin precursors was performed using 1% formic acid: methanol 60:40 v/v as eluant in the case of MeDHICA and the following gradient in the case of DHICA: 1.5% formic acid (eluant a)/ methanol (eluant b) from 5 to 90% b, 0-45 min.

Preparative HPLC was carried out on an instrument coupled with a UV detector set at 280 nm using an Econosil C18 (10 μm, 22 x 250 mm), at 15 mL/min, and 1.5% formic acid: methanol 85:15 as the eluent in the case of DHICA and 1% formic acid: methanol 60:40 v/v in the case of MeDHICA.

UV spectra were recorded on a Jasco V-730 Spectrophotometer.

EPR measurements were performed using an X-band (9 GHz) Bruker Elexys E-500 spectrometer (Bruker, Rheinstetten, Germany), equipped with a super-high sensitivity probe head.

Samples were transferred to flame-sealed glass capillaries which, in turn, were coaxially inserted in a standard 4 mm quartz sample tube. Measurements were performed at room temperature. The instrumental settings were as follows: sweep width, 100 G; resolution, 1024 points; modulation frequency, 100.00 kHz; modulation amplitude, 2.0 G. The amplitude of the field modulation was preventively checked to be low enough to avoid detectable signal overmodulation. Preliminarily, EPR spectra were measured with a microwave power of ~0.5 mW to avoid microwave saturation of resonance absorption curve. Several scans, typically 16, were accumulated to improve the signal-to-noise ratio. Successively, for power saturation experiments, the microwave power was gradually incremented from 0.02 to 160 mW. The g value and the spin density were evaluated by means of an internal standard, Mn^{2+}-doped MgO, prepared by a synthesis protocol reported in literature.[273]

Skin erythema was induced by UVB irradiation using an ultraviolet lamp (Skin-tester Kit, Cosmedico Medizintechnik GmbH, Scwennigen, Germany) which emitted in the range of UVB. The lamp is equipped with a six grid-containing square opening through which UVB-light is emitted. The grids have different abilities to attenuate the UVB-light so that the powers of the light let through the opening are different. (98.3, 122, 153, 192, 240, 300 mJ/m^2). Staff and participant wore UV protective glasses.

The induction of erythema was monitored by means of a reflectance visible spectrophotometer (X-rite mod.158- 964, Michigan USA having) 45° illumination and 0° viewing angle.

MALDI analysis mode was run on a AB Sciex TOF/TOF 5800 instrument using 2,5-dihydroxybenzoic acid as the matrix and the melanin applied to the plate from a fine suspension in ethanol obtained by homogenization in a glass to glass potter. Spectrum represents the sum of 15,000 laser pulses from randomly chosen spots per sample position. Raw data are analyzed using the computer software provided by the manufacturers and are reported as monoisotopic masses.

6.2.3 Preparation of 5,6-dihydroxyindole monomers

5,6-dihydroxyindole (DHI),[85] 5,6-dihydroxyindole-2-carboxylic acid (DHICA)[85] and 5,6-dihydroxy-*N-methyl*indole (N-MeDHI) were prepared as described.[199]

MeDHICA was prepared starting from DOPA methylester prepared by reacting DOPA (2.0 g) in methanol (20 mL) with 96% sulfuric acid (2 mL) under reflux. After 24 h the mixture was allowed to cool and sodium bicarbonate was added to neutrality. The solution thus obtained was reacted in water with potassium ferricyanide under the same conditions used for preparation of DHI[85] and after 15 min extracted with ethyl acetate to give pure Me-DHICA (1.3 g, 61% yield).

6.2.4 Preparation of 5,6-dihydroxyindole dimers

2,2'-biindolyl,[274] 2,4'-biindolyl and 2,7'-biindolyl from DHI were prepared as previously described with slight modifications. Briefly, a solution of DHI (300 mg, 2.0 mmol) in 0.05 M phosphate buffer (pH 6.8) (120 mL) was treated with horseradish peroxidase (36 U/mL) and H_2O_2 (266 μL of a 30% solution, 2.3 mmol). After 25 s, the oxidation reaction was stopped by addition of a solution of sodium dithionite and rapidly extracted with ethyl acetate. After acetylation of the residue obtained following evaporation of the combined organic layers with acetic anhydride-pyridine overnight at room temperature the mixture was fractionated by column chromatography (gradient elution, $CHCl_3$–ethyl acetate from 9:1 to 6:4) to afford the 2,7'-biindolyl (45 mg, 10% yield, >95% pure) and the 2,4'-biindolyl (53 mg, 11%, >95% pure) as acetylated derivative. For isolation of the 2,2'-biindolyl as the *O*-acetyl derivative (30 mg, 12% yield) DHI (150 mg, 1.0 mmol) was oxidized in air in 0.05 M HEPES buffer (pH 7.5) in the presence of $NiSO_4 \cdot 7H_2O$ (560 mg, 2.0 mmol). After acetylation treatment of the

ethyl acetate extracts the residue was taken up in acetone and the product was recovered by filtration as white prisms.

4,4'-Biindolyl from DHICA was prepared as previously described[29] with modifications. A solution of DHICA (100 mg, 0.51 mmol) in 0.1 M HEPES buffer (pH 7.5) (495 mL) was treated with copper acetate (1 molar equivalent) and the reaction mixture was taken under vigorous stirring. After 10 min, the oxidation reaction was stopped by addition of sodium dithionite, acidified to pH 2 and rapidly extracted with ethyl acetate. The residue obtained following evaporation of the combined organic layers was fractionated by preparative HPLC. (16 mg, 16% yield, >90% pure).

4,4'-Biindolyl from Me-DHICA was prepared as previously described[194] with modifications. A solution of Me-DHICA (110 mg, 0.51 mmol) in 0.2 M HEPES buffer (pH 7.5) (33 mL) was treated with cobalt sulfate (1 molar equivalent) and the reaction mixture was taken under vigorous stirring. After 20 min, the oxidation reaction was stopped by addition of sodium dithionite, acidified to pH 2 and rapidly extracted with ethyl acetate. The mixture was fractionated by preparative HPLC. (18 mg, 12% yield, >90% pure).

6.2.5 Oxidation of 5,6-dihydroxyindole monomers and dimers

15 μL of a 10 mM solution of the appropriate indole monomer or 4,4'DHICA-dimer were added to 3 mL of 0.1 M phosphate buffer (pH 7.0) to reach a final concentration of 50 □M followed by 2 molar equivalents of potassium ferricyanide (30 μL of a 10 mM solution in water). In the case of DOPA and DA the reaction was carried out with 6 molar equivalent of ferricyanide. The reaction mixtures were taken under vigorous stirring and periodically analyzed by UV-vis spectrophotometry. Spectra were registered at 5 min, 2 h and 24 h. After 5 min in air, reaction mixtures were degassed and kept under stirring in an argon atmosphere.

In other experiments the reaction was performed:

i) in the presence of sodium periodate (1 molar eq.)

ii) in the presence of CAN (2 molar eq.) in 0.1 M phosphate buffer (pH 3.0).

iii) adding sodium dithionite or sodium borohydride after the addition of potassium ferricyanide (2 or 40 molar equivalents).

iv) in the presence of ferric chloride or zinc sulfate or copper acetate (1 molar eq.) in 0.2 M HEPES buffer

When required, oxidation mixtures were filtered through a 0.45 micron nylon membrane.

Substrate consumption was determined by HPLC analyses under the conditions described above.

When required the reaction was carried in 0.1 M phosphate buffer (pH 7.0) containing 1% poly(vinyl alcohol) (PVA) to prevent polymer precipitation.

In the case of acetylated dimers the following protocol was followed: 5 mL of a 3.6 mM solution of the acetylated dimer in methanol were treated under an argon atmosphere with sodium *tert*-butoxide (8 molar equivalents) and after 5 min the pH of the solution was taken to 2 by addition of 4 M HCl. 42 μL of the resulting mixture was added to 3 mL of 0.1 M phosphate buffer (pH 7.0) to reach a final concentration of 50 μM followed by 2 molar equivalents of potassium ferricyanide.

6.2.6 Preparation of dioleoyl-MeDHICA

Oleoyl-MeDHICA was prepared adapting a procedure by Mainini et al. 2013.[189]

The identity of the product was secured by and LC-MS and ^{1}H- and ^{13}C NMR.

6.2.7 Preparation of DAICA

600 mg of DHICA were acetylated with 6 mL of acetic anhydride and 120 μl of pyridine at room temperature overnight. After acetylation the product was suspended in 30 mL of a methanol/water solution (1:1) under reflux. After 4 h the solid product was filtered under vacuum and was left to dry at room temperature overnight (413 mg, 43% yield).

6.2.8 Evaluation of dioleoyl-MeDHICA photoprotective properties

For each subject, the minimal erythema dose (MED) was preliminarily determined. MED is defined as the lowest time interval or dosage of UV light irradiation sufficient for producing a minimal, perceptible erythema (sunburn or redness caused by engorgement of capillaries) on unprotected skin within a few hours following exposure.

After 24 h, the exposed areas of skin were examined. Red or pink skin indicates erythema or burning. Erythematous skin exposed to the shortest duration of UV is defined as the minimal erythema dose or MED.

Three sites on the ventral surface of one forearm of each subject were chosen using a square template (1 cm^2) and demarcated with permanent ink. The creams were applied for three days on two of three sites, while a site was left untreated (control). On the third day the three sites were irradiated with the MED determined for each subject, On the fourth day the induced

erythema was monitored by means of a reflectance visible spectrophotometer, providing measures of the three coordinates of CIELAB: L*, a* and b*.

6.2.9 Preparation of melanin from DHICA and MeDHICA

Autooxidatio melanins were obtained by autoxidation of 10 mM solutions of DHICA or MeDHICA in 0.1 M phosphate buffer at pH 8.5. The oxidation mixtures were allowed to stand at room temperature under vigorous stirring. Oxidation was halted at complete monomer consumption as determined by HPLC analysis and then acidified to pH 2. The melanin precipitate was collected by centrifugation (7000 rpm, 10 min, 4 °C) and was washed three times with 15 mL of 0.01M hydrocloridric acid (95 % and 65 % yield).

In another set of experiments, 3 molar equivalents of potassium ferricyanide were added to 10 mM solutions of DHICA or MeDHICA in 0.1 M phosphate buffer at pH 7.0. The oxidation mixture was allowed to stand at room temperature under vigorous stirring for 10 min and then acified to pH 2. The melanin precipitates were collected by centrifugation (7000 rpm, 1020 min, 4 °C) and washed three times with with 15 mL of 00.1M hydrocloridric acid (86% and 93% yield).

6.2.10 Test of the solubility of melanin from DHICA and MeDHICA

Melanin prepared by autooxidation from DHICA or MeDHICA (0.3 mg/mL) were suspended/dissolved in methanol or DMSO. The materials were stirred in the appropriate solvent for 15 min and UV-vis spectra of supernatants were registered after centrifugation (5000 rpm, 10 min, and 4 °C) and appropriate dilution.

6.2.10 2,2-Diphenyl-1-picrylhydrazy (DPPH) assay

The assay was performed as previously described.[204] Briefly, to a 200 μM DPPH solution in methanol, a proper amount of a methanolic suspension of each melanin homogenized with a glass/glass potter was added and rapidly mixed. The reaction was followed by spectrophotometric analysis measuring the absorbance at 515 nm after 10 min. Values are expressed as the EC_{50} i.e. the dose of the material at which a 50% DPPH reduction is observed,

6.2.11 Ferric reducing/antioxidant power (FRAP) assay

The assay was performed as described.[205] To a solution of FRAP reagent, a proper amount of a methanolic suspension of each melanin homogenized with a glass/glass potter was added

and rapidly mixed. After 10 minutes, the absorbance at 593 nm was measured. Trolox was used as the standard and results were expressed as Trolox equivalents. The FRAP reagent was prepared freshly by mixing 0.3 M acetate buffer (pH 3.6), 10 mM 2,4,6-tris(2-pyridyl)-s-triazine in 40 mM HCl, and 20 mM ferric chloride in water, in the ratio 10 : 1 : 1, in that order.

6.3 Hyperpigmentation and strategies of control of melanin pigmentation

6.3.1 Materials

2-iodobenzoic acid, oxone®, lipoic acid (LA), sodium borohydride, sodium dithionite, 3,4-Dihydroxy-L-phenylalanine (L-DOPA), mushroom tyrosinase (EC 1.14.18.1), kojic acid, were purchased from Sigma-Aldrich. Coumaric acid (CA) was purchased by Fluka. All solvents were HPLC grade. Bidistilled deionized water was used throughout the study.

6.3.2 Methods

UV spectra were recorded on a Beckman DU 640 spectrophotometer.

NMR spectra were recorded at 400 MHz on a Bruker instrument.

HPLC analyses were performed on a Agilent 1100 binary pump instrument equipped UV-visible detector using an octadecylsilane-coated column, 250 mm x 4.6 mm, 5 μm particle size (Phenomenex Sphereclone ODS) at 0.7 mL/min, using the following gradient: 0.1% formic acid (eluant a)/ methanol (eluant b): 40% b, 0-10 min; from 40 to 80% b, 47.5-52-5 min; from 80 to 40% b, 52.5-57.5 min. Detection wavelength was set at 280 nm.

LC-MS analysis was performed on an HPLC 1100 VL series instrument with an electrospray ionization source in positive ion mode (ESI+). An Agilent Eclipse XDB-C18 (150 × 4.60 mm, 5μm) was used, with the same eluant used for the HPLC analysis at a flow rate of 0.4 mL/min. Mass spectra were registered with the nebulizer pressure 50 psi; drying gas flow 10 L/min, at 350 °C; cap voltage set at 4000 V.

6.3.3 Synthesis of 2-iodoxybenzoic acid (IBX) [275]

5.0 g of 2-iodobenzoic acid were added to 37.2 g of Oxone® previously dissolved in 200 mL of bidistilled water and the mixture was taken under stirring at 70 °C. After 1 h the solution was cooled at 4 °C for 30 min, filtered and washed with cold water (6 × 300 mL) and acetone

(2 × 30 mL). The white solid was left to dry at room temperature for 16 h and weighted (3,085g, 55% yield).

6.3.4 Preparation of DHLA (6,8-dimercaptoottanoic acid)

Preparation of DHLA (6,8-dimercaptoottanoic acid) To 1.0 g of lipoic acid, previously dissolved in 20.0 mL of an aqueous solution of $NaHCO_3$ (0.25 M), were added 740.0 mg of $NaBH_4$ (in two portions) and the mixture was taken under stirring at 0 °C. After 2 h the reaction mixture was acidified until pH 1 with HCl 6 M and extracted with toluene (5 × 20 mL). The residue was analyzed by ^{1}H NMR to give DHLA in a pure form (902mg, 89 % yield).

6.3.5 Synthesis of 2-S-lipoylcaffeic acid

A solution of *p*-coumaric acid (215. mg, 1.3 mmol) in methanol (18 mL) was treated with IBX (561 mg, 2 mmol) under vigorous stirring at room temperature. After 7 min a solution of DHLA (1.119 mg, 5.3 mmol) in methanol (18 mL) was added drop by drop. After additional 15 min the reaction mixture was dilute with water and acidified with HCl 6 M to pH 1. Then the mixture was extracted with hexane/toluene 8:2 (10 × 200 mL), chloroform (7 × 200 mL) and ethyl acetate (3×100 mL). The combined chloroform layers were dried over sodium sulfate and taken to dryness to afford pure lipoyl-CA (101 mg, 20% yield) as an oily solid.

ESI+/MS: m/z 387 ([M+H]+), 409 ([M+Na]+);

UV: λ_{max} (CH_3OH) 252, 320 nm;

^{1}H NMR (CD_3OD) δ (ppm): 1.38 (m, 1H), 1.54 (m, 1H), 1.54 (m, 2H), 1.42(m, 1H), 1.62 (m, 1H), 1.78 (m, 1H),e 1.81(m, 1H), 2.26 (m, 2H), 2.88 (m,1H), 2.90 (m, 1H), 2.96 (m, 1H), 6.29 (d, J=16 Hz, 1H), 6.86 (d, J=8.4 Hz, 1H), 7.22 (d, 1H), 8.40 (d, J= 16 Hz, 1H).

^{13}C NMR (CD_3OD) δ (ppm): 25.4 (CH2), 27.3 (CH2), 34.1 (CH2), 34.1 (CH_2), 39.4 (CH_2), 39.4 (CH_2), 40.2 (CH), 117.2 (CH), 118.1 (CH), 119.9 (CH), 121.7 (C), 130.7 (C), 144.2 (CH), 147.7 (C), 147.8 (C), 168.2 (C), 174.8 (C).

6.3.6 Assay of mushroom tyrosinase activity

100 μL of a methanolic solution of 2-S-lipoylcaffeic acid (final concentration 0.001-1mM) was incubated in 2 mL of 50 mM phosphate buffer (pH 6.8) at room temperature in the presence of mushroom tyrosinase (10 U/mL). After 10 min 20 μL of a 100 mM solution of L-

DOPA in 0.6 M HCl (final concentration 1 mM) were added and the course of the reaction was followed by spectrophotometer measuring the absorbance at 475 nm every two minutes for ten minutes.

In separate experiments the assay was run as above incubating 2-S-lipoylcaffeic acid (final concentration 250 μM) in the presence and in the absence of 20 μL of a 100 mM solution of L-DOPA in 0.6 M HCl (final concentration 1 mM) and the course of the oxidation was followed by HPLC.

6.3.7 Study of the mechanism of inhibition of mushroom tyrosinase activity

The assay was run as above, using different concentration of L-DOPA (2, 1, 0.5, 0.25 and 0.125 mM) and 2-S-lipoylcaffeic acid. (0, 2, 3 and 5 μM). Data were elaborated to build the Lineweaver-Burk plot.

6.3.8 Assay for monophenolasic mushroom tyrosinase activity

100 μL of a methanolic solution of 2-S-lipoylcaffeic acid (final concentration 0.001-1mM) was incubated in 2 mL of 50 mM phosphate buffer (pH 6.8) at room temperature in the presence of mushroom tyrosinase (10 U/mL). After 10 min 20 μL of a 100 mM solution of L-tyrosine in 0.6 M HCl (final concentration 1 mM) were added and the course of the reaction was followed by spectrophotometer measuring the absorbance at 475 nm every 20 s for 15 min.

6.3.9 Effect of the preincubation on the inhibitory activity

10 μL of a methanolic solution of 2-S-lipoylcaffeic acid (final concentration 3.7 μM) were added to 2 mL of 50 mM phosphate buffer (pH 6.8) containing mushroom tyrosinase (20 U/mL) and was followed by the immediate addition of 20 μL of a 100 mM solution of L-tyrosine in 0.6 M HCl (final concentration 1 mM). The course of the reaction was followed by spectrophotometer measuring the absorbance at 475 nm every two minutes for ten minutes.

References

1. Brenner, M. & Hearing, V. J. The protective role of melanin against UV damage in human skin. *Photochem. Photobiol.* **84,** 539–49 (2008).

2. Slominski, A. Melanin Pigmentation in Mammalian Skin and Its Hormonal Regulation. *Physiol. Rev.* **84,** 1155–1228 (2004).

3. Kollias, N., Sayre, R. M., Zeise, L. & Chedekel, M. R. Photoprotection by melanin. *J. Photochem. Photobiol. B.* **9,** 135–60 (1991).

4. Maresca, V. *et al.* UVA-induced modification of catalase charge properties in the epidermis is correlated with the skin phototype. *J. Invest. Dermatol.* **126,** 182–190 (2006).

5. Maresca, V., Flori, E. & Picardo, M. Skin phototype: A new perspective. *Pigment Cell Melanoma Res.* **28,** 378–389 (2015).

6. Printz, C. New research on melanoma risk in red-haired people. *Cancer* **119,** 1118 (2013).

7. Takeuchi, S. *et al.* Melanin acts as a potent UVB photosensitizer to cause an atypical mode of cell death in murine skin. *Proc. Natl. Acad. Sci. U. S. A.* **101,** 15076–81 (2004).

8. Ito, S. & Wakamatsu, K. Diversity of human hair pigmentation as studied by chemical analysis of eumelanin and pheomelanin. *J. Eur. Acad. Dermatology Venereol.* **25,** 1369–1380 (2011).

9. Ito, S. & Wakamatsu, K. Human hair melanins: What we have learned and have not learned from mouse coat color pigmentation. *Pigment Cell Melanoma Res.* **24,** 63–74 (2011).

10. Rouzaud, F., Kadekaro, A. L., Abdel-Malek, Z. A. & Hearing, V. J. MC1R and the response of melanocytes to ultraviolet radiation. *Mutat. Res.* **571,** 133–52 (2005).

11. Mocellin, S., Rossi, C. R., Pilati, P. & Nitti, D. Tumor necrosis factor, cancer and anticancer therapy. *Cytokine Growth Factor Rev.* **16,** 35–53 (2005).

12. Raman, D., Baugher, P. J., Thu, Y. M. & Richmond, A. Role of chemokines in tumor

growth. *Cancer Lett.* **256,** 137–165 (2007).

13. Chedekel, M. R. Photochemistry and photobiology of epidermal melanins. *Photochem. Photobiol.* **35,** 881–5 (1982).

14. Chedekel, M. R., Smith, S. K., Post, P. W., Pokora, a & Vessell, D. L. Photo Destruction of Pheomelanin Role of Oxygen. *Proc. Natl. Acad. Sci. U. S. A.* **75,** 5395–5399 (1978).

15. Harsanyi, Z. P., Post, P. W., Brinkmann, J. P., Chedekel, M. R. & Deibel, R. M. Mutagenicity of melanin from human red hair. *Experientia* **36,** 291–2 (1980).

16. Prota, G. *Melanins and melanogenesis*. (Academic Press, 1992).

17. Panzella, L., Napolitano, A. & D'Ischia, M. Is DHICA the key to dopachrome tautomerase and melanocyte functions? *Pigment Cell Melanoma Res.* **24,** 248–249 (2011).

18. Prota, G. The chemistry of melanins and melanogenesis. *Fortschr. Chem. Org. Naturst.* **64,** 93–148 (1995).

19. Ito, S. & Prota, G. A facile one-step synthesis of cysteinyldopas using mushroom tyrosinase. *Experientia* **33,** 1118–9 (1977).

20. Napolitano, A., Di Donato, P., Prota, G. & Land, E. J. Transient quinonimines and 1,4-benzothiazines of pheomelanogenesis: new pulse radiolytic and spectrophotometric evidence. *Free Radic. Biol. Med.* **27,** 521–8 (1999).

21. Di Donato, P. & Napolitano, A. 1,4-benzothiazines as key intermediates in the biosynthesis of red hair pigment pheomelanins. *Pigment Cell Res.* **16,** 532–9 (2003).

22. Palumbo, A., Nardi, G., D'Ischia, M., Misuraca, G. & Prota, G. Non-enzymic oxidation of cysteinyldopa catalyzed by metallic ions. *Gen. Pharmacol.* **14,** 253–7 (1983).

23. Napolitano, A., Di Donato, P. & Prota, G. Zinc-catalyzed oxidation of 5-S-cysteinyldopa to 2,2'-bi(2H-1,4-benzothiazine): tracking the biosynthetic pathway of trichochromes, the characteristic pigments of red hair. *J. Org. Chem.* **66,** 6958–66 (2001).

24. Napolitano, A., De Lucia, M., Panzella, L. & D'Ischia, M. The 'benzothiazine' chromophore of pheomelanins: a reassessment. *Photochem. Photobiol.* **84,** 593–9 (2008).

25. Thomson, R. H. The pigments of reddish hair and feathers. *Angew. Chem. Int. Ed. Engl.* **13,** 305–12 (1974).

26. Costantini, C., Testa, G., Crescenzi, O. & d'Ischia, M. Photochemical ring contraction of dihydro-1,4-benzothiazines. *Tetrahedron Lett.* **35,** 3365–3366 (1994).

27. Wakamatsu, K., Ohtara, K. & Ito, S. Chemical analysis of late stages of pheomelanogenesis: conversion of dihydrobenzothiazine to a benzothiazole structure. *Pigment Cell Melanoma Res.* **22,** 474–86 (2009).

28. Greco, G. *et al.* Isomeric cysteinyldopas provide a (photo)degradable bulk component and a robust structural element in red human hair pheomelanin. *Pigment Cell Melanoma Res.* **22,** 319–327 (2009).

29. Nezirević Dernroth, D. *et al.* Pheomelanin-related benzothiazole isomers in the urine of patients with diffuse melanosis of melanoma. *Clin. Chim. Acta.* **411,** 1195–203 (2010).

30. Greco, G., Panzella, L., Verotta, L., D'Ischia, M. & Napolitano, A. Uncovering the structure of human red hair pheomelanin: Benzothiazolylthiazinodihydroisoquinolines as key building blocks. *J. Nat. Prod.* **74,** 675–682 (2011).

31. Greco, G., Panzella, L., Napolitano, A. & D'Ischia, M. The fundamental building blocks of red human hair pheomelanin are isoquinoline-containing dimers. *Pigment Cell Melanoma Res.* **25,** 110–112 (2012).

32. Thureau, P. *et al.* Probing the motional behavior of eumelanin and pheomelanin with solid-state NMR spectroscopy: new insights into the pigment properties. *Chemistry* **18,** 10689–700 (2012).

33. Land, E. J., Ito, S., Wakamatsu, K. & Riley, P. A. Rate constants for the first two chemical steps of eumelanogenesis. *Pigment cell Res.* **16,** 487–93 (2003).

34. Ito, S. & Wakamatsu, K. Chemistry of mixed melanogenesis - Pivotal roles of dopaquinone. *Photochem. Photobiol.* **84,** 582–592 (2008).

35. Simon, J. D., Peles, D., Wakamatsu, K. & Ito, S. Current challenges in understanding

melanogenesis: Bridging chemistry, biological control, morphology, and function. *Pigment Cell Melanoma Res.* **22,** 563–579 (2009).

36. Ullrich, S. E. Photoimmune suppression and photocarcinogenesis. *Front. Biosci.* **7,** d684-703 (2002).

37. Schreier, W. J. *et al.* Thymine dimerization in DNA is an ultrafast photoreaction. *Science* **315,** 625–9 (2007).

38. Vink, A. A. & Roza, L. Biological consequences of cyclobutane pyrimidine dimers. *J. Photochem. Photobiol. B.* **65,** 101–4 (2001).

39. Brash, D. E. *et al.* A role for sunlight in skin cancer: UV-induced p53 mutations in squamous cell carcinoma. *Proc. Natl. Acad. Sci. U. S. A.* **88,** 10124–8 (1991).

40. Brash, D. E. UV Signature Mutations. *Photochem. Photobiol.* **91,** 15–26 (2015).

41. Tewari, A., Sarkany, R. P. & Young, A. R. UVA1 Induces Cyclobutane Pyrimidine Dimers but Not 6-4 Photoproducts in Human Skin In Vivo. *J. Invest. Dermatol.* **132,** 394–400 (2012).

42. Young, A. R. *et al.* Human melanocytes and keratinocytes exposed to UVB or UVA in vivo show comparable levels of thymine dimers. *J. Invest. Dermatol.* **111,** 936–40 (1998).

43. Applegate, L. A., Scaletta, C., Panizzon, R., Niggli, H. & Frenk, E. In vivo induction of pyrimidine dimers in human skin by UVA radiation: initiation of cell damage and/or intercellular communication? *Int. J. Mol. Med.* **3,** 467–72 (1999).

44. Douki, T., Reynaud-Angelin, A., Cadet, J. & Sage, E. Bipyrimidine photoproducts rather than oxidative lesions are the main type of DNA damage involved in the genotoxic effect of solar UVA radiation. *Biochemistry* **42,** 9221–6 (2003).

45. Cadet, J., Douki, T. & Ravanat, J.-L. Oxidatively generated damage to cellular DNA by UVB and UVA radiation. *Photochem. Photobiol.* **91,** 140–55 (2015).

46. Noonan, F. P. *et al.* Melanoma induction by ultraviolet A but not ultraviolet B radiation requires melanin pigment. *Nat. Commun.* **3,** 884 (2012).

47. Premi, S. *et al.* Photochemistry. Chemiexcitation of melanin derivatives induces DNA

photoproducts long after UV exposure. *Science* **347,** 842–7 (2015).

48. Taylor, J.-S. The dark side of sunlight. *Science* **347,** 31–35 (2015).

49. Abdel-Malek, Z. A. & Cassidy, P. Dark CPDs and photocarcinogenesis: the party continues after the lights go out. *Pigment Cell Melanoma Res.* **28,** 373–374 (2015).

50. Knudsen, F. S. *et al.* Chemiluminescent aldehyde and beta-diketone reactions promoted by peroxynitrite. *Chem. Res. Toxicol.* **13,** 317–26 (2000).

51. Lamola, A. A. Production of pyrimidine dimers in DNA in the dark. *Biochem. Biophys. Res. Commun.* **43,** 893–8 (1971).

52. Napolitano, A., Pezzella, A., Vincensi, M. R. & Prota, G. Oxidative degradation of melanins to pyrrole acids: A model study. *Tetrahedron* **51,** 5913–5920 (1995).

53. Epstein, F. H., Gilchrest, B. A., Eller, M. S., Geller, A. C. & Yaar, M. The Pathogenesis of Melanoma Induced by Ultraviolet Radiation. *N. Engl. J. Med.* **340,** 1341–1348 (1999).

54. Armstrong, B. K. & Kricker, A. The epidemiology of UV induced skin cancer. *J. Photochem. Photobiol. B.* **63,** 8–18 (2001).

55. Routaboul, C., Denis, A. & Vinche, A. Immediate pigment darkening: description, kinetic and biological function. *Eur. J. Dermatol.* **9,** 95–9 (1999).

56. Moyal, D., Chardon, A. & Kollias, N. Determination of UVA protection factors using the persistent pigment darkening (PPD) as the end point. (Part 1). Calibration of the method. *Photodermatol. Photoimmunol. Photomed.* **16,** 245–9 (2000).

57. Moyal, D., Wichrowski, K. & Tricaud, C. In vivo persistent pigment darkening method: a demonstration of the reproducibility of the UVA protection factors results at several testing laboratories. *Photodermatol. Photoimmunol. Photomed.* **22,** 124–8 (2006).

58. Parrish, J. A., Jaenicke, K. F. & Anderson, R. R. Erythema and melanogenesis action spectra of normal human skin. *Photochem. Photobiol.* **36,** 187–91 (1982).

59. Friedmann, P. S. & Gilchrest, B. A. Ultraviolet radiation directly induces pigment production by cultured human melanocytes. *J. Cell. Physiol.* **133,** 88–94 (1987).

60. Meredith, P. & Sarna, T. The physical and chemical properties of eumelanin. *Pigment Cell Res.* **19,** 572–594 (2006).

61. Hoogduijn, M. J. *et al.* Melanin protects melanocytes and keratinocytes against H2O2-induced DNA strand breaks through its ability to bind Ca2+. *Exp. Cell Res.* **294,** 60–7 (2004).

62. Kipp, C. & Young, A. R. The soluble eumelanin precursor 5,6-dihydroxyindole-2-carboxylic acid enhances oxidative damage in human keratinocyte DNA after UVA irradiation. *Photochem. Photobiol.* **70,** 191–8 (1999).

63. Kvam, E. & Tyrrell, R. M. The Role of Melanin in the Induction of Oxidative DNA Base Damage by Ultraviolet A Irradiation of DNA or Melanoma Cells. *J. Invest. Dermatol.* **113,** 209–213 (1999).

64. Kvam, E. & Dahle, J. Melanin synthesis may sensitize melanocytes to oxidative DNA damage by ultraviolet A radiation and protect melanocytes from direct DNA damage by ultraviolet B radiation. *Pigment cell Res.* **17,** 549–50 (2004).

65. Korytowski, W., Pilas, B., Sarna, T. & Kalyanaraman, B. Photoinduced generation of hydrogen peroxide and hydroxyl radicals in melanins. *Photochem. Photobiol.* **45,** 185–90 (1987).

66. Marrot, L., Belaidi, J. P., Meunier, J. R., Perez, P. & Agapakis-Causse, C. The human melanocyte as a particular target for UVA radiation and an endpoint for photoprotection assessment. *Photochem. Photobiol.* **69,** 686–93 (1999).

67. Hill, H. Z. The function of melanin or six blind people examine an elephant. *Bioessays* **14,** 49–56 (1992).

68. Chedekel, M. R., Post, P. W., Deibel, R. M. & Kalus, M. Photodestruction of phaeomelanin. *Photochem. Photobiol.* **26,** 651–3 (1977).

69. Rees, J. L. Genetics of hair and skin color. *Annu. Rev. Genet.* **37,** 67–90 (2003).

70. Box, N. F., Wyeth, J. R., O'Gorman, L. E., Martin, N. G. & Sturm, R. A. Characterization of melanocyte stimulating hormone receptor variant alleles in twins with red hair. *Hum. Mol. Genet.* **6,** 1891–1897 (1997).

71. Healy, E. *et al.* Functional variation of MC1R alleles from red-haired individuals.

Hum. Mol. Genet. **10,** 2397–2402 (2001).

72. Le Pape, E., Wakamatsu, K., Ito, S., Wolber, R. & Hearing, V. J. Regulation of eumelaninpheomelanin synthesis and visible pigmentation in melanocytes by ligands of the melanocortin 1 receptor. *Pigment Cell Melanoma Res.* **21,** 477–486 (2008).

73. Candille, S. I. *et al.* A -Defensin Mutation Causes Black Coat Color in Domestic Dogs. *Science* **318,** 1418–1423 (2007).

74. Song, X. *et al.* alpha-MSH activates immediate defense responses to UV-induced oxidative stress in human melanocytes. *Pigment Cell Melanoma Res.* **22,** 809–18 (2009).

75. Panzella, L., Szewczyk, G., D'Ischia, M., Napolitano, A. & Sarna, T. Zinc-induced structural effects enhance oxygen consumption and superoxide generation in synthetic pheomelanins on UVA/visible light irradiation. *Photochem. Photobiol.* **86,** 757–764 (2010).

76. Wenczl, E. *et al.* (Pheo)melanin photosensitizes UVA-induced DNA damage in cultured human melanocytes. *J. Invest. Dermatol.* **111,** 678–82 (1998).

77. Korytowski, W., Kalyanaraman, B., Menon, I. A., Sarna, T. & Sealy, R. C. Reaction of superoxide anions with melanins: electron spin resonance and spin trapping studies. *Biochim. Biophys. Acta* **882,** 145–53 (1986).

78. Abdel-Malek, Z. A. & Ito, S. Being in the red: A no-win situation with melanoma. *Pigment Cell and Melanoma Research* (2013). doi:10.1111/pcmr.12061

79. Mitra, D. *et al.* An ultraviolet-radiation-independent pathway to melanoma carcinogenesis in the red hair/fair skin background. *Nature* **491,** 449–453 (2012).

80. Morgan, A. M., Lo, J. & Fisher, D. E. How does pheomelanin synthesis contribute to melanomagenesis?: Two distinct mechanisms could explain the carcinogenicity of pheomelanin synthesis. *BioEssays* **35,** 672–676 (2013).

81. Napolitano, A., Panzella, L., Monfrecola, G. & d'Ischia, M. Pheomelanin-induced oxidative stress: bright and dark chemistry bridging red hair phenotype and melanoma. *Pigment Cell Melanoma Res.* **27,** 721–733 (2014).

82. Greco, G. *et al.* A melanin-inspired pro-oxidant system for dopa(mine) polymerization:

mimicking the natural casing process. *Chem. Commun. (Camb).* **47,** 10308–10 (2011).

83. Suzukawa, A. A. *et al.* Novel properties of melanins include promotion of DNA strand breaks, impairment of repair, and reduced ability to damage DNA after quenching of singlet oxygen. *Free Radic. Biol. Med.* **52,** 1945–1953 (2012).

84. Panzella, L. *et al.* Red human hair pheomelanin is a potent pro-oxidant mediating UV-independent contributory mechanisms of melanomagenesis. *Pigment Cell Melanoma Res.* **27,** 244–252 (2014).

85. d'Ischia, M. *et al.* Melanins and melanogenesis: methods, standards, protocols. *Pigment Cell Melanoma Res.* **26,** 616–33 (2013).

86. Wakamatsu, K., Nakanishi, Y., Miyazaki, N., Kolbe, L. & Ito, S. UVA-induced oxidative degradation of melanins: Fission of indole moiety in eumelanin and conversion to benzothiazole moiety in pheomelanin. *Pigment Cell Melanoma Res.* **25,** 434–445 (2012).

87. Liu, Y. & Simon, J. D. The effect of preparation procedures on the morphology of melanin from the ink sac of Sepia officinalis. *Pigment Cell Res.* **16,** 72–80 (2003).

88. Ito, S. Reexamination of the structure of eumelanin. *Biochim. Biophys. Acta* **883,** 155–61 (1986).

89. Novellino, L., Napolitano, A. & Prota, G. Isolation and characterization of mammalian eumelanins from hair and irides. *Biochim. Biophys. Acta* **1475,** 295–306 (2000).

90. Panzella, L., Manini, P., Monfrecola, G., d'Ischia, M. & Napolitano, A. An easy-to-run method for routine analysis of eumelanin and pheomelanin in pigmented tissues. *Pigment Cell Res.* **20,** 128–33 (2007).

91. Lin, Z.-Q., Kondo, T., Ishida, Y., Takayasu, T. & Mukaida, N. Essential involvement of IL-6 in the skin wound-healing process as evidenced by delayed wound healing in IL-6-deficient mice. *J. Leukoc. Biol.* **73,** 713–21 (2003).

92. Derynck, R. & Feng, X. H. TGF-beta receptor signaling. *Biochim. Biophys. Acta* **1333,** F105–F150 (1997).

93. Kolb, R., Liu, G.-H. H., Janowski, A. M., Sutterwala, F. S. & Zhang, W. Inflammasomes in cancer: A double-edged sword. *Protein Cell* **5,** 12–20 (2014).

94. Boyan, B. D. *et al.* Evidence for distinct membrane receptors for 1 alpha,25-(OH)(2)D(3) and 24R,25-(OH)(2)D(3) in osteoblasts. *Steroids* **67,** 235–46 (2002).

95. Mårs, U. & Larsson, B. S. Pheomelanin as a binding site for drugs and chemicals. *Pigment Cell Res.* **12,** 266–74 (1999).

96. Slominski, A., Paus, R. & Schadendorf, D. Melanocytes as "sensory" and regulatory cells in the epidermis. *J. Theor. Biol.* **164,** 103–20 (1993).

97. Mayevsky, A. & Rogatsky, G. G. Mitochondrial function in vivo evaluated by NADH fluorescence : from animal models to human studies. *Am. J. Cell Physiol.* **292,** C615–C640 (2007).

98. Liu, Y. *et al.* Comparisons of the structural and chemical properties of melanosomes isolated from retinal pigment epithelium, iris and choroid of newborn and mature bovine eyes. *Photochem. Photobiol.* **81,** 510–6

99. Liu, Y. *et al.* Comparison of structural and chemical properties of black and red human hair melanosomes. *Photochem. Photobiol.* **81,** 135–44

100. Jimbow, K. *et al.* Characterization of melanogenesis and morphogenesis of melanosomes by physicochemical properties of melanin and melanosomes in malignant melanoma. *Cancer Res.* **44,** 1128–1134 (1984).

101. Jimbow, K. *et al.* Combined chemical and electron microscopic studies of pheomelanosomes in human red hair. *J. Invest. Dermatol.* **81,** 506–11 (1983).

102. Yagi, K. in *Free Radical and Antioxidant Protocols* **108,** 107–110 (Humana Press, 1998).

103. Meffert, H., Diezel, W. & Sönnichsen, N. Stable lipid peroxidation products in human skin: detection, ultraviolet light-induced increase, pathogenic importance. *Experientia* **32,** 1397–8 (1976).

104. Bickers, D. R. & Athar, M. Oxidative Stress in the Pathogenesis of Skin Disease. *J. Invest. Dermatol.* **126,** 2565–2575 (2006).

105. Schneider, S. L., Ross, A. L. & Grichnik, J. M. Do inflammatory pathways drive melanomagenesis? *Exp. Dermatol.* **24,** 86–90 (2015).

106. Kuźbicki, Ł., Lange, D., Strączyńska-Niemiec, A. & Chwirot, B. W. The value of cyclooxygenase-2 expression in differentiating between early melanomas and histopathologically difficult types of benign human skin lesions. *Melanoma Res.* **22,** 70–6 (2012).

107. Della Vecchia, N. F. N. F. *et al.* Tailoring melanins for bioelectronics: polycysteinyldopamine as an ion conducting redox-responsive polydopamine variant for pro-oxidant thin films. *J. Mater. Chem. C* **3,** 6525–6531 (2015).

108. Li, H. & Dryhurst, G. Oxidative metabolites of 5-S-cysteinyldopamine inhibit the pyruvate dehydrogenase complex. *J. Neural Transm.* **108,** 1363–74 (2001).

109. Wakamatsu, K., Murase, T., Zucca, F. A., Zecca, L. & Ito, S. Biosynthetic pathway to neuromelanin and its aging process. *Pigment Cell Melanoma Res.* **25,** 792–803 (2012).

110. Aureli, C. *et al.* 5-S-cysteinyldopamine neurotoxicity: Influence on the expression of α-synuclein and ERp57 in cellular and animal models of Parkinson's disease. *J. Neurosci. Res.* (2014). doi:10.1002/jnr.23318

111. Zamir, E. & Bastiaens, P. I. H. Reverse engineering intracellular biochemical networks. *Nat. Chem. Biol.* **4,** 643–7 (2008).

112. Tarabella, G. *et al.* Irreversible evolution of eumelanin redox states detected by an organic electrochemical transistor: en route to bioelectronics and biosensing. *J. Mater. Chem. B* **1,** 3843–3849 (2013).

113. Kim, E., Gordonov, T., Liu, Y., Bentley, W. E. & Payne, G. F. Reverse engineering to suggest biologically relevant redox activities of phenolic materials. *ACS Chem. Biol.* **8,** 716–724 (2013).

114. Liu, Y., Kim, E., White, I. M., Bentley, W. E. & Payne, G. F. Information processing through a bio-based redox capacitor: Signatures for redox-cycling. *Bioelectrochemistry* **98,** 94–102 (2014).

115. Kim, E. *et al.* Reverse Engineering Applied to Red Human Hair Pheomelanin Reveals Redox-Buffering as a Pro-Oxidant Mechanism. *Sci. Rep.* **5,** (2015).

116. Dessinioti, C., Antoniou, C., Katsambas, A. & Stratigos, A. J. Melanocortin 1 receptor variants: Functional role and pigmentary associations. *Photochem. Photobiol.* **87,** 978–

987 (2011).

117. García-Borrón, J. C. *et al.* MC1R, the cAMP pathway, and the response to solar UV: Extending the horizon beyond pigmentation. *Pigment Cell Melanoma Res.* **27,** 699–720 (2014).

118. Kadekaro, A. L. *et al.* Cutaneous photobiology. The melanocyte vs. the sun: who will win the final round? *Pigment cell Res.* **16,** 434–47 (2003).

119. Prota, G. Pigment cell research: what directions? *Pigment cell Res.* **10,** 5–11

120. Gauden, M. *et al.* Role of solvent, pH, and molecular size in excited-state deactivation of key eumelanin building blocks: Implications for melanin pigment photostability. *J. Am. Chem. Soc.* **130,** 17038–17043 (2008).

121. Memoli, S. *et al.* Diffusible melanin-related metabolites are potent inhibitors of lipid peroxidation. *Biochim. Biophys. Acta* **1346,** 61–8 (1997).

122. Novellino, L., d'Ischia, M. & Prota, G. Nitric oxide-induced oxidation of 5,6-dihydroxyindole and 5,6-dihydroxyindole-2-carboxylic acid under aerobic conditions: non-enzymatic route to melanin pigments of potential relevance to skin (photo)protection. *Biochim. Biophys. Acta* **1425,** 27–35 (1998).

123. Novellino, L., Napolitano, A. & Prota, G. 5,6-Dihydroxyindoles in the fenton reaction: a model study of the role of melanin precursors in oxidative stress and hyperpigmentary processes. *Chem. Res. Toxicol.* **12,** 985–92 (1999).

124. Zhang, X., Erb, C., Flammer, J. & Nau, W. M. Absolute rate constants for the quenching of reactive excited states by melanin and related 5,6-dihydroxyindole metabolites: implications for their antioxidant activity. *Photochem. Photobiol.* **71,** 524–33 (2000).

125. Kadekaro, A. L. *et al.* Melanocortin 1 receptor genotype: an important determinant of the damage response of melanocytes to ultraviolet radiation. *FASEB J.* **24,** 3850–3860 (2010).

126. Maresca, V. *et al.* MC1R stimulation by alpha-MSH induces catalase and promotes its re-distribution to the cell periphery and dendrites. *Pigment Cell Melanoma Res.* **23,** 263–75 (2010).

127. Denat, L., Kadekaro, A. L., Marrot, L., Leachman, S. A. & Abdel-Malek, Z. A. Melanocytes as instigators and victims of oxidative stress. *J. Invest. Dermatol.* **134,** 1512–8 (2014).

128. Hauser, J. E. *et al.* Melanin content and MC1R function independently affect UVR-induced DNA damage in cultured human melanocytes. *Pigment cell Res.* **19,** 303–14 (2006).

129. Kadekaro, A. L. *et al.* Alpha-Melanocyte-Stimulating Hormone Suppresses Oxidative Stress through a p53-Mediated Signaling Pathway in Human Melanocytes. *Mol. Cancer Res.* **10,** 778–786 (2012).

130. Yin, K., Sturm, R. A. & Smith, A. G. MC1R and NR4A receptors in cellular stress and DNA repair: implications for UVR protection. *Exp. Dermatol.* **23,** 449–52 (2014).

131. Haycock, J. W. *et al.* Alpha-melanocyte-stimulating hormone reduces impact of proinflammatory cytokine and peroxide-generated oxidative stress on keratinocyte and melanoma cell lines. *J. Biol. Chem.* **275,** 15629–36 (2000).

132. Kadekaro, A. L. *et al.* -Melanocortin and Endothelin-1 Activate Antiapoptotic Pathways and Reduce DNA Damage in Human Melanocytes. *Cancer Res.* **65,** 4292–4299 (2005).

133. Böhm, M. *et al.* alpha-Melanocyte-stimulating hormone protects from ultraviolet radiation-induced apoptosis and DNA damage. *J. Biol. Chem.* **280,** 5795–802 (2005).

134. Swope, V. *et al.* Significance of the melanocortin 1 receptor in the DNA damage response of human melanocytes to ultraviolet radiation. *Pigment Cell Melanoma Res.* **27,** 601–610 (2014).

135. Arzillo, M. *et al.* Eumelanin Buildup on the Nanoscale: Aggregate Growth/Assembly and Visible Absorption Development in Biomimetic 5,6-Dihydroxyindole Polymerization. *Biomacromolecules* **13,** 2379–2390 (2012).

136. Clancy, C. M. R. & Simon, J. D. Ultrastructural organization of eumelanin from Sepia officinalis measured by atomic force microscopy. *Biochemistry* **40,** 13353–13360 (2001).

137. Ghiani, S. *et al.* Characterization of human hair melanin and its degradation products

by means of magnetic resonance techniques. *Magn Reson Chem* **46,** 471–479 (2008).

138. Kaxiras, E., Tsolakidis, A., Zonios, G. & Meng, S. Structural model of eumelanin. *Phys. Rev. Lett.* **97,** 1–4 (2006).

139. Liu, Y. & Simon, J. D. Isolation and Biophysical Studies of Natural Eumelanins: Applications of Imaging Technologies and Ultrafast Spectroscopy. *Pigment Cell Res.* **16,** 606–618 (2003).

140. Meng, S. *et al.* Theoretical Models of Eumelanin Protomolecules and their Optical Properties. *J. Org. Chem.* **72,** 9225–9230 (2007).

141. Stark, K. B. *et al.* Effect of Stacking and Redox State on Optical Absorption Spectra of Melanins - Comparison of Theoretical and Experimental Results. **109,** 1970–1977 (2005).

142. Corani, A. *et al.* Superior photoprotective motifs and mechanisms in eumelanins uncovered. *J. Am. Chem. Soc.* **136,** 11626–35 (2014).

143. Mostert, A. B. *et al.* Hydration-Controlled X-Band EPR Spectroscopy: A Tool for Unravelling the Complexities of the Solid-State Free Radical in Eumelanin. *J. Phys. Chem. B* **117,** 4965–4972 (2013).

144. Panzella, L. *et al.* Atypical structural and π-electron features of a melanin polymer that lead to superior free-radical-scavenging properties. *Angew. Chemie - Int. Ed.* **52,** 12684–12687 (2013).

145. Blois, M. S., Zahalan, A. B. & Maling, J. E. Electron spin resonance studies on melanin. *Biophys. J.* **4,** 471–90 (1964).

146. Simon, J. D. & Peles, D. N. The Red and the Black. *Acc. Chem. Res.* **43,** 1452–1460 (2010).

147. d'Ischia, M. *et al.* Melanins and melanogenesis: from pigment cells to human health and technological applications. *Pigment Cell Melanoma Res.* **28,** 520–44 (2015).

148. Borovanský, J. & Riley, P. A. (Patrick A. *Melanins and melanosomes : biosynthesis, biogenesis, physiological, and pathological functions*. (Wiley-Blackwell, 2011).

149. Tran, M. L., Powell, B. J. & Meredith, P. Chemical and structural disorder in

eumelanins: a possible explanation for broadband absorbance. *Biophys. J.* **90,** 743–52 (2006).

150. Pezzella, A. *et al.* Disentangling eumelanin 'black chromophore': visible absorption changes as signatures of oxidation state- and aggregation-dependent dynamic interactions in a model water-soluble 5,6-dihydroxyindole polymer. *J. Am. Chem. Soc.* **131,** 15270–5 (2009).

151. Tran, M. L., Powell, B. J. & Meredith, P. Chemical and Structural Disorder in Eumelanins - A Possible Explanation for Broad Band Absorbance. *Biophys. J.* **90,** 28 (2005).

152. d'Ischia, M. *et al.* Structural effects on the electronic absorption properties of 5,6-dihydroxyindole oligomers: the potential of an integrated experimental and DFT approach to model eumelanin optical properties. *Photochem. Photobiol.* **84,** 600–7 (2008).

153. Ascione, L., Pezzella, A., Ambrogi, V., Carfagna, C. & d'Ischia, M. Intermolecular π-Electron Perturbations Generate Extrinsic Visible Contributions to Eumelanin Black Chromophore in Model Polymers with Interrupted Interring Conjugation. *Photochem. Photobiol.* **89,** 314–318 (2013).

154. Pezzella, A. *et al.* Lack of visible chromophore development in the pulse radiolysis oxidation of 5,6-dihydroxyindole-2-carboxylic acid oligomers: DFT investigation and implications for eumelanin absorption properties. *J. Org. Chem.* **74,** 3727–3734 (2009).

155. Chen, C.-T. *et al.* Excitonic effects from geometric order and disorder explain broadband optical absorption in eumelanin. *Nat. Commun.* **5,** 3859 (2014).

156. Tuna, D., Udvarhelyi, A., Sobolewski, A. L., Domcke, W. & Domratcheva, T. Onset of the Electronic Absorption Spectra of Isolated and π-Stacked Oligomers of 5,6-Dihydroxyindole: An Ab Initio Study of the Building Blocks of Eumelanin. *J. Phys. Chem. B* **120,** 3493–502 (2016).

157. Prampolini, G. *et al.* Intermolecular interactions in eumelanins: a computational bottom-up approach. I. small building blocks. *RSC Adv.* **5,** 38513–38526 (2015).

158. Assis Oliveira, L. B., L Fonseca, T., Costa Cabral, B. J., Coutinho, K. & Canuto, S. Hydration effects on the electronic properties of eumelanin building blocks. *J. Chem.*

Phys. **145,** 84501 (2016).

159. Pezzella, A. *et al.* Free radical coupling of o-semiquinones uncovered. *J. Am. Chem. Soc.* **135,** 12142–9 (2013).

160. Pezzella, A. *et al.* Short-Lived Quinonoid Species from 5,6-Dihydroxyindole Dimers en Route to Eumelanin Polymers: Integrated Chemical, Pulse Radiolytic, and Quantum Mechanical Investigation. *J. Am. Chem. Soc.* **128,** 15490–15498 (2006).

161. Barone, V. *et al.* Unraveling the interplay of different contributions to the stability of the quinhydrone dimer. *RSC Adv.* **4,** 876 (2014).

162. Micillo, R., Panzella, L., Fabbrocini, G., Ayala, F. & Monfrecola, G. A reappraisal of the biological functions of melanins and melanogens: The role of 5,6-dihydroxyindole-2-carboxylic acid (DHICA) in skin (photo)protection. *J. Plast. Dermatology* **10,** 69–74 (2014).

163. Prota, G. The role of peroxidase in melanogenesis revisited. *Pigment cell Res.* **Suppl 2,** 25–31 (1992).

164. Olivares, C. & Solano, F. New insights into the active site structure and catalytic mechanism of tyrosinase and its related proteins. *Pigment Cell Melanoma Res.* **22,** 750–760 (2009).

165. Ito, S. & IFPCS. The IFPCS presidential lecture: a chemist's view of melanogenesis. *Pigment cell Res.* **16,** 230–6 (2003).

166. Michard, Q. *et al.* TRP-2 specifically decreases WM35 cell sensitivity to oxidative stress. *Free Radic. Biol. Med.* **44,** 1023–31 (2008).

167. Pak, B. J. *et al.* Radiation resistance of human melanoma analysed by retroviral insertional mutagenesis reveals a possible role for dopachrome tautomerase. *Oncogene* **23,** 30–8 (2004).

168. Chu, W. *et al.* Tyrosinase-related protein 2 as a mediator of melanoma specific resistance to cis-diamminedichloroplatinum(II): therapeutic implications. *Oncogene* **19,** 395–402 (2000).

169. Sendoel, A., Kohler, I., Fellmann, C., Lowe, S. W. & Hengartner, M. O. HIF-1 antagonizes p53-mediated apoptosis through a secreted neuronal tyrosinase. *Nature*

465, 577–83 (2010).

170. Nishioka, E. *et al.* Expression of tyrosinase, TRP-1 and TRP-2 in ultraviolet-irradiated human melanomas and melanocytes: TRP-2 protects melanoma cells from ultraviolet B induced apoptosis. *Melanoma Res.* **9,** 433–43 (1999).

171. Jiang, S. *et al.* Regulation of DHICA-mediated antioxidation by dopachrome tautomerase: Implication for skin photoprotection against UVA radiation. *Free Radic. Biol. Med.* **48,** 1144–1151 (2010).

172. Hara, H., Walsh, N., Yamada, K. & Jimbow, K. High plasma level of a eumelanin precursor, 6-hydroxy-5-methoxyindole-2-carboxylic acid as a prognostic marker for malignant melanoma. *J. Invest. Dermatol.* **102,** 501–505 (1994).

173. Kovacs, D. *et al.* The eumelanin intermediate 5,6-dihydroxyindole-2-carboxylic acid is a messenger in the cross-talk among epidermal cells. *J. Invest. Dermatol.* **132,** 1196–205 (2012).

174. Yohn, J. J. *et al.* Disparate antioxidant enzyme activities in cultured human cutaneous fibroblasts, keratinocytes, and melanocytes. *J. Invest. Dermatol.* **97,** 405–9 (1991).

175. Briganti, S. & Picardo, M. Antioxidant activity, lipid peroxidation and skin diseases. What's new. *J. Eur. Acad. Dermatol. Venereol.* **17,** 663–669 (2003).

176. Dummer, R. & Maier, T. UV protection and skin cancer. *Recent Results Cancer Res.* **160,** 7–12 (2002).

177. Morabito, K., Shapley, N. C., Steeley, K. G. & Tripathi, A. Review of sunscreen and the emergence of non-conventional absorbers and their applications in ultraviolet protection. *International Journal of Cosmetic Science* **33,** 385–390 (2011).

178. Victor, F. C., Cohen, D. E. & Soter, N. A. A 20-year analysis of previous and emerging allergens that elicit photoallergic contact dermatitis. *J. Am. Acad. Dermatol.* **62,** 605–610 (2010).

179. Gaspar, L. R., Tharmann, J., Maia, P. M. B. G. & Liebsch, M. Toxicology in Vitro Skin phototoxicity of cosmetic formulations containing photounstable and photostable UV-filters and vitamin A palmitate. *Toxicol. Vitr.* **27,** 418–425 (2013).

180. Wong, T. & Orton, D. Sunscreen allergy and its investigation. *Clin. Dermatol.* **29,**

306–310 (2011).

181. Sarveiya, V., Risk, S. & Benson, H. A. E. Liquid chromatographic assay for common sunscreen agents: Application to in vivo assessment of skin penetration and systemic absorption in human volunteers. *J. Chromatogr. B Anal. Technol. Biomed. Life Sci.* **803,** 225–231 (2004).

182. Wermuth, C. G., Ganellin, C. R., Lindberg, P. & Mitscher, L. A. Glossary of terms used in medicinal chemistry (IUPAC Recommendations 1998). *Pure Appl. Chem.* **70,** 1129–1143 (1998).

183. Imai, T., Takase, Y., Iwase, H. & Hashimoto, M. Involvement of Carboxylesterase in Hydrolysis of Propranolol Prodrug during Permeation across Rat Skin. *Pharmaceutics* **5,** 371–384 (2013).

184. Hewitt, P. G., Perkins, J. & Hotchkiss, S. A. M. Metabolism of fluroxypyr, fluroxypyr methyl ester, and the herbicide fluroxypyr methylheptyl ester. I: during percutaneous absorption through fresh rat and human skin in vitro. *Drug Metab. Dispos.* **28,** 748–754 (2000).

185. Jewell, C. *et al.* Hydrolysis of a series of parabens by skin microsomes and cytosol from human and minipigs and in whole skin in short-term culture. *Toxicol. Appl. Pharmacol.* **225,** 221–228 (2007).

186. Naik, A., Pechtold, L. A. R. M., Potts, R. O. & Guy, R. H. Mechanism of oleic acid-induced skin penetration enhancement in vivo in humans. *J. Control. Release* **37,** 299–306 (1995).

187. Touitou, E., Godin, B., Karl, Y., Bujanover, S. & Becker, Y. Oleic acid, a skin penetration enhancer, affects Langerhans cells and corneocytes. *J. Control. Release* **80,** 1–7 (2002).

188. Cardoso, C. R. *et al.* Oleic acid modulation of the immune response in wound healing: A new approach for skin repair. *Immunobiology* **216,** 409–415 (2011).

189. Mainini, F. *et al.* Synthesis, molecular characterization and preliminary antioxidant activity evaluation of quercetin fatty esters. *JAOCS, J. Am. Oil Chem. Soc.* **90,** 1751–1759 (2013).

190. Dawson, J. B. *et al.* A theoretical and experimental study of light absorption and scattering by in vivo skin. *Phys Med Biol* **25,** 695–709 (1980).

191. Andersen, P. H., Abrams, K., Bjerring, P. & Maibach, H. A time-correlation study of ultraviolet B-induced erythema measured by reflectance spectroscopy and laser Doppler flowmetry. *Photodermatol. Photoimmunol. Photomed.* **8,** 123–8 (1991).

192. Micillo, R. *et al.* 'Fifty Shades' of Black and Red or How Carboxyl Groups Fine Tune Eumelanin and Pheomelanin Properties. *Int. J. Mol. Sci.* **17,** 746 (2016).

193. Palumbo, P., d'Ischia, M. & Prota, G. Tyrosinase-promoted oxidation of 5, 6-dihydroxyindole-2-carboxy1ic acid to melanin. Isolation and characterization of oligomer intermediates. *Tetrahedron* **43,** 4203–4206 (1987).

194. Palumbo, A., d'Ischia, M., Misuraca, G. & Prota, G. Effect of metal ions on the rearrangement of dopachrome. *Biochim. Biophys. Acta* **925,** 203–9 (1987).

195. Palumbo, A. *et al.* Comparative action of dopachrome tautomerase and metal ions on the rearrangement of dopachrome. *Biochim. Biophys. Acta* **1115,** 1–5 (1991).

196. Tsukamoto, K., Palumbo, A., D'Ischia, M., Hearing, V. J. & Prota, G. 5,6-Dihydroxyindole-2-carboxylic acid is incorporated in mammalian melanin. *Biochem. J.* **286 (Pt 2),** 491–5 (1992).

197. d'Ischia, M., Napolitano, A. & Pezzella, A. 5,6-Dihydroxyindole Chemistry: Unexplored Opportunities Beyond Eumelanin. *European J. Org. Chem.* **2011,** 5501–5516 (2011).

198. Pezzella, A. *et al.* 5,6-Dihydroxyindole Tetramers with 'Anomalous' Interunit Bonding Patterns by Oxidative Coupling of 5,5',6,6'-Tetrahydroxy-2,7'-biindolyl: Emerging Complexities on the Way toward an Improved Model of Eumelanin Buildup. *J. Org. Chem.* **72,** 9225–9230 (2007).

199. Corradini, M. G., Napolitano, A. & Prota, G. A biosynthetic approach to the structure of eumelanins. The isolation of oligomers from 5,6-dihydroxy-1-methylindole. *Tetrahedron* **42,** 2083–2088 (1986).

200. Pezzella, A., Vogna, D. & Prota, G. Synthesis of optically active tetrameric melanin intermediates by oxidation of the melanogenic precursor 5,6-dihydroxyindole-2-

carboxylic acid under biomimetic conditions. *Tetrahedron: Asymmetry* **14,** 1133–1140 (2003).

201. Pezzella, A., Vogna, D. & Prota, G. Atropoisomeric melanin intermediates by oxidation of the melanogenic precursor 5,6-dihydroxyindole-2-carboxylic acid under biomimetic conditions. *Tetrahedron* **58,** 3681–3687 (2002).

202. Rienecker, S. B., Mostert, A. B., Schenk, G., Hanson, G. R. & Meredith, P. Heavy Water as a Probe of the Free Radical Nature and Electrical Conductivity of Melanin. *J. Phys. Chem. B* **119,** 14994–15000 (2015).

203. Pezzella, A., Napolitano, A., d'Ischia, M. & Prota, G. Oxidative polymerisation of 5,6-dihydroxyindole-2-carboxylic acid to melanin: A new insight. *Tetrahedron* **52,** 7913–7920 (1996).

204. Goupy, P., Dufour, C., Loonis, M. & Dangles, O. Quantitative kinetic analysis of hydrogen transfer reactions from dietary polyphenols to the DPPH radical. *J. Agric. Food Chem.* **51,** 615–22 (2003).

205. Benzie, I. F. F. & Strain, J. J. The Ferric Reducing Ability of Plasma (FRAP) as a Measure of 'Antioxidant Power': The FRAP Assay. *Anal. Biochem.* **239,** 70–76 (1996).

206. Virador, V. *et al.* Production of melanocyte-specific antibodies to human melanosomal proteins: expression patterns in normal human skin and in cutaneous pigmented lesions. *Pigment Cell Res.* **14,** 289–297 (2001).

207. Gunia-Krzyżak, A., Popiol, J. & Marona, H. Melanogenesis Inhibitors: Strategies for Searching for and Evaluation of Active Compounds. *Curr. Med. Chem.* **23,** 3548–3574 (2016).

208. Ebanks, J. P., Wickett, R. R. & Boissy, R. E. Mechanisms regulating skin pigmentation: the rise and fall of complexion coloration. *Int. J. Mol. Sci.* **10,** 4066–87 (2009).

209. Hearing, V. J. & Tsukamoto, K. Enzymatic control of pigmentation in mammals. *FASEB J.* **5,** 2902–9 (1991).

210. Land, E. J., Ramsden, C. A. & Riley, P. A. Tyrosinase Autoactivation and the Chemistry of ortho -Quinone Amines. *Acc. Chem. Res.* **36,** 300–308 (2003).

211. Riley, P. A. Tyrosinase Kinetics: A Semi-quantitative Model of the Mechanism of Oxidation of Monohydric and Dihydric Phenolic Substrates. *J. Theor. Biol.* **203,** 1–12 (2000).

212. Ramsden, C. A. & Riley, P. A. Bioorganic & Medicinal Chemistry Tyrosinase : The four oxidation states of the active site and their relevance to enzymatic activation , oxidation and inactivation. *Bioorg. Med. Chem.* **22,** 2388–2395 (2014).

213. Shibahara, S. *et al.* Microphthalmia-Associated Transcription Factor (MITF): Multiplicity in Structure, Function, and Regulation. *J. Investig. Dermatology Symp. Proc.* **6,** 99–104 (2001).

214. Tachibana, M. *et al.* Ectopic expression of MITF, a gene for Waardenburg syndrome type 2, converts fibroblasts to cells with melanocyte characteristics. *Nat. Genet.* **14,** 50–4 (1996).

215. Levy, C., Khaled, M. & Fisher, D. E. MITF: master regulator of melanocyte development and melanoma oncogene. *Trends Mol. Med.* **12,** 406–14 (2006).

216. Napolitano, A., d'Ischia, M., Prota, G., Havens, M. & Tramposch, K. 2-Aryl-1,3-thiazolidines as masked sulfhydryl agents for inhibition of melanogenesis. *Biochim. Biophys. Acta* **1073,** 416–22 (1991).

217. Ha, Y. M. *et al.* Design, synthesis and biological evaluation of 2-(substituted phenyl)thiazolidine-4-carboxylic acid derivatives as novel tyrosinase inhibitors. *Biochimie* **94,** 533–540 (2012).

218. Han, Y. K. *et al.* Characterization of a novel tyrosinase inhibitor, (2RS,4R)-2-(2,4-dihydroxyphenyl)thiazolidine-4-carboxylic acid (MHY384). *Biochim. Biophys. Acta - Gen. Subj.* **1820,** 542–549 (2012).

219. Moon, K. M. *et al.* Antimelanogenic activity of MHY384 via inhibition of NO-induced cGMP signalling. *Exp. Dermatol.* **25,** 652–654 (2016).

220. Roméro-Graillet, C., Aberdam, E., Clément, M., Ortonne, J. P. & Ballotti, R. Nitric oxide produced by ultraviolet-irradiated keratinocytes stimulates melanogenesis. *J. Clin. Invest.* **99,** 635–642 (1997).

221. Horikoshi, T. *et al.* Involvement of nitric oxide in UVB-induced pigmentation in

guinea pig skin. *Pigment Cell Res* **13,** 358–363 (2000).

222. Napolitano, A., Micillo, R. & Monfrecola, G. Melanin pigmentation control by 1,3-thiazolidines: does NO scavenging play a critical role? *Exp. Dermatol.* **25,** 596–597 (2016).

223. d'Ischia, M., Panzella, L., Manini, P. & Napolitano, A. The chemical basis of the antinitrosating action of polyphenolic cancer chemopreventive agents. *Curr. Med. Chem.* **13,** 3133–44 (2006).

224. Prütz, W. A., Mönig, H., Butler, J. & Land, E. J. Reactions of nitrogen dioxide in aqueous model systems: oxidation of tyrosine units in peptides and proteins. *Arch. Biochem. Biophys.* **243,** 125–34 (1985).

225. van der Vliet, A., Eiserich, J. P., Kaur, H., Cross, C. E. & Halliwell, B. Nitrotyrosine as biomarker for reactive nitrogen species. *Methods Enzymol.* **269,** 175–84 (1996).

226. Solano, F., Briganti, S., Picardo, M. & Ghanem, G. Hypopigmenting agents: An updated review on biological, chemical and clinical aspects. *Pigment Cell Research* **19,** 550–571 (2006).

227. Lee, C. S. *et al.* Different effects of five depigmentary compounds, rhododendrol, raspberry ketone, monobenzone, rucinol and AP736 on melanogenesis and viability of human epidermal melanocytes. *Exp. Dermatol.* **25,** 44–49 (2016).

228. Okura, M. *et al.* Effects of rhododendrol and its metabolic products on melanocytic cell growth. *J. Dermatol. Sci.* **80,** 142–149 (2015).

229. Ito, S., Ojika, M., Yamashita, T. & Wakamatsu, K. Tyrosinase-catalyzed oxidation of rhododendrol produces 2-methylchromane-6,7-dione, the putative ultimate toxic metabolite: implications for melanocyte toxicity. *Pigment Cell Melanoma Res.* **27,** 744–53 (2014).

230. Ito, S. *et al.* Human tyrosinase is able to oxidize both enantiomers of rhododendrol. *Pigment Cell Melanoma Res.* **27,** 1149–53 (2014).

231. Briganti, S., Camera, E. & Picardo, M. Chemical and instrumental approaches to treat hyperpigmentation. *Pigment Cell Res.* **16,** 101–110 (2003).

232. Amorati, R., Fumo, M. G., Menichetti, S., Mugnaini, V. & Pedulli, G. F. Electronic

and hydrogen bonding effects on the chain-breaking activity of sulfur-containing phenolic antioxidants. *J. Org. Chem.* **71,** 6325–6332 (2006).

233. Bilska, A. & Włodek, L. Biologic properties of lipoic acid. *Postepy Hig. Med. Dosw.* **56,** 201–219 (2002).

234. Reed, L. J. From lipoic acid to multi-enzyme complexes. *Protein Sci.* **7,** 220–4 (1998).

235. Reed, L. J., DeBusk, B. G., Gunsalus, I. C. & Hornberger, C. S. Crystalline alpha-lipoic acid; a catalytic agent associated with pyruvate dehydrogenase. *Science* **114,** 93–4 (1951).

236. Packer, L., Witt, E. H. & Tritschler, H. J. alpha-Lipoic acid as a biological antioxidant. *Free Radic. Biol. Med.* **19,** 227–50 (1995).

237. Biewenga, G., Haenen, G. R. & Bast, A. The role of lipoic acid in the treatment of diabetic polyneuropathy. *Drug Metab. Rev.* **29,** 1025–54 (1997).

238. Kojima, M. *et al.* Efficacy of α-Lipoic Acid Against Diabetic Cataract in Rat. *Jpn. J. Ophthalmol.* **51,** 10–13 (2007).

239. Ono, K., Hirohata, M. & Yamada, M. Alpha-lipoic acid exhibits anti-amyloidogenicity for beta-amyloid fibrils in vitro. *Biochem. Biophys. Res. Commun.* **341,** 1046–52 (2006).

240. Ono, K., Naiki, H. & Yamada, M. The development of preventives and therapeutics for Alzheimer's disease that inhibit the formation of beta-amyloid fibrils (fAbeta), as well as destabilize preformed fAbeta. *Curr. Pharm. Des.* **12,** 4357–75 (2006).

241. Holmquist, L. *et al.* Lipoic acid as a novel treatment for Alzheimer's disease and related dementias. *Pharmacol. Ther.* **113,** 154–164 (2007).

242. Di Stefano, A. *et al.* L-dopa- and dopamine-(R)-alpha-lipoic acid conjugates as multifunctional codrugs with antioxidant properties. *J. Med. Chem.* **49,** 1486–93 (2006).

243. Tsuji-Naito, K., Hatani, T., Okada, T. & Tehara, T. Evidence for covalent lipoyl adduction with dopaquinone following tyrosinase-catalyzed oxidation. *Biochem. Biophys. Res. Commun.* **343,** 15–20 (2006).

244. Tsuji-Naito, K., Hatani, T., Okada, T. & Tehara, T. Modulating effects of a novel skin-lightening agent, alpha-lipoic acid derivative, on melanin production by the formation of DOPA conjugate products. *Bioorg. Med. Chem.* **15,** 1967–75 (2007).

245. Chung, T.-W. *et al.* Novel and therapeutic effect of caffeic acid and caffeic acid phenyl ester on hepatocarcinoma cells: complete regression of hepatoma growth and metastasis by dual mechanism. *FASEB J.* **18,** 1670–81 (2004).

246. Kwak, S.-Y. Y., Lee, S., Choi, H.-R. R., Park, K.-C. C. & Lee, Y.-S. S. Dual effects of caffeoyl-amino acidyl-hydroxamic acid as an antioxidant and depigmenting agent. *Bioorganic Med. Chem. Lett.* **21,** 5155–5158 (2011).

247. Cheynier, V. & Moutounet, M. Oxidative reactions of caffeic acid in model systems containing polyphenol oxidase. *J. Agric. Food Chem.* **40,** 2038–2044 (1992).

248. Schurink, M., van Berkel, W. J. H., Wichers, H. J. & Boeriu, C. G. Novel peptides with tyrosinase inhibitory activity. *Peptides* **28,** 485–495 (2007).

249. Tada, T., Ohnishi, K., Komiya, T. & Imai, K. Synthetic Search for Cosmetic Ingredients: Preparations, Tyrosinase Inhibitory and Antioxidant Activities of Caffeic Amides. *J. Oleo Sci.* **51,** 19–27 (2002).

250. Pezzella, A., Lista, L., Napolitano, A. & D'Ischia, M. An expedient one-pot entry to catecholestrogens and other catechol compounds via IBX-mediated phenolic oxygenation. *Tetrahedron Lett.* **46,** 3541–3544 (2005).

251. Magdziak, D., Rodriguez, A. A., Van De Water, R. W. & Pettus, T. R. R. Regioselective oxidation of phenols to o-quinones with o-iodoxybenzoic acid (IBX). *Org. Lett.* **4,** 285–288 (2002).

252. Gunsalus, I. C., Barton, L. S. & Gruber, W. Biosynthesis and Structure of Lipoic Acid Derivatives. *J. Am. Chem. Soc.* **78,** 1763–1766 (1956).

253. Panzella, L., De Lucia, M., Napolitano, A. & D'Ischia, M. The first expedient entry to the human melanogen 2-S-cysteinyldopa exploiting the anomalous regioselectivity of 3,4-dihydroxycinnamic acid–thiol conjugation. *Tetrahedron Lett.* **48,** 7650–7652 (2007).

254. Panzella, L., Napolitano, A. & d'Ischia, M. Oxidative conjugation of chlorogenic acid

with glutathione. Structural characterization of addition products and a new nitrite-Promoted pathway. *Bioorg. Med. Chem.* **11,** 4797–805 (2003).

255. Chiari, M. E. *et al.* Bioorganic & Medicinal Chemistry Tyrosinase inhibitory activity of a 6-isoprenoid-substituted flavanone isolated from Dalea elegans. *Bioorg. Med. Chem.* **19,** 3474–3482 (2011).

256. Liang, C., Lim, J.-H., Kim, S.-H. & Kim, D.-S. Dioscin: A synergistic tyrosinase inhibitor from the roots of Smilax china. *Food Chem.* **134,** 1146–1148 (2012).

257. Delogu, G. *et al.* Synthesis and biological evaluation of a novel series of bis-salicylaldehydes as mushroom tyrosinase inhibitors. *Bioorg. Med. Chem. Lett.* **20,** 6138–6140 (2010).

258. Yamazaki, Y., Kawano, Y., Yamanaka, A. & Maruyama, S. N-[(Dihydroxyphenyl)acyl]serotonins as potent inhibitors of tyrosinase from mouse and human melanoma cells. *Bioorg. Med. Chem. Lett.* **19,** 4178–82 (2009).

259. Ubo, K., Chen, Q.-X. & Kubo, I. Kinetics of Mushroom Tyrosinase Inhibition by Quercetin. *J. Agric. Food Chem.* **50,** 4108–4112 (2002).

260. Chang, T. S. An updated review of tyrosinase inhibitors. *Int. J. Mol. Sci.* **10,** 2440–2475 (2009).

261. Chen, J. S., Wei, C. I. & Marshall, M. R. Inhibition mechanism of kojic acid on polyphenol oxidase. *J. Agric. Food Chem.* **39,** 1897–1901 (1991).

262. Espín, J. C. *et al.* Kinetic characterization of the substrate specificity and mechanism of mushroom tyrosinase. *Eur. J. Biochem.* **267,** 1270–9 (2000).

263. Hajdú, I., Szilágyi, A., Kardos, J. & Závodszky, P. A link between hinge-bending domain motions and the temperature dependence of catalysis in 3-isopropylmalate dehydrogenase. *Biophys. J.* **96,** 5003–12 (2009).

264. Tarafder, A. K. *et al.* Rab11b mediates melanin transfer between donor melanocytes and acceptor keratinocytes via coupled exo/endocytosis. *J. Invest. Dermatol.* **134,** 1056–66 (2014).

265. Lawrie, K. J., Meredith, P. & McGeary, R. P. Synthesis and polymerization studies of organic-soluble eumelanins. *Photochem. Photobiol.* **84,** 632–8 (2008).

266. Ambrico, M. *et al.* A photoresponsive red-hair-inspired polydopamine-based copolymer for hybrid photocapacitive sensors. *Adv. Funct. Mater.* **24,** 7161–7172 (2014).

267. Bernsmann, F.; Ponche, A.; Ringwald, C.; Hemmerl_e, J.; Raya, J.; Bechinger, B. . & Voegel, J. C.; Schaaf, P.; Ball, V. J. Characterization of dopamine-melanin growth on silicon oxide. *J. Phys. Chem. C* **113,** 8234–8242 (2009).

268. Napolitano, A., Vincensi, M. R., Di Donato, P., Monfrecola, G. & Prota, G. Microanalysis of melanins in mammalian hair by alkaline hydrogen peroxide degradation: Identification of a new structural marker of pheomelanins. *J. Invest. Dermatol*. **114,** 1141–1147 (2000).

269. Napolitano, A., Palumbo, A., D'Ischia, M. & Prota, G. Mechanism of selective incorporation of the melanoma seeker 2-thiouracil into growing melanin. *J. Med. Chem.* **39,** 5192–5201 (1996).

270. Liu, Y. *et al.* Ion-exchange and adsorption of Fe(III) by Sepia melanin. *Pigment Cell Res.* **17,** 262–269 (2004).

271. Livak, K. J. & Schmittgen, T. D. Analysis of relative gene expression data using real-time quantitative PCR and. *Methods* **25,** 402–408 (2001).

272. Yagi, K., Shidoji, Y., Komura, S., Kojima, H. & Ohishi, N. Dissipation of mitochondrial membrane potential by exogenous phospholipid monohydroperoxide and protection against this effect by transfection of cells with phospholipid hydroperoxide glutathione peroxidase gene. *Biochem. Biophys. Res. Commun.* **245,** 528–33 (1998).

273. Yordanov, N. D., Gancheva, V. & Pelova, V. A. Studies on some materials suitable for use as internal standards in high energy EPR dosimetry. *J. Radioanal. Nucl. Chem.* **240,** 619–622 (1999).

274. Napolitano, A., Corradini M.G., Prota, G. A reinvestigation of the structure of melanochrome. *Tetrahedron Lett.* **26,** 2805–2808 (1985).

275. Frigerio, M., Santagostino, M. & Sputore, S. A user-friendly entry to 2-iodoxybenzoic acid (IBX). *J. Org. Chem.* **64,** 4537–4538 (1999).